RECEPTOR BINDING AND EARLY STEPS OF

CELLULAR INFECTION BY PARVOVIRUSES

A Dissertation

Presented to the Faculty of the Graduate School

of Cornell University

In Partial Fulfillment of the Requirements for the Degree of

Doctor of Philosophy

by

Carole Elizabeth Harbison

May 2011

RECEPTOR BINDING AND EARLY STEPS OF CELLULAR INFECTION BY
PARVOVIRUSES

Carole Elizabeth Harbison, D.V.M

Cornell University 2011

Parvoviruses are small, non-enveloped, single stranded DNA viruses. The specific attributes of the capsid and genome dictate how the virus interacts with the environment and the host cell in terms of transmission, tissue tropism, anti-viral immunity, and disease states.

A major focus of these studies is viral entry into host cells. During infection, the parvovirus capsid hijacks cellular pathways to reach the nucleus for genome replication. Receptor binding is critical for determining host range and tissue tropism, and various receptors are utilized by different parvoviruses. However, the intracellular trafficking pathways followed by viruses after endocytosis are poorly understood. Chapter 2 examines the dynamic nature of parvoviral uptake and entry by wild type viruses, while chapter 3 examines the ability of these viruses to use variant receptors for uptake and infection.

In addition to successfully navigating entry into host cells, parvoviruses must survive in the environment and evade host defenses. Humoral immunity plays a particularly important role in the control of these viruses. This is a benefit as vaccination is generally successful in controlling parvoviral disease, but is a challenge that must be overcome in the development of adeno-associated viruses as gene therapy vectors.

The studies that follow expand our knowledge about the interaction of antibodies with a newly described variant of CPV in raccoons, RPV-2 (Chapter 4) and the adeno-associated virus capsid (Chapter 5).

One final aspect of parvoviral biology addressed in this work is how changes in host range, antigenicity, and receptor interactions have evolved with small numbers of capsid changes in these closely related viruses. The trafficking studies in chapters 2 and 3 were performed within this contextual framework to examine the differences in the interactions of FPV and CPV with host cells. Chapter 4 describes the phylogenetic origin, host range, and receptor binding properties of several recently characterized parvovirus strains isolated from raccoons, and places this animal as an important intermediate host in the evolution of CPV. Finally, two of the more dissimilar serotypes of AAV were examined in Chapter 5 to look at the interaction of antibodies with capsids displaying somewhat different surface features.

BIOGRAPHICAL SKETCH

Carole grew up in Rochester, NY and received her undergraduate training leading to a Bachelor of Arts in Biology with honors from Oberlin College in 2000. Her undergraduate thesis studied the reproductive ecology of jack-in-the-pulpit (*Arisaema triphyllum*), and she held various summer research positions during this time studying topics ranging from foot and mouth disease to plant phylogenetics and rattlesnake behavior. After graduation, she worked at Genencor International, a biotechnology company in the San Francisco area, for four years before deciding to pursue veterinary research training.

Carole began the dual DVM/Ph.D program in 2004 at the Cornell University College of Veterinary Medicine, and joined the laboratory of Dr. Colin Parrish in 2005. She completed the requirements for the DVM program in May 2010, graduating with distinction. In April 2010, she was the recipient of the Merck Manual Award and the Frank L. Bloom award for excellence in pathology. After completing the Ph.D, she plans to find a challenging position that will utilize both aspects of her training for the advancement of human and/or animal health.

Dedicated to the loving memory of Caroline Coffey, an inspired scientist and devoted

friend taken from us many, many years too soon.

ACKNOWLEDGMENTS

There is a saying that it takes a community to raise a child, but as it also takes a community to raise a Ph.D student I have many people to thank. Foremost, I would like to thank my Ph.D mentor Colin Parrish for bearing with me for seven years as I bounced back and forth between the veterinary and research portions of the program, for providing guidance while also letting me find my own way and explore areas of interest, and for keeping me regularly caffeinated. I would also like to thank the other past and present members of my Ph.D committee, Drs. Eric Denkers, William Brown, Julia Felippe, and Timothy O'Brien for providing their time and input during the key periods in the development of this research program. Thank you to the dual degree oversight committee and graduate administration office, Casey and Janna. You guys work so hard, and it doesn't go unnoticed!

I have been fortunate to be part of a wonderful community in the Parrish lab and at the Baker Institute as a whole. Thank you particularly to Wendy Weichert, to whom the epithet "lab mom" seems particularly fitting. She has not only provided tireless technical support, but also made herself available on countless occasions for both scientific and personal discussions. Could not have done it without you! Thank you to past and present Parrish lab members; Karla for showing me the ropes as a dual degree student and for endless optimism, Christian for tin-foil art and beer-thirties, Swaantje and Jess for support and motivation to regularly swim at 7 AM, Jason for respecting my endless authority as senior student, and also to Michael, two Lauras, and Candy for making the lab a fun place to work. Thanks to Virginia, Erica, and Alicia for excellent technical support and for keeping the lab running smoothly, and to Shelagh for somehow keeping

v

TABLE OF CONTENTS

Chapter Two: Early Steps in Cellular Infection by Parvoviruses: Host-Specific

Differences in Receptor Binding but Similar Endosomal

Chapter Three: Endocytosis of canine and feline parvoviruses: Altering receptor transmembrane and cytoplasmic sequences to show requirements for infection

LIST OF FIGURES

LIST OF ABBREVIATIONS

AAV: Adeno-associated virus(es)

Ad: Adenovirus(es)

AMDV: Aleutian mink disease virus

AP-2: Adaptor protein 2

CA: Constitutively active

CHO: Chinese hamster ovary

CPV: Canine parvovirus

CRFK: Crandall-Rees feline kidney

DMEM: Dulbecco's Modified Eagle Medium

DN: Dominant negative

EDTA: Ethylenediaminetetraacetic acid

FFPE: Formalin-fixed paraffin-embedded

FPV: Feline panleukopenia virus

GFP: Green fluorescent protein

HA: Hemagglutination

HI: Hemagglutination inhibition

HBSS: Hank's buffered saline solution

HSPG: Heparin sulfate proteoglycan

mAB: monoclonal antibody

MFI: Mean fluorescence intensity

MVM: Minute virus of mice

NLFK: Norden Laboratory feline kidney

NLS: Nuclear localization signal

NPC: Nuclear pore complex

PBS: Phosphate buffered saline

PCR: Polymerase chain reaction

PPV: Porcine parvovirus

qPCR: quantitative polymerase chain reaction

PFA: Paraformaldehyde

PLA-2: Phospholipase A_2

RPV: Raccoon parvovirus

$TCID_{50}$: Fifty percent tissue culture infectious dose

Tf: Transferrin

TfR: Transferrin receptor

WGA: Wheat germ agglutinin

CHAPTER 1: INTRODUCTION

1.1 Taxonomy

The family *Parvoviridae* is divided into two subfamilies. The *Parvovirinae* infect vertebrate hosts and the *Densovirinae* infect invertebrates; only the former will be considered here. Within the *Parvovirinae* are several genera including Parvovirus and Dependovirus. Many parvoviruses of veterinary importance are contained within the genus Parvovirus, including feline panleukopenia virus (FPV), canine parvovirus (CPV), porcine parvovirus (PPV), and minute virus of mice (MVM). The adeno-associated viruses (AAVs) are within the genus Dependovirus, so named for their dependence on helper viruses for replication. The other genera within the family include Erythrovirus, of which the human B19 virus is a member, Amdovirus, containing the Aleutian mink disease virus (AMDV), and Betaparvovirus.

1.2 Parvovirus capsid structure

All of the Parvoviridae have small (~25 nm diameter), non-enveloped capsids with T=1 icosahedral symmetry. The CPV capsid is comprised of 60 copies total of the major capsid proteins, VP1 and VP2. In general, 90% of the capsid protein is comprised of the 65 kDa VP2, with several copies of the 83 kDa VP1 per capsid. In full capsids, 19 amino acids may be cleaved off the amino (N) terminus of some VP2 copies to form the 63 kDa VP3 (96). The carboxyl (C) terminus of each of these proteins is identical, and the unique 143 base pair N terminus of VP1 contains sequences with phospholipase A_2 and nuclear targeting activity (82, 100). These sequences are not exposed in the intact capsid, but are released during viral entry and play an essential role in infectivity. VP2 alone can assemble into capsids, but these virions are non-infectious (85, 152, 159).

The core of the CPV capsid is formed by an 8-stranded anti-parallel β-barrel

structure commonly found in icosahedral viruses, which internally contacts the single

stranded DNA viral genome through hydrogen bonding interactions (20, 58). The

intervening loops between the β strands contain the most variable sequences between

different viruses and are responsible for the major surface features of the capsid,

including the three-fold spike, the five-fold cylinder surrounding a pore, a deep canyon

surrounding the five-fold cylinder, and a depression (dimple) at the two-fold axis of

symmetry (Figure 1.1a) (151, 173). The pore at the five-fold axis is ~8 Å wide, large

enough to accommodate one peptide or DNA molecule at a time, and is the site for VP1

N terminus and genome extrusion during entry and DNA packaging (12, 43). In

structures solved by cryo-electron microscopy or X-ray crystallography, the N termini of

both VP1 and VP2 are disordered, indicative of their flexibility (43, 96). These features

are shared between many members of the *Parvoviridae* with the exception of the

human virus B19, which appears to lack the prominent three-fold spike and the pore at

the five-fold axis (69).
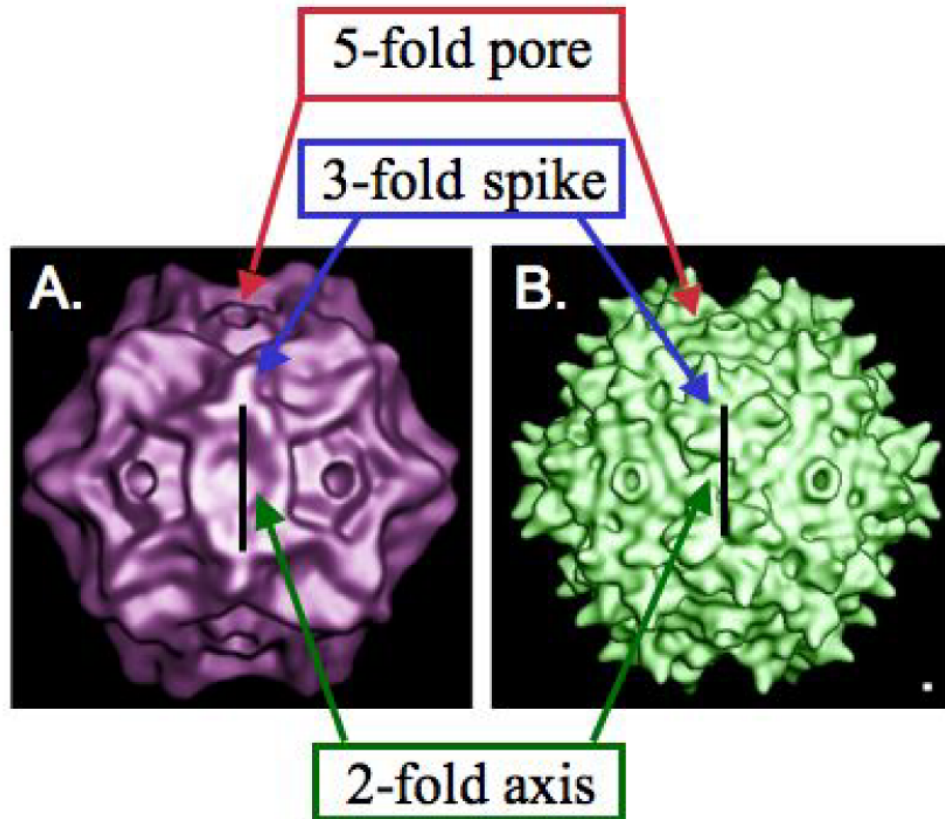
FIGURE 1.1. Parvovirus capsid structure. Cryo-electron microscopy reconstruction of A) CPV and B) AAV-2 capsids at 21Å resolution. The major surface features are indicated; note the overall similar topology between the capsids. Modified from Walters, R. W. et al. 2004. J. Virol. 78(7): 3361-3371, with permission.

The adeno-associated viruses also show variations on this structural theme. The AAV capsid is made up of 3 capsid proteins, VP1, VP2, and VP3, in an approximately 1:1:10 ratio, and like the autonomous parvoviruses these proteins contain shared C terminal regions. 12 AAV serotypes have been described that possess varying host ranges, tissue tropisms, and receptor binding properties (30). The differences between the serotypes stem primarily from mutations within the surface-oriented loops located between the β strands, whose sequences are less conserved than the β-barrel capsid core. Serotypes 1, 2, 3, and 6 share ~85% of their capsid sequence with each other,

while AAV5 is the most divergent and shares only ~55% capsid sequence identity (33, 162). Furthermore, the capsid genes share only about 10-20% identity with the CPV VP2 protein (21). Nonetheless, the internal structure and same basic surface topology is present, as described above, except that that three-fold spike of CPV is instead a trimer of spikes with an intervening depression at the three-fold axis (Figure 1.1b) (75, 97, 172).

1.3 Genome organization and gene components

The ~5.1 kb, usually negative sense, single-stranded DNA genome of CPV contains two open reading frames that encode the non-structural (NS1, NS2) and structural (VP1, VP2) proteins. Alternate RNA splicing gives rise to the two different gene products from each open reading frame. Two promoters drive gene transcription and are named for their genomic position (p4 and p38, respectively). There is a single polyadenylation site on the right hand end of the genome, and the terminal sequences are comprised of palindromic sequences that organize into variable hairpin secondary structures (Figure 1.2a) (121).
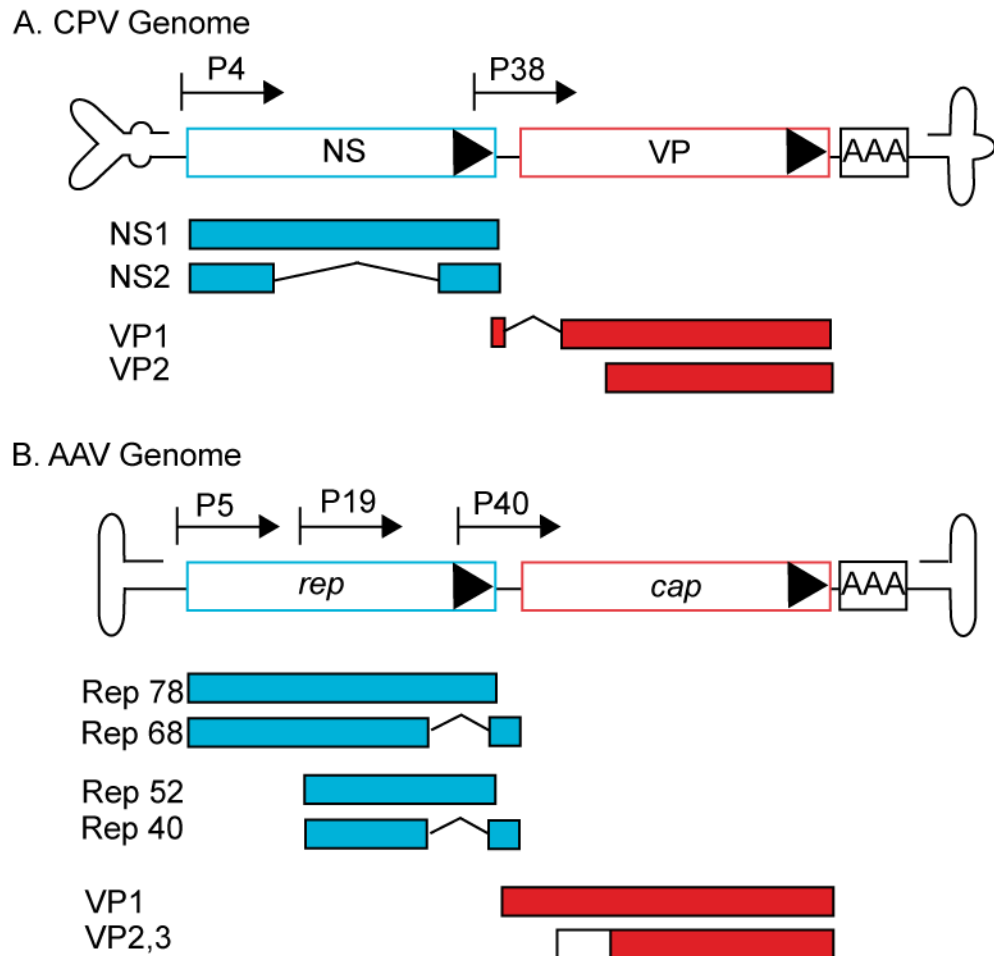
FIGURE 1.2. Parvovirus genome organization. Schematic representation of the A) CPV and B) AAV viral genomes, including the major transcripts encoding the non-structural (NS, Rep) and structural (VP) proteins. Other features shown are the locations of the various promoters, the single polyadenylation sequence within each genome, and the secondary structure formed by the inverted terminal repeats or hairpins (not to scale).

The non-structural proteins perform supportive roles in parvoviral replication. Neither protein has DNA polymerase activity, and the viruses depend on cellular proteins or helper viruses for this functionality. The 83 kDa NS1 protein is known to initiate replication by binding to and nicking the right-hand hairpin to start the process of secondary strand synthesis (167). It also has helicase and ATPase functions, is a

regulator of both viral promoters, and mediates RNA splicing and cytotoxic effects (1).

Phosphorylation by the cellular factor phosphokinase C is required for one or more of

these functions (76). The smaller NS2 protein is not required for infection in all cases,

and its function(s) have not been completely elucidated. For example, the Parvovirus

H1 NS2 is required for infection in rats, but not for infection of hamster or human cells

(79). In MVM, NS2 has been show to support capsid assembly and translation of the

capsid protein mRNA, and infection is inhibited in mutants lacking a functional version of

the protein (40). NS2 also binds to regulatory proteins in the cytoplasm (14-3-3 proteins)

and nucleus (Crm1) and may play a role in cell cycle control or other intracellular cell

signaling pathways (16). In CPV, however, no specific role for the the19 kDa protein has

been identified, and it appears to be dispensable for infection (165, 175).

The 4.7kb AAV genome is organized similarly to that of the autonomous

parvoviruses. There are four non-structural rep genes (large reps: Rep 68/78 and small

reps: Rep 52/40) that are analogous to the NS1 and NS2 genes, respectively (11). RNA

splicing and alternate translational start sites allow for the generation of these multiple

gene products as in the autonomous parvoviruses. These transcripts, as well as the

structural cap genes, are driven by separate promoters within the viral genome (p5, p19

and p40) (Figure 1.2b). Like the NS genes, they are involved in several aspects of the

AAV life cycle including replication, transcription, packaging, and integration. Though

both large and small Rep proteins contain helicase domains, the helicase function

provided by the small Rep protein is essential for complete genome packaging. The

large Rep proteins also have DNA binding, helicase, and ATPase activity like the

autonomous parvovirus NS1 protein described above. These proteins also interact with

the helper virus to modify its replication in some cases (146).

1.4 Parvovirus evolution

The structural and functional differences between FPV and CPV strains arise primarily from a small number of VP2 capsid protein mutations that affect receptor binding, host range, antigenicity, and capsid flexibility. CPV-2 emerged in the mid-1970s, and was first recognized in 1978 as a novel disease of dogs that rapidly spread worldwide to cause a global pandemic (107, 114). It arose during a host-switching event as a monophyletic clade from FPV, or an FPV like virus, and this process may have involved other carnivore intermediate hosts (61, 139). Within two years of CPV-2's emergence, new antigenic strains emerged that quickly replaced the original circulating strains in the wild, though the reasons these strains possess evidently enhanced fitness have not been determined. Of the newer antigenic variants, CPV-2a emerged in 1981, CPV-2b in the late 1980s, and CPV-2c in the early 2000s (18, 110, 113). These more recent strains are co-circulating to this day in different proportions varying by geographic area, and new mutations continue to arise. For a DNA virus, CPV has a relatively high rate of mutation that is comparable to the levels found in RNA viruses ($\sim 1.7 \times 10^4$ substitutions per site per year). The majority of the positively selected mutation sites are located within the VP2 gene (129).

The different parvovirus strains have distinct host ranges *in vitro* and *in vivo*, largely based on their ability to bind to the transferrin receptor of the host species (108). *In vitro*, FPV can only bind to and infect feline cells, while CPV variants can bind to and infect both canine and feline cells, although to different levels (101). *In vivo*, FPV infects a wide variety of carnivores but does not cause disease in dogs. Interestingly, however,

FPV can infect canine thymocytes, but this phenomenon has not been investigated in detail (111, 150). CPV-2 gained the ability to infect dogs by capsid changes at residues 93 and 323 that allowed it to bind the canine cellular receptor, but in that process lost the ability to infect cats due to concurrent changes at residues 80, 564, and 568 (Figure 1.3) (109, 148). The more recent CPV antigenic variants maintained the canine host range but regained the ability to infect cats through the acquisition of novel mutations at residues 87, 300, and 305 and not through back mutation to the feline residues at the sites listed above (149). CPV-2b and -2c are defined by a single point mutation at residue 426, which has undergone repeated changes (it is an Asn in FPV, CPV-2, and -2a, Asp in CPV-2b, and Glu in CPV-2c). Other changes of unknown significance are present in various recent isolates, such as Ser297Ala, which emerged in CPV strains in the mid 1990s, and Ile101Thr. Furthermore, the importance of CPV infections in cats is not well understood, but has been recognized in the literature as an occasional cause of generally mild disease (32, 67, 94, 149).
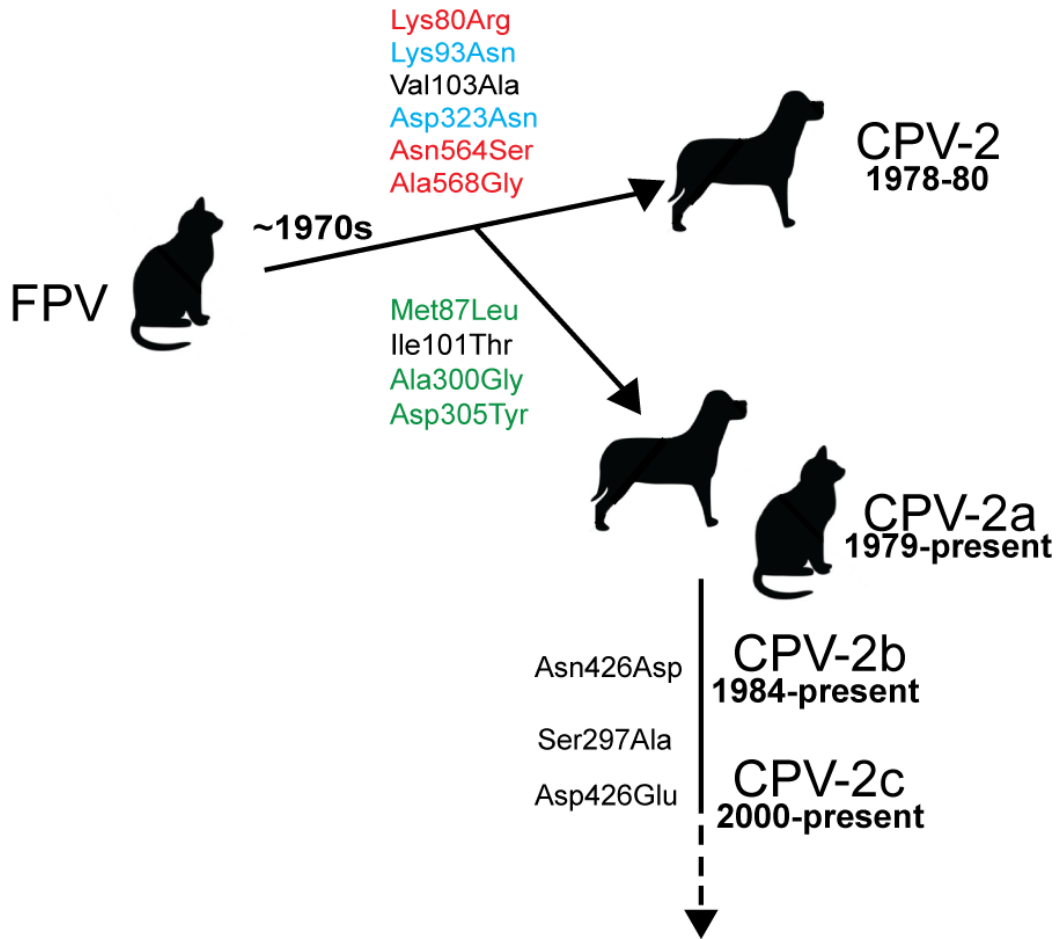
FIGURE 1.3. Classical view of CPV Evolution. Changes in the VP2 capsid protein during the evolution of CPV resulted in alterations in host range and antigenicity. Mutations in blue are responsible for the gain of canine host range. Mutations in red are important for loss of the feline host range during the evolution of CPV-2, while those in green are the compensating mutations in CPV-2a that allowed it to regain the ability to infect cats. Point mutations at residue 426 define the difference between CPV-2a and more recent variants, all of which can infect both cats and dogs.

Structurally, some of these mutations affect flexibility in the capsid by altering hydrogen-bonding patterns between surface residues. Within the threefold spike of CPV, mutations in surface loops 1 and 2 remove a hydrogen bond that is present in FPV between residues 93 with 225 and 227. This residue is a Lys in FPV and an Asn in CPV. An additional hydrogen bond is present between Asp323 and Arg377 in FPV that is abolished with the Asp323Asn mutation in CPV (63). FPV and CPV capsids also have

different numbers of associated divalent cations that affect stability. The surface oriented loop 3 (residues 359-75) organizes two calcium ions in CPV, but three in FPV due to the presence of an Asp at positions 373 and 375 (CPV is Asn375). This loop affects the sialic acid binding properties and controls the pH and temperature dependence of hemagglutination. FPV requires acidic pH to hemagglutinate red blood cells, while CPV can bind sialic acids at acidic and neutral pH (81, 132).

Because naturally circulating strains are often found to contain multiple concurrent residue changes, experimental site-directed mutagenesis has been useful in investigating the functional significance of individual residue changes. Following *in vitro* selection in feline cells, for example, a CPV-2 Ala300Asp mutation was selected. This strain has altered structure compared to CPV-2 due to the creation of a salt bridge between the Asp300 and Arg81, which changes the antigenicity and *in vitro* host range as infection of canine cells is significantly inhibited (112). This mutation was also seen in the wild in CPV-2a-derived isolates from wild leopard cats in Vietnam, and was also present in CPV-like isolates from raccoons described in chapter 4 (66, 68). Confusingly, this mutation was also designated CPV-2c by some authors, though is unrelated to the Glu426 strains described above. Other experimental mutations have mapped important host range-determining residues to VP2 299, 301, and 387, and have identified additional residues important for hemagglutination at VP2 377, 396, and 397 (81, 105).

1.5 Transferrin receptor-Cellular receptor for CPV, FPV

CPV and FPV use the transferrin receptor type-1 (TfR) for entry into host cells, and TfR expression is sufficient to allow infection in otherwise non-permissive Chinese hamster ovary (CHO) cells (104). The TfR is a 90 kDa, 760-residue type II membrane

protein, meaning that its N terminus is on the cytoplasmic side of the membrane (2).

The cellular function of TfR is to allow the regulated uptake of iron via iron-loaded

transferrin (Tf) (119). Iron is an essential cofactor in a wide variety of cellular proteins

including hemoglobin and lipoxygenase, an enzyme involved in arachadonic acid

metabolism. The TfR is an essential protein, and the TfR knockout mutation in mice is

embryonic lethal due to anemia based on a lack of functional, oxygen carrying red blood

cells (95). While nearly ubiquitously expressed on most cell types, the expression levels

of TfR are highest on rapidly dividing cells, which is a useful feature for this group of

viruses that requires cellular S phase to complete their replication.

At the cell surface (pH 7.4), TfR binds one or two molecules of the bilobed

transferrin protein (Tf) that, in turn, carries one or two ferric iron (Fe^{3+}) atoms per

holoTf. The iron-free form, apoTf, binds poorly to TfR at this pH. Once bound, the

targeting sequence Tyr-Thr-Arg-Phe on the cytoplasmic portion of TfR interacts with the

clathrin endocytic machinery through adaptor protein 2 (AP-2) for rapid endocytosis

(48). Deletion of this tail decreases the Tf internalization rate by ~90%, with the residual

endocytosis occurring by non-specific membrane turnover (27). The receptor and its

cargo are delivered sequentially to the early and recycling endosomal compartments,

where the iron is released in response to a low pH signal that results in a conformational

change of Tf. The iron-depleted apoTf remains bound at acidic pH and is recycled with

the receptor back to the cell surface, where it is released to make the TfR available for

another round of uptake. Clustering the TfR with oligomeric transferrin diverts the

receptor into a longer-lived perinuclear recycling compartment and acts as a luminal

retention signal to delay recycling. This phenomenon is not dependent on the

cytoplasmic tail, and likely has relevance for the trafficking of multivalent ligands such as viral capsids (87). Under normal conditions, a single transferrin receptor can undergo approximately 100 rounds of endocytosis during its normal lifespan before being targeted for degradation by ubiquitination and proteosomal digestion (42, 46).

1.6 Transferrin receptor structure

The crystal structure of the soluble human TfR ectodomain has been determined at pH 6.7, and is likely similar to that of the canine and feline TfRs which share ~80% sequence identity (63, 78). The tertiary structure of the transferrin receptor can be divided into several functional domains: the apical domain (residues 189-383, human TfR numbering), the protease-like domain (residues 127-188 and 384-606), the helical domain (607-760), a 30Å perimembrane stalk (90-126), the transmembrane domain (62-89), and an amino-terminal 61 amino acid cytoplasmic tail. The protease-like domain is located adjacent to the membrane and has an overall structure similar to carboxy- and amino-peptidases, although functionally the TfR has no protease activity. The apical domain is distal to the membrane and is made up of a β-sandwich flanked by two α-helices. No known cellular function for this domain has been identified. The helical domain, as the name suggests, consists of a four-helix bundle and two α-hairpins. The intervening loops between the helices are important for dimerization and accurate protein folding. The specific residues involved in Tf binding are located within the helical and protease-like domains, and vary slightly depending on the iron-loaded status of Tf (23, 46). In its native form, the protein exists as a homodimer on the surface of the cell and has a butterfly-like shape with the apical and protease-like domains forming the bipartite wing and the helical domain comprising the body (Figure 1.4) (2).
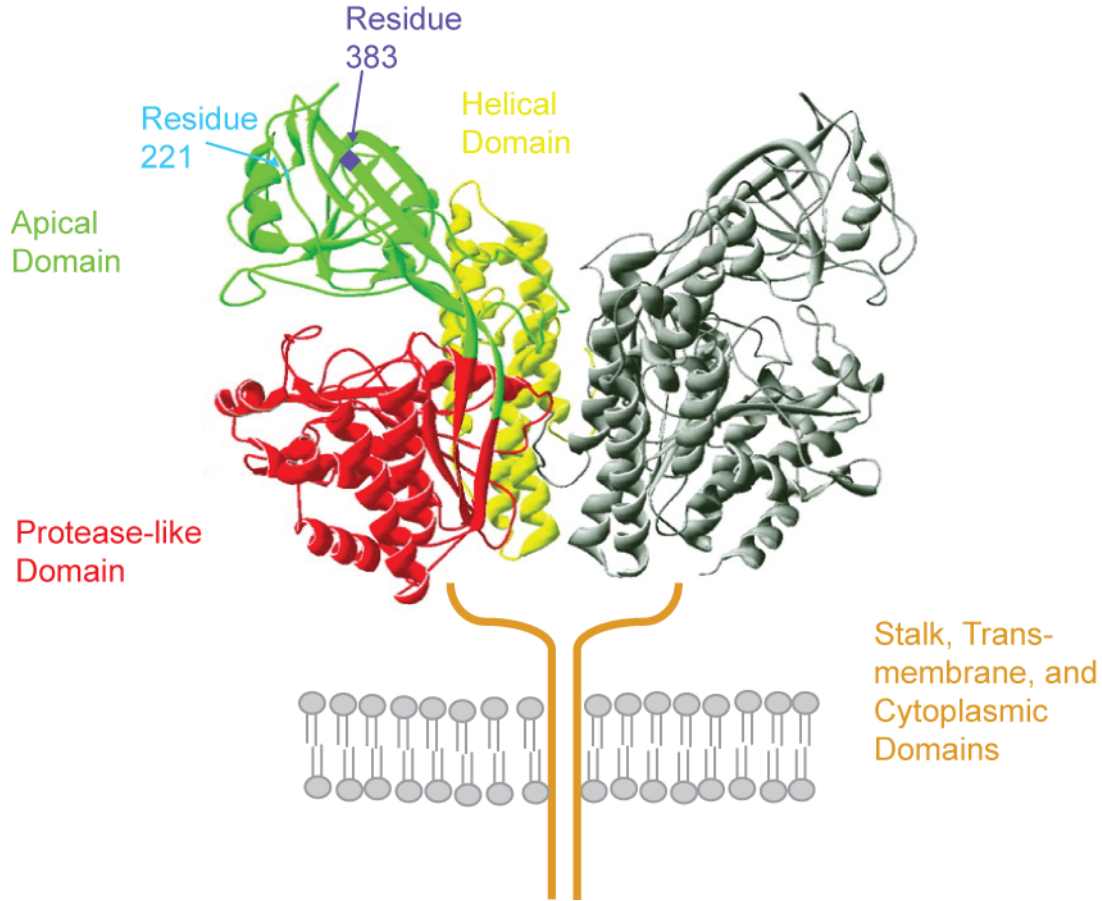
FIGURE 1.4. Human transferrin receptor structure. The different domains of the dimeric transferrin receptor are indicated on one monomer. The crystal structures of the stalk, transmembrane, and cytoplasmic domains have not been determined and are indicated schematically. Apical domain residues important for parvovirus binding are highlighted; a Leu221Ser feline TfR mutant is unable to bind CPV or FPV capsids, and residue 383 contains a glycosylation site contributing to viral host range that is present in the canine but not the feline TfR (79).

CPV and FPV bind to the apical domain for cellular entry, and do not sterically inhibit Tf binding (102). One major difference between the canine and feline TfRs controls parvovirus host range; the presence of a glycosylation site in the canine TfR at residue 383 prevents FPV binding and thus, infection of canine cells. Mutational analysis of the TfR only identified one mutation that completely knocked out parvovirus

binding, TfR Leu221Ser, though Thr300Asp and Asp369Lys mutations partially reduced binding and infection (Figure 1.4)(49, 101). Several residues in the virus capsid control viral host range by affecting binding to the TfR, and these are located over a relatively large area around the shoulder of the three-fold spike. Cryo-electron microscopy studies have identified this footprint, and have shown asymmetric binding whereby each capsid associates with only one or a small number of receptors (54).

CPV and FPV can also bind sialic acids on the surface of cells. These viruses bind specifically to the sialic acid moiety N-glycolylneuraminic acid (NeuGC), present on feline but not canine red blood cells. However, the significance of these interactions, and their role in the viral life cycle, is unclear; treating cells with neuraminidases does not inhibit CPV/FPV binding or infection and a non-hemagglutinating virus mutant is still infectious (8, 63, 102, 147).

1.7 Parvoviral disease, pathogenesis, and control

The small, non-enveloped parvoviral capsid provides protection from a wide variety of environmental conditions outside the host, including variations in pH, temperature, and humidity, and the presence of detergents (15). Harsh cleaners such as bleach or Virkon-S (potassium peroxymonosulfate) are required to kill the virus, as hot water, alcohol, grapefruit extract, and quaternary ammonium compounds are ineffective (41).

Because maternal antibodies and appropriate vaccination are protective against disease, unvaccinated or incompletely vaccinated animals and newborns from unvaccinated bitches/queens are most commonly affected by parvoviruses. CPV also appears to have some breed predispositions among dogs, with disease

overrepresented in "black and tan" breeds such as Rottweilers and Doberman Pinschers (31). The age window between 6 and 16 weeks is the highest risk period for puppies and kittens, even for those receiving the vaccination series. This is the period where maternal antibody levels are waning and may no longer be protective against disease but may still be high enough to interfere with vaccination efficacy. Multiple vaccinations (every 3-4 weeks between 6-8 and 14-16 weeks) are recommended to give the highest chance of protection (19).

For CPV and FPV, direct fecal-oral transmission is the primary route of disease spread between animals, but given the stability of the capsid fomites commonly play a role. In addition, vertical transmission to the developing fetus has been demonstrated for CPV (72). In the acute phase the virus is shed in large quantities in feces and may be present in other bodily fluids. Shedding may last up to several weeks or months in some cases, but for CPV and FPV, there appears to be no long-term carrier phase (77). Other parvoviruses are spread by alternate routes, such as respiratory transmission for human B19 virus and venereal transmission for porcine parvovirus (17, 130). AMDV is shed in the urine, and is an example of a parvovirus that can set up a persistent infection in the kidneys and other tissues (116).

Following oral inoculation, CPV and FPV first infect the dividing lymphocytes in the tonsils and oral lymphoid tissue. The virus then spreads systemically through free viremia and/or in association with the infected lymphocytes to secondary sites such as the intestine and bone marrow (92). The TfR is highly expressed on rapidly dividing cells including lymphocyte precursors and gastrointestinal epithelium, and the viral replication requirement for cellular passage through S phase helps to account for the

major symptoms of disease.

Some parvoviruses, most notably AAV, are non-pathogenic. Others can cause severe and often fatal disease. The clinical manifestations of CPV and FPV reflect the tissue tropisms of the virus. The most common manifestation of CPV is segmental enteritis with copious, foul smelling diarrhea, often containing frank blood. Small intestinal histopathology shows necrosis of the enteric crypt cells (crypts of Lieberkühn), villous effacement, and intranuclear inclusion bodies (118). Other common clinical signs include fever, inappetence, vomiting, and severe dehydration. Lymphopenia and generalized leukopenia are common laboratory findings, and along with the breakdown in the intestinal barrier this often results in secondary systemic bacterial infections and sepsis. No specific anti-viral treatment exists, but aggressive supportive care is usually required to combat the ongoing fluid losses and to prevent or control secondary infections. Without treatment, many cases are often acutely fatal, and severely affected cases may die even when treatment is administered. Those animals that recover from disease retain long lasting, likely life-long, immunity (164).

In the developing fetus, abortion occurs when the animal is infected with CPV or FPV during the first half of gestation. This is a common syndrome associated with infection by other parvoviruses including bovine and porcine parvovirus, as well as the human B19 virus. CPV and FPV infections occurring later in gestation or just after birth may lead to localized disease including cerebellar hypoplasia in kittens and myocarditis in puppies (9, 71).

1.8 The parvovirus life cycle

Successful entry into animal cells by viruses requires a series of interactions that culminates in the release of viral genetic material into a compartment permissive for replication. Many viruses utilize cellular receptor-mediated endocytic and vesicular trafficking pathways for uptake and directed, cytoskeleton-dependent transport (88, 131, 133). The choice of receptor can determine host specificity and tissue tropism and influences the subsequent endosomal trafficking within the cell. For the parvoviruses, infection and intracellular trafficking can be divided into five main stages: receptor binding and uptake, vesicular trafficking, endosomal escape, cytoplasmic trafficking, and nuclear entry. Where it has been examined the particle-to-infection ratio of most parvoviruses is typically high (>1000:1), and thus the majority of entering particles appear to be trafficked through a non-productive entry pathway.

1.8a Receptor-dependent virus internalization

The pathways of endosomal uptake and trafficking are summarized in Figure 1.5. All parvoviruses utilize receptor-mediated endocytosis for cellular uptake, and a wide variety of glycoproteins, glycans, and glycolipids function as receptors for various viruses (Table 1.1).
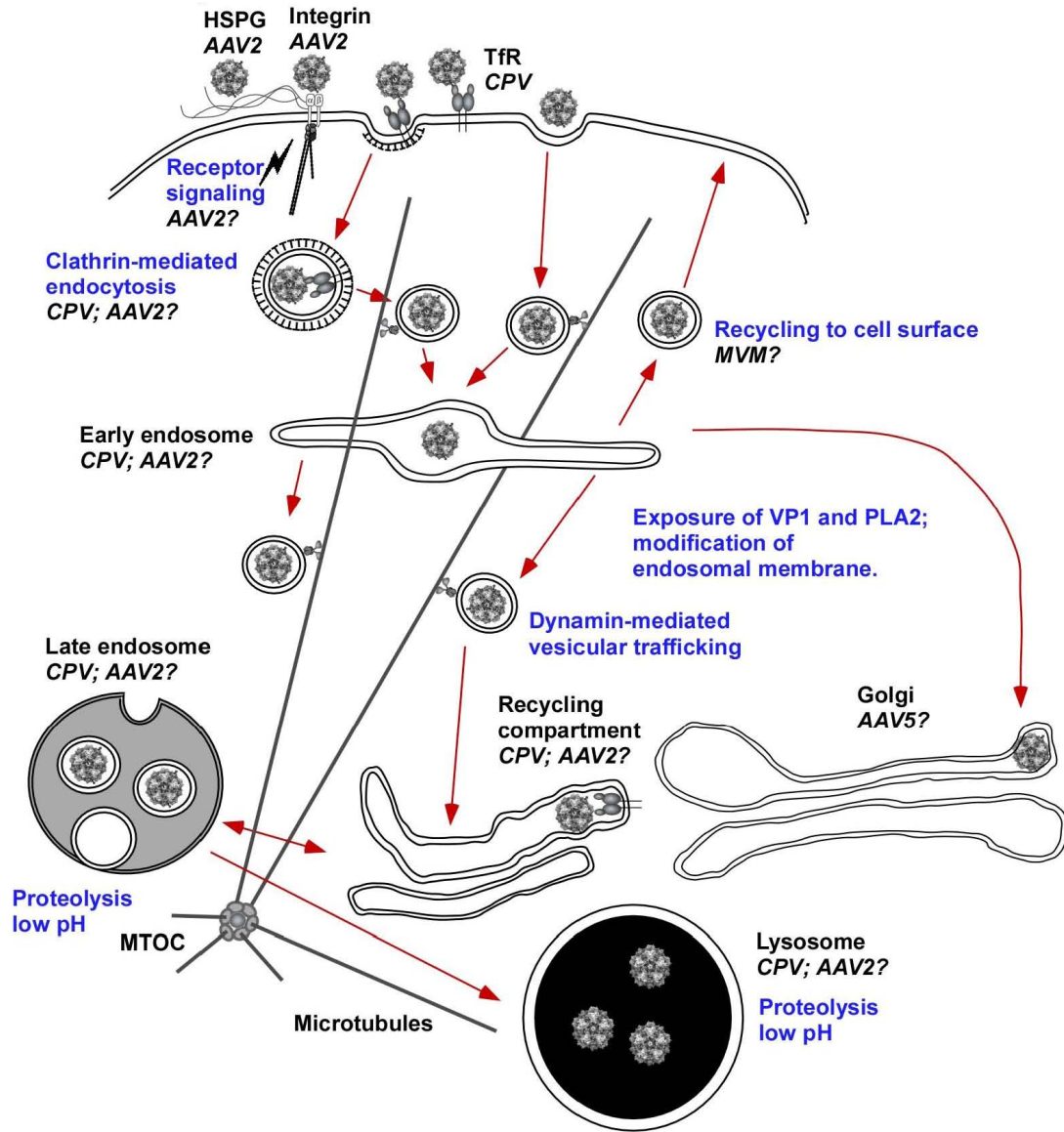
FIGURE 1.5. Parvovirus endocytosis. The processes of cellular uptake and endosomal trafficking by the different parvoviruses are shown, outlining the conserved pathways and the various steps that appear to differ between viruses. Capsids are shown in association with viral receptors including the TfR (CPV), αVβ5 integrin (AAV2), or heparin sulfate proteoglycan (HSPG) (AAV2). Uptake from the cell surface mostly appears to be clathrin-mediated, but other uptake pathways may be possible. Red arrows indicate intracellular pathways that have been identified for various viruses, but may differ depending on the cell type and specific experimental conditions used to examine virus trafficking.

Table 1.1. Parvoviral Receptors. Receptors defined as binding to parvoviruses, which in most cases also mediate the process of cell infection.

Virus	Cell-surface receptors and binding molecules	Hosts
Minute Virus of Mice	Sialic acids	Rodents
Human B19 virus	Globotriaosylceramide or globoside erythrocyte P antigen	Humans (primates)
FPV and CPV	Transferrin receptor-1, Sialic acid in some breeds	Cats, dogs, other carnivores
AAV2	Heparin sulfate proteoglycan, αVβ5 integrin, fibroblast growth factor receptor 1	Humans
AAV4	O-linked α2–3 sialic acid	Humans
AAV5	N-linked α2–3 sialic acid, platelet-derived growth factor receptor	Humans
AAV6	N-linked α2–3 and α2–6 sialic acid	Humans
AAV8	37/67-kDa laminin receptor	Humans
Bovine AAV	Gangliosides	Bovines

Some viruses use multiple receptors, and there is sometimes uncertainty exactly how those interact to allow optimal infection under different circumstances. CPV and FPV bind the TfR for infection, and are primarily endocytosed by clathrin-mediated endocytosis (103). However, altering the TfR Tyr-Thr-Arg-Phe (YTRF) internalization signal or expressing a dominant negative dynamin-2 construct that interferes with clathrin-mediated endocytosis reduces and delays, but does not abolish, uptake and infection by CPV indicating that other uptake mechanisms can also be used (37, 62, 104). MVM and AAV2 capsids are also taken up by clathrin-mediated endocytosis, despite using primary receptors that are not specifically associated with this pathway (sialic acids and heparin sulfate proteoglycan (HSPG), respectively) (10, 80). Other potential routes of uptake into the cell include macropinocytosis, caveolin-mediated endocytosis, and other less well-defined, clathrin- and caveolin-independent mechanisms (88, 90, 133). For example, porcine parvovirus binds sialic acids on the

cell surface and appears to use macropinocytosis and other uncharacterized pathways in addition to clathrin-mediated endocytosis for uptake, with viral aggregates preferentially using non-clathrin mediated uptake mechanisms (13). The specific pathways of uptake may also vary by cell type. AAV5 appears to use clathrin- and caveolin- mediated endocytosis in D7 cells, whereas in HeLa cells clathrin-mediated endocytosis is exclusively used. In HeLa cells in particular, capsids were seen concentrating on filopodia and at cell-cell junctions, a phenomenon observed in CPV binding to canine cells in chapter 2. The significance of this phenomenon is still being investigated (5).

An unresolved question for most parvoviruses is the specific role that receptor binding and/or clustering plays in initiating cellular signaling pathways to enhance viral uptake or alter cellular gene expression. AAV2, for example, binds and clusters $\alpha V\beta 5$ integrins, which signal through Notch1 and Rac to enhance the rate of internalization by clathrin-mediated endocytosis (127). Receptor clustering and cross linking may also affect the intracellular trafficking of the receptor-virus complex (87). Interestingly, in some cases viruses bind and are internalized into cells but infection is nonetheless blocked, possibly due to some alteration in trafficking that prevents viral release. For example, transduction of recombinant AAV2 capsids is more efficient from the basolateral surface of polarized human airway epithelia compared with the apical, despite similar numbers of particles entering from each surface (38). Similarly, chimeric TfRs with the cytoplasmic and transmembrane sequences replaced with those of the influenza neuraminidase or the extracellular domain replaced with an anti-viral antibody fragment both bind and take up CPV but do not allow infection (62). However, the

specific intracellular blocks to infection in these cases have not been determined.

1.8b Trafficking within the endosomal system

The rapid dynamics and complexity of viral movement within and between endosomal compartments is becoming increasingly appreciated. Somewhat different pictures of viral entry are seen when intracellular capsid distribution is examined by live-cell microscopy versus analysis of capsids in formaldehyde fixed cells. For CPV, viral uptake into cells that are subsequently fixed and stained with antibodies show capsid accumulation in perinuclear vesicles within 30 minutes (103), and this pattern can be disrupted by depolymerization of the microtubule network with nocodazole, low temperature, or by expression of a dynamin-2 Lys44Ala dominant negative mutant. These treatments also reduce infection, however it is difficult to distinguish direct effects on viral infectivity from indirect effects on cell viability and progression through the cell cycle (142, 158). After uptake, capsids are found in several intracellular locations, but dissecting the infectious pathway and determining from which endosomal compartment(s) the viruses escape into the cytoplasm has proven a difficult task (141). Furthermore, the number of entering virions actually completing the replication cycle is very low for this family of viruses, and particle to infectivity ratios have been calculated as low as 250:1 but may be much higher in some cases (177). The infectious proportion of the entering virions appear to stay associated with the TfR in the endosomal system for four hours or more, as infection can be blocked up to that time by intracellular microinjection of an antibody against the TfR cytoplasmic tail. After fixing the cells at different times after uptake, CPV and AAV capsids can be stained and co-localized with markers of the early endosome, late endosome, recycling endosome, and lysosome

within the first hours of infection (10, 35, 36, 103). Live cell analysis with fluorescently labeled particles, which more accurately represents the dynamic nature of the processes compared to fixed cell work, indicates there are several overlapping types and rates of particle movement within the vesicular system (128).

The intracellular trafficking patterns of AAVs differ by viral serotype. For example, capsids of AAV5 but not other examined serotypes accumulate in the Golgi complex (6). Cell type and capsid concentration also affect both the distribution of AAV2 particles in endosomes as well as the efficiency of transduction (36, 56). When cells are fixed after viral uptake using low multiplicities of infection, AAV2 capsids localize primarily in Rab7-labeled vesicles (late endosomes), while at high multiplicities they are found preferentially in Rab11-positive vesicles (recycling endosomes). Studies where Rab7 or Rab11 are overexpressed or are inhibited by RNAi treatments, suggest that the Rab11 pathway allows more efficient transduction of AAV2 compared with the Rab7 pathway (36). However, other studies suggest that AAV2 escapes from an early endosomal compartment and thus trafficking to later compartments is dispensable for entry (10, 85). The reasons for these differences are unclear, but are likely due to the use of different experimental approaches or analytical methods and to the complex nature of the trafficking that may be difficult to define when only fixed cells are examined.

Endosomal acidification is essential for infection by all parvoviruses examined to date, although the specific function(s) in triggering the initiation of viral infection are not yet resolved. Bafilomycin A1 inhibits the ATPase responsible for endosomal acidification, while NH_4Cl directly neutralizes the endosomal pH, and both significantly reduce infection if added within 30 minutes of AAV inoculation or within 90 minutes for

CPV. Prior low pH incubation of capsids does not substitute for the cellular block *in vivo* (10, 103, 142). The results of these experiments suggest that low pH may trigger a required conformational change in the capsid that must occur in the context of the intracellular environment. Some reversible changes occur in the capsid structures when incubated at low pH *in vitro*, and internal components of the capsids such as the VP1 unique region may be more easily released in these conditions (43, 85, 159). Alternatively, the viruses may require the activity of an acid-dependent host factor present in specific endosomal compartments (such as acid-dependent proteases), or the endosomal trafficking and vesicular fusion pathways themselves may be directly affected by endosomal neutralization (3, 135, 156, 158). Both the choice of which trafficking pathway is followed and the stage at which the particles leave the endosome are emerging as critical to the transduction activity of AAV gene therapy vectors (3).

1.8c Capsid structural changes and endosomal escape

The parvovirus capsid is a very stable structure, and neither major conformational changes nor complete capsid disassembly have been detected during the viral entry process. The details of the responses to low pH and proteases vary between different parvoviruses, suggesting that there are virus-specific processing requirements. Parvovirus B19 is sensitive to inactivation at low pH and exposes both the VP1 unique N terminus and the genome under these conditions, while CPV and MVM capsids remain intact and infectious (14, 125, 132). CPV replicates in and is shed from the intestine, and is therefore likely required to be more stable than B19, which appears to use mainly respiratory routes of infection and spread. The full capsids of autonomous parvoviruses such as MVM and CPV expose a proportion of the VP2

protein N-termini, and 19 to 22 residues of that sequence may be cleaved off to form VP3 (153, 166). In the case of MVM, this sequence is cleaved during viral entry, enhancing the release of the VP1 N terminal sequences and capsid recycling to the cell surface (124). Whether this happens with CPV has not been determined, nor have inhibitor studies identified the protease responsible for the cleavage of MVM VP2 to VP3 (166).

The N termini of VP1 proteins contain both phospholipase A_2 (PLA-2) sequences and basic nuclear localization signals (NLSs), and both activities are required for infection (157, 177). This sequence becomes exposed during uptake, but may not require acidification for release. CPV capsids show VP1 exposure even in the presence of endosomal neutralizing drugs, and MVM and AAV2 will expose their VP1 N termini *in vitro* in response to urea or heat treatment (74, 85, 141). PLA-2 activity appears to be either directly or indirectly responsible for endosomal escape by MVM and AAV2, as non-infectious point mutants lacking PLA-2 activity may infect when complemented in trans by treatments that lyse endosomes, such as polyethylene imine or adenovirus capsids. This effect can be separated from the helper virus functions of adenovirus (Ad) as the rescue of these PLA-2 mutants does not occur with Ad variants that are deficient for endosomal escape (43, 138).

Exposure of AAV to acidic conditions also results in conformational changes that activate or expose the PLA-2 domain of AAV2 capsids. PLA-2 active site mutations had no influence on capsid assembly, packaging of viral genomes into particles, or binding and entry into HeLa cells. Early viral gene expression, however, was delayed in cells incubated with these mutants, suggesting this region is important during viral entry (47).

Furthermore, as with other parvoviruses, capsid mutations that block exposure of the PLA-2 domain dramatically decrease infectivity (12, 51).

PLA-2s modify membranes and induce curvature by modifying the lipid head groups and changing their packing in the membrane, but the connection to viral membrane penetration has not yet been specifically determined. Furthermore, the contribution of other viral or cellular factors and the details of the mechanism of escape are both unknown. Pore formation is more likely than wholesale endosomal lysis for CPV escape, as neither α-sarcin nor large dextrans enter the cytoplasm with incoming viral capsids (103, 141).

1.8d Viral trafficking in the cytoplasm and access to the nucleus

The capsid processes that operate in the cytoplasm and are associated with nuclear entry are summarized in Figure 1.6. Although some conformational changes begin in the endosome, there is evidence for further capsid processing in the cytoplasm. Treating cells with protease inhibitors reduces MVM and PPV infectivity if added 3-12 hours after infection, late enough to affect a cytoplasmic proteosomal processing event (13). The proteasome may cleave the capsid VP2 at specific sites to initiating disassembly, but does not seem to be involved in the specific cleavage of VP2 to VP3 or in the externalization of the VP1 N terminus. Viruses infecting cells in the presence of protease inhibitors accumulate at the cytoplasmic side of the nuclear membrane but were not see to enter the nucleus (124, 136). However, this treatment can affect a variety of cellular enzymes including those within endosomes, and they are also generally toxic to the cells, which may non-specifically reduce viral replication.
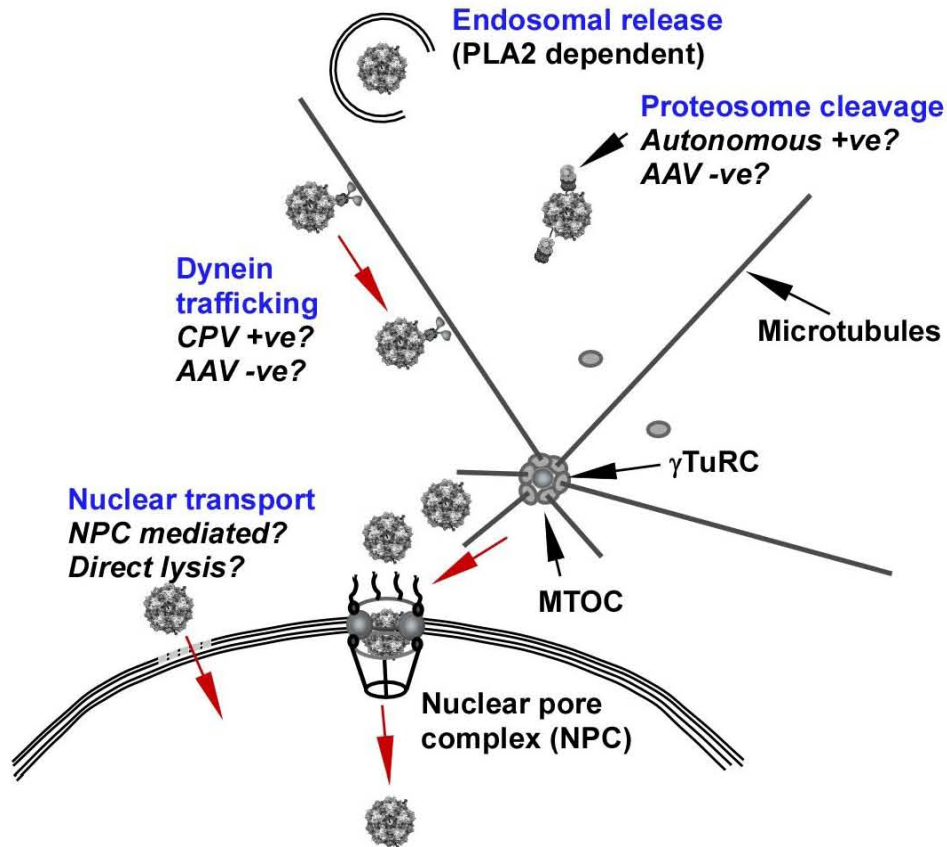
FIGURE 1.6. The cytoplasmic and nuclear trafficking of viral capsids. Viral release occurs from the endosome after PLA-2 modification, although the process is not completely understood. In the cytoplasm capsids may be susceptible to digestion by the proteosome, with enhancing or inhibitory effects depending on the virus. The involvement of microtubules and microtubule-associated motors (particularly dynein) may vary. The process of nuclear entry may involve direct transport through the nuclear pore by the more-or-less intact capsid or may directly or indirectly affect the nuclear membrane structure.

In contrast, various proteases appear to play both positive and negative roles in AAV infection. The proteosome plays an inhibitory role in AAV entry. Treatment with proteasome inhibitors enhances AAV transduction, perhaps by altering endosomal trafficking or processing of capsids or by decreasing ubiquitination-dependent degradation of viral capsids. Intact particles appear not to be ubiquitinated, and endosomal processing and partial disassembly may be required to prime AAV capsids

for ubiquitination (174).

Cathepsins B and L, on the other hand, interact with AAV2 or AAV8 proteins as shown by yeast two hybrid screening, and inhibiting these proteases decreases *in vivo* transduction (3). Trypsin cleavage sites have also been identified on the AAV2 capsid surface, and may be involved in structural rearrangements that increase capsid flexibility in preparation for uncoating. While the particles remain intact during protease treatment *in vitro*, differences in negative staining suggest structural rearrangement or flexibility due to the cleavage event. Prolonged incubation with these proteases reduces the infectivity of the particle as a result of loss of heparin binding activity, but may assist in uncoating and release of the viral genome once inside the cell (154). Microinjection of particles treated with various proteases into cells would show whether these post-entry modifications are sufficient to activate the particles. Indeed, some capsid processing steps are essential, as microinjecting AAV2 virions into the cytoplasm did not result to productive infection even in the presence of Ad5 (136). Cleavage of capsid proteins may directly lead to DNA uncoating or may be required to prime the capsids for ubiquitination (179).

From the site of endosomal release, the capsids must be further transported to the nucleus to allow genome replication. If transported to an immediately perinuclear position within endosomes, an active mechanism for transporting free capsids in the cytoplasm may not be required. Regardless, microtubules may be used by incoming CPV capsids for targeting to this location, as treating cells with nocodazole leads to a redistribution of microinjected capsids so that they become scattered throughout the cytoplasm (160). However, more recent data in another study conflicts with this finding,

as microinjected CPV capsids were observed to remain stationary within the cytoplasm at the site of injection for long periods of time, indicating a lack of interaction with cytoskeletal components (S. Lyi, unpublished data).

For AAV, the details of cytoplasmic trafficking and interactions with the cytoskeleton are also not well resolved. AAV2, 5 and rh10 strains have been observed to interact with microtubule-associated proteins (70), but different studies show various effects of nocodazole or other microtubule-directed drug treatment on virus infection or transduction. In some cases, these treatments prevented directed motion of viral particles in the cytoplasm and nucleus, while in others they had little effect on transduction (127, 128). Paclitaxol (taxol) treatment, which stabilizes microtubules, gave a mild enhancement of transduction by AAV2 in one study (60).

1.8e Nuclear entry and uncoating

For most of these viruses, the proportion of capsids that enter the nucleus is quite small, and the majority appears to persist in a perinuclear location (most likely in a non-degradative endosomal compartment) for several hours. Theoretically, the 26 nm diameter capsids should be able to pass through the nuclear pore complex (NPC) intact, as this is seen for newly synthesized capsids during viral egress (93). The role of potential NLS sequences in AAV capsid nuclear trafficking has been examined. Expression of the VP1 basic region sequence (PARKRLNF) on the exterior of the capsid was found to allow infection of otherwise non-infectious particles made up of only VP3, indicating that the NLS plays an important role in targeting the incoming capsids to the nucleus (51). However, some evidence suggests that MVM may not enter the nucleus through the NPC and may instead use a pore-independent entry mechanism,

despite the presence of NLSs in the unique N terminus of VP1 that become exposed during entry. In one study, disruption of the outer nuclear envelope was seen when MVM capsids were microinjected into the cytoplasm of *Xenopus* oocytes, and blocking the nuclear pore by adding wheat germ agglutinin (WGA) did not inhibit nuclear entry by the injected capsids (26). This phenomenon was also seen during entry into mouse fibroblast cells (25). For the parvovirus H1, in mammalian cells permeabilized with digitonin nuclear envelope breakdown following virus addition resulted in chromatin extrusion, possibly via activation of caspases (M. Kann, unpublished data). Finally, AAVs were found to enter isolated nuclei in the absence of cytoplasmic factors required for transport through the pore, and this was also unaffected by WGA addition (57). A role for the NLS in these viruses may therefore be to target the capsid to the nuclear membrane and/or dock it at the NPC, instead of directing transport through the pore. However, further studies are required to define the mechanisms involved in productive infection.

The capsid form that enters the nucleus is also still unresolved, and may vary between viruses. Although MVM capsid proteins have not been detected in the nucleus, this may simply indicate a low efficiency of transfer or may suggest that the capsids dock at the NPC (85). Conversely, in some studies microinjected CPV capsids appear to enter the nucleus intact, though after a delay of three to six hours (159, 166). For AAV, there is conflicting evidence whether uncoating occurs before or after nuclear entry. Fluorescently labeled AAV2 capsids were detected by microscopy within the nucleus within 2 hours (10), and some particles were seen within membrane invaginations of the nuclear envelope after only 15 minutes in studies utilizing single

particle tracking technology (128). Co-infection with adenovirus was found to enhance

nuclear entry of AAV capsids, though the process was still inefficient and the majority

(>90%) of particles remained outside the nucleus (83, 170). The results of two additional

studies suggest that the AAV genome is associated with the capsid when it contacts the

nucleus (136, 145). Microinjection of anti-capsid antibodies into the nucleus was found

to block infection in one study, and exposure of capsids to nuclear extracts in another

had the ability to induce genome release *in vitro*. Taken together, these results may

suggest that uncoating occurs dynamically during or shortly after the process of nuclear

entry, and this step may represent a bottleneck in the efficiency of infection by

parvoviruses.

The uncoating mechanism of parvoviruses is also not well understood, but in

general the particle is quite robust and complete disassembly may not be required for

genome release (96). Instead, the viral DNA may be extruded or extracted from

relatively intact capsids (28). In support of this hypothesis, a fluorescently labeled probe

for the 5' end of the MVM genome detected the partial exposure of DNA from VP2 5-

fold cylinder mutants in the cytoplasm while the 3' end (which would prime new DNA

synthesis) remained inside the capsid (85, 125). In a more recent study with wild-type

virions, however, genome extrusion occurred from the 3' to 5' direction (designated a

"pass-though" or "second portal" model) in capsids depleted of divalent cations. These

results further support a role for capsid conformational changes during the entry

process that allow the DNA to be released in a form immediately permissive for second

strand synthesis, though the *in vivo* trigger remains to be defined (28). As with nuclear

entry, genome release from the capsid occurs slowly and inefficiently for autonomous

parvoviruses, as microinjecting antibodies to the capsid into cells could block CPV

infection even when administered several hours after inoculation (160).

1.8f Parvoviral replication

Parvoviral replication is dependant on exogenous DNA polymerases, as the

viruses do not encode their own. The autonomous parvoviruses are dependent on

cellular S phase for replication, in accordance with their tropism for rapidly dividing cells,

while AAVs generally also require co-infection with helper viruses such as adenoviruses

or herpesviruses. In the absence of helper virus infection, AAV can establish latency

either by integration into the host chromosome or by maintenance as an episomal

concatemer. Treatment of cells with UV light, heat, or cyclohexamine can also induce

AAV replication, likely by stimulating DNA damage-repair mechanisms within the cell

(11).

Once inside the nucleus, CPV has been shown to cause rearrangements of the

nuclear architecture, though parvoviruses are unable to directly stimulate cellular

division. Late in the process of replication, DNA "replication bodies" may fill the majority

of the nucleus, with the cellular chromatin marginated at the nuclear periphery (64).

The parvoviruses replicate by a rolling-hairpin mechanism that proceeds through

a variety of duplex intermediates culminating in the release of genomes with a NS1

protein covalently linked to the 5' end. After the MVM genome is released from the

capsid the first step in replication is the synthesis of the second (complimentary) DNA

strand, which is primed using the 3' terminal hairpins and elongated by cellular

polymerases. The right-handed terminal hairpin is joined to the end of the elongating

strand, and then is nicked by the viral NS1 protein to allow the second strand to be fully

extended (167). The secondary structure at the ends is then restored, and the new 3'

hairpin can be used to prime further rounds of DNA elongation. Single stranded

genomes are released by additional DNA binding, nicking, and helicase activities of

NS1 (65).

The replication of AAV is similar, except that helper viruses facilitate DNA

synthesis instead of cellular polymerases, and the large Rep proteins take the role of

NS1. AAV replication may also be completed in a helper virus-free manner by co-

transfection of the individual helper genes, specifically adenovirus E1A/B E2A, E4orf6,

and VA RNA (126). These genes act to facilitate RNA processing, regulate viral

promoters, and inhibit cellular antiviral responses (89).

1.8g Capsid assembly and viral egress

The details of capsid assembly remain elusive, but the most likely pathway

involves the capsid proteins (VP1 and VP2) assembling into dimer, trimer, and/or

pentamer intermediates, before or after transport into the nucleus (175). VP1 contains

four basic regions that have been shown to function as NLSs, and the MVM VP2 also

contains a putative NLS and a nuclear localization motif that is functional after VP2

trimerization (29, 82, 159). Once inside the nucleus, several highly conserved

hydrophobic amino acids along the interface between the trimers likely facilitate this

spontaneous organization (122). Not all trimers include a VP1 molecule, and complete

capsids can assemble from only VP2, though they are non-infectious (123, 152). The

subsequent steps from trimerization to complete capsid formation have not been

determined, but appear to occur before DNA incorporation into the capsid.

While empty capsid assembly can occur within minutes, mature, genome-containing capsids can take up to an hour or more to be produced. The genome is packaged 3' end first into the intact, empty capsid through the five-fold pore. The process appears to proceed quickly for the first 2kb of packaging, but then stalls and requires the helicase action of NS1 (or the small rep proteins for AAV) for completion. This reaction may be facilitated by structural interactions between the DNA backbone and the capsid that help to reduce the energy required for packaging. Even in the complete, mature capsid, about 21 bp of the 5' end of the genome remains exposed on the capsid surface with a covalently linked NS1 protein attached (175). During packaging, in some cases the VP2 N termini are extruded from the five-fold pores to expose sequences necessary for nuclear export of the mature virion (a process which does not readily occur in empty capsids) (86). The autonomous parvoviruses package 99% negative strand genomes, while AAV packages approximately 40% positive strand DNA. Secondary structure formation within the genome may interfere with efficient packaging, and may explain why positive strand DNA is poorly encapsidated in some but not all viruses. Furthermore, structural limitations on genome packaging may also be an overlooked complication in cases of limited yields during gene therapy vector production (29).

Mature viral capsids are released from dying cells in a process that involves NS1-mediated cytotoxicity but is not well understood. A recent study identified markers of early apoptosis in CPV-infected NLFK cells, but the process of apoptotic was incomplete (98). Thus virus release may simply be a passive process of membrane permeabilization accompanying cell death, but the viruses may also be playing more of

an active role in tailoring how the cell dies and may be changing the organization of the cytoskeleton at this stage (7, 22).

1.9 Introduction to antibody neutralization

In an effort to prevent or contain viral spread, the infected host produces antibodies to bind and inactivate the viral capsids. The mechanism of antibody neutralization is direct or indirect interference with the functions of the viral capsid proteins. Antibodies can aggregate viral particles in solution and reduce the number of virions available to infect cells; however, this mechanism is often reversible and/or incomplete. Antibodies can also inhibit the interaction of viral surface proteins with the cellular receptor. They can either compete directly for the receptor binding site, or in some cases may coat the virus in an apparently non-specific way to sterically prevent interaction with the cell. However, given that the receptor-binding site is likely to have sequence constraints necessary to maintain the requisite structural interactions with the cellular receptor, these areas make good antigenic targets, particularly when they are located on a highly accessible portion of the capsid.

Various models of neutralization exist, including the single and multiple hit models (106). The single hit model emphasizes the importance of antibody binding to a key site on the viral capsid. Inactivation is achieved, for example, by the induction of structural rearrangements that renders the capsid non-infectious (34). This model does not, however, explain neutralization in all virus systems and if it occurs is likely uncommon (73). The multiple hit model explains neutralization as the result of antibodies coating the surface of the capsid by occupying a certain threshold percentage of available epitopes. Determinants of the stoichiometry of neutralization, or

the number of antibodies per viral capsid needed to prevent cellular infection *in vivo*, include capsid size, epitope accessibility, and the organization of the viral surface proteins. For icosahedral viruses, capsid size is generally proportional to the number of antibodies needed to neutralize and is related to the surface area that must be directly or sterically inhibited from interacting with host cells. Other details such as the location of the antigenic epitopes on raised or depressed areas of the capsid, as well as the spacing and density of the epitopes, may affect neutralization properties. For Picornaviruses, different antibodies have been shown behave according to the tenets of each of these models. A single hit antibody, for example, can mimic receptor binding and lead to premature uncoating in solution, while multiple hit antibodies must reach a certain occupancy before successfully being able to block cellular receptor binding. Not all of the accessible epitopes need to be coated in order to neutralize, and the required stoichiometry varies by antibody (117). Bivalent binding and steric hindrance by antibodies may decrease the threshold for neutralization.

Neutralization may also occur after virus attachment, for example if antibody binding inhibits interaction with intracellular cofactors required for infection. Antibodies can also facilitate or block conformational changes in the capsid and may interfere with intracellular events such as endosomal trafficking, release of the viral capsid into the cytoplasm, and genome uncoating. Antibodies directed against a flexible region on the West Nile virus capsid, for example, act at a post-attachment step by inhibiting intracellular fusion of the viral envelope with cellular membranes to prevent genome release (161).

In vivo, activation of complement, antibody dependent cellular toxicity, and other Fc related functionality further contribute to protection against infection. Specifically, interaction with TRIM-21 was recently identified as a method for degrading antibody coated viral capsids, regardless of the specific antibody-virus interaction (84). Given the wide range of neutralization mechanisms, *in vitro* neutralization does not always correlate to the efficacy of protection *in vivo* (99). For example, anti-West Nile virus Fab antibody fragments selected for neutralization ability *in vitro* provided poor neutralizing ability *in vivo*, though the mechanism behind this phenomenon was not further investigated (39).

1.10 Antigenicity of the CPV capsid

Antibodies are an essential part of the immune response against CPV. The major antigenic sites on the capsid are located within the surface oriented loops between the β strands, with loops 1 and 3 containing the most antigenically important residues. Furthermore, while many parvoviruses that infect carnivores are antigenically indistinguishable from FPV (such as viruses from raccoons, mink enteritis virus, and blue fox parvovirus), these sites are useful for distinguishing between FPV and the various CPV antigenic types based on monoclonal antibody binding patterns. These sites contain conformational epitopes, and have been grouped into 2 partially overlapping areas, named the "A site" and the "B site" (Figure 1.7) (53, 140).
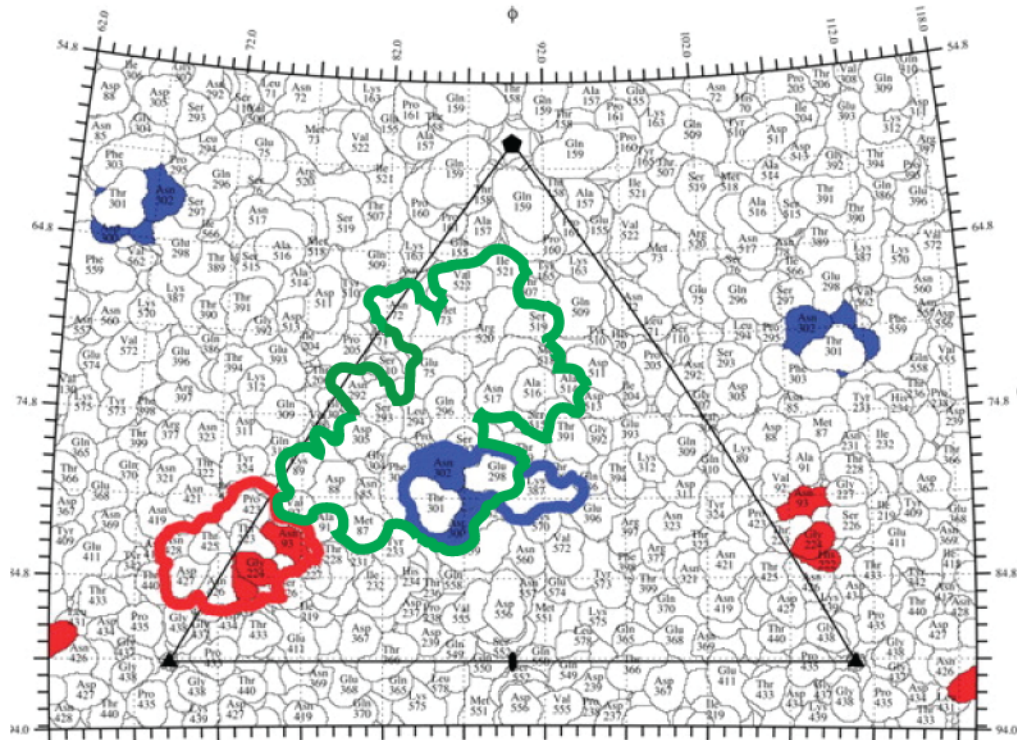
FIGURE 1.7. CPV antigenicity. The two major antigenic sites on the CPV capsid are projected onto a roadmap of the capsid asymmetric unit. The "A site" is outlined in red, and the "B site" is outlined in blue. The area outlined in green includes residues important for receptor binding. Modified from (53), with permission.

The "A site" contains VP2 residues near the tip of the three fold spike, including 93, 222, 224, and 426, important in the antigenic differentiation of CPV-like strains isolated from raccoons (chapter 3) and CPV-2c from other CPV strains. The "B site" contains residues located on the shoulder of the 3-fold spike, including the CPV-2 to CPV-2a mutations of Ala300Gly and Asp305Tyr as well as residues 299 and 302. This epitope partially overlaps with the receptor-binding site, and suggests that inhibition of receptor binding is one mechanism of neutralization used against these viruses. Other residues important for antigenicity lie under the capsid surface but have indirect effects on its structure, namely 80, 101, 103, 375, 564, 588 (140). Note that several of these antigenically important residues also affect receptor binding properties and host range,

(93, 300, etc.) and that both pressures likely influence selection of specific amino acids at these sites (61).

1.11 Adeno-associated viruses (AAVs) as gene therapy vectors

AAV is currently under investigation as a vector for therapeutic gene delivery. A variety of features make AAV an attractive vector, including the stability of the capsid, the inability of the virus to replicate without helper genes, the lack of disease associated with infection, the ability to induce long term expression of packaged genes, and the ability to transduce a variety of cells, both dividing and non-dividing (134, 137, 155).

This group of viruses was first discovered in the 1960s as a contaminant in adenovirus preparations (4). 12 different serotypes have been discovered in different host species to date, and of those AAV2 was the first serotype studied and is the best characterized. The cellular receptor for AAV2 is heparin sulfate proteoglycan (HSPG), though the virus can use $\alpha V\beta 5$ integrins as co-receptors and has also been shown to interact with the basic fibroblast growth factor receptor 1 (FGFR1) (120, 143). Other serotypes examined for use in different target tissues include AAV1 based on its superior ability to transduce muscle and hematopoitic stem cells compared to other AAV serotypes (178) and AAV5 for efficient transduction of muscle, airway epithelia, and brain tissues compared to AAV2 (176). Both of these serotypes utilize sialic acids as a cellular receptor (163), and AAV5 additionally binds to the platelet derived growth factor receptor (PDGF) as a co-receptor (115).

The AAV genome lends itself naturally to replacement with small gene products. Transgenes may be efficiently packaged into the AAV capsid by flanking any gene with the AAV inverted terminal repeats (ITRs), without including any viral proteins otherwise

encoded by the genome. Furthermore, despite small intrinsic genome size, strategies have been developed for the delivery of genes larger than the normal AAV packaging capacity (~5 kb) (45). Though naturally found in association with adenoviruses in nature, various helper virus-free production systems have emerged. Often, this involves transducing mammalian cells with the capsid gene of interest, two AAV Rep genes (p78/68), the adenovirus helper genes (E2A, E4, VA), and the genome to be packaged (52, 171).

1.12 Immunity to adeno-associated viruses

Despite a relatively low immunogenicity compared to other viral vector systems, humoral immunity leading to virus neutralization is a major challenge for gene therapy. Natural antibodies exist in up to 30%-80% of subjects in different studies, and these antibodies may be capable of preventing gene transduction by neutralizing the virus even at the first administration. Reactivity against serotypes 1, 2, 3, and 5 appears to be the most common, with variation according to geographic location and age of the subject. Furthermore, elicitation of memory B cell responses can preclude the implementation of repeat dosing schedules where necessary for sustained treatment. These responses are affected by the route, dose, and serotype of the administered virus, as well as the identity, expression level, and promoter of the transgene product (59, 144).

Pseudotyping the transgene using different serotypes of AAV has been attempted to circumvent the problems encountered with multiple administrations, as the capsids can very in up to 20% of amino acid residues such that antibodies tend not to cross-react significantly between serotypes (55, 169). Re-dosing with serotypes AAV5,

7, and 8 are of current interest because they are the most divergent from AAV2 and have lower levels of pre-existing immunity in some studies (24, 44). Concurrently dosing immunosuppressants to reduce reactivity to the AAV vector has also been attempted with some success in clinical trials. This strategy is of particular benefit when the immune response is directed against the transgene itself.

In addition to humoral immunity, innate and cell-mediated immune mechanisms may also play roles in interfering with the delivery of gene therapy vectors. On their own, most AAV capsids poorly transduce antigen presenting cells and are below the threshold of immunogenicity needed to strongly prime innate effector functions or cytotoxic T lymphocytes (CTLs). However, in some conditions such as expression of an immunogenic transgene or delivery into inflamed tissues, the immune system can be sufficiently activated to destroy transduced cells. As with the humoral immune response, this activity varies by capsid serotype, gene promoter, and target cell type (91).

1.13 Structural basis of the antibody response to AAV

The structure of AAV1, 2, and 5 has been solved alone and in complex with several Fab fragments. By way of review, Fab fragments are obtained by digesting antibodies with papain to release the variable domains and one constant region of both the heavy and light chain. Thus, two Fab fragments and a single Fc portion are produced per IgG. The Fab fragments contain a single antigen-binding site, cannot crosslink virus capsids, and do not generally retain any of the constant region functionality. In addition, they are smaller than intact IgGs and thus have a smaller area of steric inhibition.

In contrast to previous work showing a variety of structural conformational epitopes, the results of recent structural analyses show that most anti-AAV antibodies bind within a relatively limited footprint on raised areas around the threefold axis (168). Like other parvoviruses, in most serotypes the spikes at the three-fold axis of symmetry are the major feature projecting from the surface of the capsid. The receptor binding sites vary by serotype and specific cellular receptor, but where known tend to be located on these spikes (172). Interestingly, none of the antibodies tested against AAV or the autonomous parvoviruses bound to the other main raised feature of the viral capsid: the cylinder at the five-fold axis. Despite being accessible to the solvent, this loop may be a more flexible structure than the three-fold spike, and therefore less able to stimulate an effective antibody response (50). Alternatively, this structure may be partially covered by protein (the VP2 N terminus in the case of CPV) or the genome protruding from the pore at the five-fold axis.

Of several recently produced anti-AAV1 monoclonal antibodies, one (AA4E4.G7) bound on the shoulder of the threefold spike, away from the receptor-binding site, whereas others were expected to overlap with this site (AA5H7.Dii, ADK1a)(B. Gurda, unpublished data). The antibodies analyzed in this study also bound with different stoichiometries; occupying from 33% (AA4E4.G7, 5H7.D11) to 100% (ADK1a) of the available epitopes. This distribution of antigenic epitopes and the differences in structural interaction is reminiscent of other parvoviruses, where two overlapping regions of antibody binding have been described: one surrounding and one relatively distinct from the receptor-binding site. These differences in antibody interaction were

shown to be functionally relevant in previous studies of CPV infection, as antibodies were varyingly neutralizing as intact IgGs and as Fab fragments (53).

1.14 Dissertation outline

This thesis explores various aspects of parvovirus-host interactions. Chapters 2 and 3 examine the interaction of the viruses with the host cell during viral entry. Chapter 2 examines the early stages of entry of wild type viruses into host cells of different species, and underscores the complexity and rapid dynamics of viral endocytosis and intracellular trafficking. In Chapter 3, the role that the transferrin receptor cytoplasmic tail plays in directing the virus into the cell during infection is determined by the evaluation of receptor mutants where this domain is mutated or replaced with cytoplasmic tails from other type II membrane proteins.

Chapter 4 discusses the interaction of the viruses with different hosts on the whole organism level, addressing aspects of Parvoviral evolution and the role of raccoons as an intermediate host. My role in this work was to examine the binding and uptake properties of recently described CPV-like viral strains isolated from raccoons as related to in vitro host range, and to characterize antigenic variation between these strains and other carnivore parvoviruses.

Chapter 5 examines the interaction of the parvoviral capsid with the host immune system, specifically neutralizing antibodies. In this chapter, the mechanism of neutralization was evaluated for several anti-AAV1 and one anti-AAV5 monoclonal antibody.

Finally, Chapter 6 summarizes the significance of the research contained herein and provides suggestions for future investigation.

1.15 References

1.   **Adeyemi, R. O., S. Landry, M. E. Davis, M. D. Weitzman, and D. J. Pintel.** Parvovirus minute virus of mice induces a DNA damage response that facilitates viral replication. PLoS Pathog **6**.

2.   **Aisen, P.** 2004. Transferrin receptor 1. Int J Biochem Cell Biol **36:**2137-43.

3.   **Akache, B., D. Grimm, X. Shen, S. Fuess, S. R. Yant, D. S. Glazer, J. Park, and M. A. Kay.** 2007. A two-hybrid screen identifies cathepsins B and L as uncoating factors for adeno-associated virus 2 and 8. Mol Ther **15:**330-9.

4.   **Atchison, R. W., B. C. Casto, and W. M. Hammon.** 1965. Adenovirus-Associated Defective Virus Particles. Science **149:**754-6.

5.   **Bantel-Schaal, U., I. Braspenning-Wesch, and J. Kartenbeck.** 2009. Adeno-associated virus type 5 exploits two different entry pathways in human embryo fibroblasts. J Gen Virol **90:**317-22.

6.   **Bantel-Schaal, U., B. Hub, and J. Kartenbeck.** 2002. Endocytosis of adeno-associated virus type 5 leads to accumulation of virus particles in the Golgi compartment. J Virol **76:**2340-9.

7.   **Bar, S., L. Daeffler, J. Rommelaere, and J. P. Nuesch.** 2008. Vesicular egress of non-enveloped lytic parvoviruses depends on gelsolin functioning. PLoS Pathog **4:**e1000126.

8.   **Barbis, D. P., S.-F. Chang, and C. R. Parrish.** 1992. Mutations adjacent to the dimple of canine parvovirus capsid structure affect sialic acid binding. Virology **191:**301-308.

9.   **Barker, I. K., and C. R. Parrish.** 2001. Parvovirus Infections. . *In* E. Williams and I. Barker (ed.), Infectious Diseases of wild mammals, 3rd ed.

10.   **Bartlett, J. S., R. Wilcher, and R. J. Samulski.** 2000. Infectious entry pathway of adeno-associated virus and adeno-associated virus vectors. J Virol **74:**2777-2785.

11.   **Berns, K. I.** 1990. Parvovirus replication. Microbiol Rev **54:**316-29.

12.   **Bleker, S., F. Sonntag, and J. A. Kleinschmidt.** 2005. Mutational analysis of narrow pores at the fivefold symmetry axes of adeno-associated virus type 2 capsids reveals a dual role in genome packaging and activation of phospholipase A2 activity. J Virol **79:**2528-40.

13. **Boisvert, M., S. Fernandes, and P. Tijssen.** 2010. Multiple pathways involved in porcine parvovirus cellular entry and trafficking toward the nucleus. J Virol **84:**7782-92.

14. **Boschetti, N., I. Niederhauser, C. Kempf, A. Stuhler, J. Lower, and J. Blumel.** 2004. Different susceptibility of B19 virus and mice minute virus to low pH treatment. Transfusion **44:**1079-86.

15. **Boschetti, N., K. Wyss, A. Mischler, T. Hostettler, and C. Kempf.** 2003. Stability of minute virus of mice against temperature and sodium hydroxide. Biologicals **31:**181-5.

16. **Brockhaus, K., S. Plaza, D. J. Pintel, J. Rommelaere, and N. Salome.** 1996. Nonstructural proteins NS2 of minute virus of mice associate in vivo with 14-3-3 protein family members. J Virol **70:**7527-7534.

17. **Brown, K. E., and N. S. Young.** 1995. Parvovirus B19 infection and hematopoiesis. Blood Rev **9:**176-82.

18. **Buonavoglia, C., V. Martella, A. Pratelli, M. Tempesta, A. Cavalli, D. Buonavoglia, G. Bozzo, G. Elia, N. Decaro, and L. Carmichael.** 2001. Evidence for evolution of canine parvovirus type 2 in Italy. J Gen Virol **82:**3021-5.

19. **Carmichael, L. E., J. C. Joubert, and R. V. H. Pollock.** 1983. A modified canine parvovirus vaccine 2. Immune response. Cornell Vet. **73:**13-29.

20. **Chapman, M. S., and M. G. Rossmann.** 1995. Single-stranded DNA-protein interactions in canine parvovirus. Structure **3:**151-162.

21. **Chapman, M. S., and M. G. Rossmann.** 1993. Structure, sequence, and function correlations among parvoviruses. Virology **194:**491-508.

22. **Chen, A. Y., E. Y. Zhang, W. Guan, F. Cheng, S. Kleiboeker, T. M. Yankee, and J. Qiu.** 2010. The small 11 kDa nonstructural protein of human parvovirus B19 plays a key role in inducing apoptosis during B19 virus infection of primary erythroid progenitor cells. Blood **115:**1070-80.

23. **Cheng, Y., O. Zak, P. Aisen, S. C. Harrison, and T. Walz.** 2004. Structure of the human transferrin receptor-transferrin complex. Cell **116:**565-576.

24. **Chiorini, J. A., F. Kim, L. Yang, and R. M. Kotin.** 1999. Cloning and characterization of adeno-associated virus type 5. J Virol **73:**1309-19.

25. **Cohen, S., A. R. Behzad, J. B. Carroll, and N. Pante.** 2006. Parvoviral nuclear import: bypassing the host nuclear-transport machinery. The Journal of general virology **87:**3209-13.

26. **Cohen, S., and N. Pante.** 2005. Pushing the envelope: microinjection of Minute virus of mice into Xenopus oocytes causes damage to the nuclear envelope. J Gen Virol **86:**3243-52.

27. **Collawn, J. F., A. Lai, D. Domingo, M. Fitch, S. Hatton, and I. S. Trowbridge.** 1993. YTRF is the conserved internalization signal of the transferrin receptor, and a second YTRF signal at position 31-34 enhances endocytosis. J Biol Chem **268:**21686-92.

28. **Cotmore, S. F., S. Hafenstein, and P. Tattersall.** 2010. Depletion of virion-associated divalent cations induces parvovirus minute virus of mice to eject its genome in a 3'-to-5' direction from an otherwise intact viral particle. J Virol **84:**1945-56.

29. **Cotmore, S. F., and P. Tattersall.** 2005. Encapsidation of minute virus of mice DNA: aspects of the translocation mechanism revealed by the structure of partially packaged genomes. Virology **336:**100-12.

30. **Daly, T. M.** 2004. Overview of adeno-associated viral vectors. Methods Mol Biol **246:**157-65.

31. **Davies, M.** 2008. Canine parvovirus strains identified from clinically ill dogs in the United Kingdom. Vet Rec **163:**543-4.

32. **Decaro, N., D. Buonavoglia, C. Desario, F. Amorisco, M. L. Colaianni, A. Parisi, V. Terio, G. Elia, M. S. Lucente, A. Cavalli, V. Martella, and C. Buonavoglia.** 2010. Characterisation of canine parvovirus strains isolated from cats with feline panleukopenia. Res Vet Sci **89:**275-8.

33. **DiMattia, M., L. Govindasamy, H. C. Levy, B. Gurda-Whitaker, A. Kalina, E. Kohlbrenner, J. A. Chiorini, R. McKenna, N. Muzyczka, S. Zolotukhin, and M. Agbandje-McKenna.** 2005. Production, purification, crystallization and preliminary X-ray structural studies of adeno-associated virus serotype 5. Acta Crystallogr Sect F Struct Biol Cryst Commun **61:**917-21.

34. **Dimmock, N. J.** 1993. Neutralization of animal viruses. Curr Top Microbiol Immunol **183:**1-149.

35. **Ding, W., L. Zhang, Z. Yan, and J. F. Engelhardt.** 2005. Intracellular trafficking of adeno-associated viral vectors. Gene Ther **12:**873-80.

36. **Ding, W., L. N. Zhang, C. Yeaman, and J. F. Engelhardt.** 2006. rAAV2 traffics through both the late and the recycling endosomes in a dose-dependent fashion. Mol Ther.

37.   **Duan, D., Q. Li, A. W. Kao, Y. Yue, J. E. Pessin, and J. F. Engelhardt.** 1999. Dynamin is required for recombinant adeno-associated virus type 2 infection. J Virol **73:**10371-10376.

38.   **Duan, D., Y. Yue, Z. Yan, P. B. McCray, Jr., and J. F. Engelhardt.** 1998. Polarity influences the efficiency of recombinant adenoassociated virus infection in differentiated airway epithelia. Hum Gene Ther **9:**2761-76.

39.   **Duan, T., M. Ferguson, L. Yuan, F. Xu, and G. Li.** 2009. Human Monoclonal Fab Antibodies Against West Nile Virus and its Neutralizing Activity Analyzed in Vitro and in Vivo. J Antivir Antiretrovir **1:**36-42.

40.   **Eichwald, V., L. Daeffler, M. Klein, J. Rommelaere, and N. Salome.** 2002. The NS2 proteins of parvovirus minute virus of mice are required for efficient nuclear egress of progeny virions in mouse cells. J Virol **76:**10307-19.

41.   **Eleraky, N. Z., L. N. Potgieter, and M. A. Kennedy.** 2002. Virucidal efficacy of four new disinfectants. J Am Anim Hosp Assoc **38:**231-4.

42.   **Enns, C. A.** 2002. The transferrin receptor, p. 71-94. *In* D. M. Templeton (ed.), Molecular and cellular iron transport. Marcel Dekker, New York.

43.   **Farr, G. A., and P. Tattersall.** 2004. A conserved leucine that constricts the pore through the capsid fivefold cylinder plays a central role in parvoviral infection. Virology **323:**243-56.

44.   **Gao, G. P., M. R. Alvira, L. Wang, R. Calcedo, J. Johnston, and J. M. Wilson.** 2002. Novel adeno-associated viruses from rhesus monkeys as vectors for human gene therapy. Proc Natl Acad Sci U S A **99:**11854-9.

45.   **Ghosh, A., Y. Yue, Y. Lai, and D. Duan.** 2008. A hybrid vector system expands adeno-associated viral vector packaging capacity in a transgene-independent manner. Mol Ther **16:**124-30.

46.   **Giannetti, A. M., P. M. Snow, O. Zak, and P. J. Bjorkman.** 2003. Mechanism for multiple ligand recognition by the human transferrin receptor. PLoS Biol **1:**E51.

47.   **Girod, A., C. E. Wobus, Z. Zadori, M. Ried, K. Leike, P. Tijssen, J. A. Kleinschmidt, and M. Hallek.** 2002. The VP1 capsid protein of adeno-associated virus type 2 is carrying a phospholipase A2 domain required for virus infectivity. J Gen Virol **83:**973-8.

48.   **Girones, N., E. Alverez, A. Seth, I. M. Lin, D. A. Latour, and R. J. Davis.** 1991. Mutational analysis of the cytoplasmic tail of the human transferrin receptor.

Identification of a sub-domain that is required for rapid endocytosis. J Biol Chem **266:**19006-19012.

49.   **Goodman, L. B., S. M. Lyi, N. C. Johnson, J. O. Cifuente, S. L. Hafenstein, and C. R. Parrish.** Binding site on the transferrin receptor for the parvovirus capsid and effects of altered affinity on cell uptake and infection. J Virol **84:**4969-78.

50.   **Govindasamy, L., K. Hueffer, C. R. Parrish, and M. Agbandje-McKenna.** 2003. Structures of host range-controlling regions of the capsids of canine and feline parvoviruses and mutants. J Virol **77:**12211-21.

51.   **Grieger, J. C., J. S. Johnson, B. Gurda-Whitaker, M. Agbandje-McKenna, and R. J. Samulski.** 2007. Surface-exposed adeno-associated virus Vp1-NLS capsid fusion protein rescues infectivity of noninfectious wild-type Vp2/Vp3 and Vp3-only capsids but not that of fivefold pore mutant virions. J Virol **81:**7833-43.

52.   **Grieger, J. C., and R. J. Samulski.** 2005. Adeno-associated virus as a gene therapy vector: vector development, production and clinical applications. Adv Biochem Eng Biotechnol **99:**119-45.

53.   **Hafenstein, S., V. D. Bowman, T. Sun, C. D. Nelson, L. M. Palermo, P. R. Chipman, A. J. Battisti, C. R. Parrish, and M. G. Rossmann.** 2009. Structural comparison of different antibodies interacting with parvovirus capsids. J Virol **83:**5556-66.

54.   **Hafenstein, S., L. M. Palermo, V. A. Kostyuchenko, C. Xiao, M. C. Morais, C. D. Nelson, V. D. Bowman, A. J. Battisti, P. R. Chipman, C. R. Parrish, and M. G. Rossmann.** 2007. Asymmetric binding of transferrin receptor to parvovirus capsids. Proc Natl Acad Sci U S A **104:**6585-9.

55.   **Halbert, C. L., E. A. Rutledge, J. M. Allen, D. W. Russell, and A. D. Miller.** 2000. Repeat transduction in the mouse lung by using adeno-associated virus vectors with different serotypes. J Virol **74:**1524-32.

56.   **Hansen, J., K. Qing, and A. Srivastava.** 2001. Adeno-associated virus type 2-mediated gene transfer: altered endocytic processing enhances transduction efficiency in murine fibroblasts. J Virol **75:**4080-90.

57.   **Hansen, J., K. Qing, and A. Srivastava.** 2001. Infection of purified nuclei by adeno-associated virus 2. Mol Ther **4:**289-96.

58.   **Harrison, L. R.** 2001. Principles of Virus Structure. *In* H. Knipe (ed.), Fundamental Virology, fourth ed. Lippincott, Williams & Wilkins.

59. **Hernandez, Y. J., J. Wang, W. G. Kearns, S. Loiler, A. Poirier, and T. R. Flotte.** 1999. Latent adeno-associated virus infection elicits humoral but not cell-mediated immune responses in a nonhuman primate model. J Virol **73:**8549-58.

60. **Hirosue, S., K. Senn, N. Clement, M. Nonnenmacher, L. Gigout, R. M. Linden, and T. Weber.** 2007. Effect of inhibition of dynein function and microtubule-altering drugs on AAV2 transduction. Virology.

61. **Hoelzer, K., L. A. Shackelton, C. R. Parrish, and E. C. Holmes.** 2008. Phylogenetic analysis reveals the emergence, evolution and dispersal of carnivore parvoviruses. J Gen Virol **89:**2280-9.

62. **Hueffer, K., L. M. Palermo, and C. R. Parrish.** 2004. Parvovirus infection of cells by using variants of the feline transferrin receptor altering clathrin-mediated endocytosis, membrane domain localization, and capsid-binding domains. J Virol **78:**5601-5611.

63. **Hueffer, K., J. S. Parker, W. S. Weichert, R. E. Geisel, J. Y. Sgro, and C. R. Parrish.** 2003. The natural host range shift and subsequent evolution of canine parvovirus resulted from virus-specific binding to the canine transferrin receptor. J. Virol. **77:**1718-1726.

64. **Ihalainen, T. O., E. A. Niskanen, J. Jylhava, O. Paloheimo, N. Dross, H. Smolander, J. Langowski, J. Timonen, and M. Vihinen-Ranta.** 2009. Parvovirus induced alterations in nuclear architecture and dynamics. PLoS One **4:**e5948.

65. **Ihalainen, T. O., E. A. Niskanen, J. Jylhava, T. Turpeinen, J. Rinne, J. Timonen, and M. Vihinen-Ranta.** 2007. Dynamics and interactions of parvoviral NS1 protein in the nucleus. Cell Microbiol **9:**1946-59.

66. **Ikeda, Y., M. Mochizuki, R. Naito, K. Nakamura, T. Miyazawa, T. Mikami, and E. Takahashi.** 2000. Predominance of canine parvovirus (CPV) in unvaccinated cat populations and emergence of new antigenic types of CPVs in cats. Virology **278:**13-9.

67. **Ikeda, Y., K. Nakamura, T. Miyazawa, E. Takahashi, and M. Mochizuki.** 2002. Feline host range of canine parvovirus: recent emergence of new antigenic types in cats. Emerg Infect Dis **8:**341-6.

68. **Kapil, S., G. Rezabek, B. Germany, and L. Johnston.** 2010. Isolation of a virus related to canine parvovirus type 2 from a raccoon (Procyon lotor). Vet Rec **166:**24-5.

69. **Kaufmann, B., A. A. Simpson, and M. G. Rossmann.** 2004. The structure of human parvovirus B19. Proc Natl Acad Sci U S A **101:**11628-33.

70. **Kelkar, S., B. P. De, G. Gao, J. M. Wilson, R. G. Crystal, and P. L. Leopold.** 2006. A common mechanism for cytoplasmic dynein-dependent microtubule binding shared among adeno-associated virus and adenovirus serotypes. J Virol **80:**7781-5.

71. **Kerr, J. R., S. F. Cotmore, M. E. Bloom, R. M. Linden, and C. R. Parrish.** 2006. Parvoviruses. Hodder Arnold, London.

72. **Kilham, L., G. Margolis, and E. D. Colby.** 1967. Congenital infections of cats and ferrets by feline panleukopenia virus manifested by cerebella hypoplasia. Lab. Invest. **17:**465-480.

73. **Klasse, P. J., and Q. J. Sattentau.** 2001. Mechanisms of virus neutralization by antibody. Curr Top Microbiol Immunol **260:**87-108.

74. **Kronenberg, S., B. Bottcher, C. W. von der Lieth, S. Bleker, and J. A. Kleinschmidt.** 2005. A conformational change in the adeno-associated virus type 2 capsid leads to the exposure of hidden VP1 N termini. J Virol **79:**5296-303.

75. **Kronenberg, S., J. A. Kleinschmidt, and B. Bottcher.** 2001. Electron cryo-microscopy and image reconstruction of adeno-associated virus type 2 empty capsids. EMBO Rep **2:**997-1002.

76. **Lachmann, S., J. Rommeleare, and J. P. Nuesch.** 2003. Novel PKCeta is required to activate replicative functions of the major nonstructural protein NS1 of minute virus of mice. J Virol **77:**8048-60.

77. **Lamm, C. G., and G. B. Rezabek.** 2008. Parvovirus infection in domestic companion animals. Vet Clin North Am Small Anim Pract **38:**837-50, viii-ix.

78. **Lawrence, C. M., S. Ray, M. Babyonyshev, R. Galluser, D. W. Borhani, and S. C. Harrison.** 1999. Crystal structure of the ectodomain of human transferrin receptor. Science **286:**779-782.

79. **Li, X., and S. L. Rhode.** 1991. Nonstructural protein NS2 of parvovirus H-1 is required for efficient viral protein synthesis and virus production in rat cells in vivo and in vitro. Virology **184:**117-130.

80. **Linser, P., H. Bruning, and R. W. Armentrout.** 1977. Specific binding sites for a parvovirus, minute virus of mice, on cultured mouse cells. J.Virol. **41:**211-221.

81. **Llamas-Saiz, A. L., M. Agbandje-McKenna, J. S. L. Parker, A. T. M. Wahid, C. R. Parrish, and M. G. Rossmann.** 1996. Structural analysis of a mutation in canine parvovirus which controls antigenicity and host range. Virology **225:**65-71.

82.   **Lombardo, E., J. C. Ramirez, J. Garcia, and J. M. Almendral.** 2002. Complementary roles of multiple nuclear targeting signals in the capsid proteins of the parvovirus minute virus of mice during assembly and onset of infection. J Virol **76:**7049-59.

83.   **Lux, K., N. Goerlitz, S. Schlemminger, L. Perabo, D. Goldnau, J. Endell, K. Leike, D. M. Kofler, S. Finke, M. Hallek, and H. Buning.** 2005. Green fluorescent protein-tagged adeno-associated virus particles allow the study of cytosolic and nuclear trafficking. J Virol **79:**11776-87.

84.   **Mallery, D. L., W. A. McEwan, S. R. Bidgood, G. J. Towers, C. M. Johnson, and L. C. James.** Antibodies mediate intracellular immunity through tripartite motif-containing 21 (TRIM21). Proc Natl Acad Sci U S A **107:**19985-90.

85.   **Mani, B., C. Baltzer, N. Valle, J. M. Almendral, C. Kempf, and C. Ros.** 2006. Low pH-dependent endosomal processing of the incoming parvovirus minute virus of mice virion leads to externalization of the VP1 N-terminal sequence (N-VP1), N-VP2 cleavage, and uncoating of the full-length genome. J Virol **80:**1015-24.

86.   **Maroto, B., N. Valle, R. Saffrich, and J. M. Almendral.** 2004. Nuclear export of the nonenveloped parvovirus virion is directed by an unordered protein signal exposed on the capsid surface. J Virol **78:**10685-94.

87.   **Marsh, E. W., P. L. Leopold, N. L. Jones, and F. R. Maxfield.** 1995. Oligomerized transferrin receptors are selectively retained by a lumenal sorting signal in a long-lived endocytic recycling compartment. J Cell Biol **129:**1509-1522.

88.   **Marsh, M., and A. Helenius.** 2006. Virus entry: open sesame. Cell **124:**729-40.

89.   **Matsushita, T., T. Okada, T. Inaba, H. Mizukami, K. Ozawa, and P. Colosi.** 2004. The adenovirus E1A and E1B19K genes provide a helper function for transfection-based adeno-associated virus vector production. J Gen Virol **85:**2209-14.

90.   **Mayor, S., and R. E. Pagano.** 2007. Pathways of clathrin-independent endocytosis. Nat Rev Mol Cell Biol **8:**603-12.

91.   **Mays, L. E., and J. M. Wilson.** The complex and evolving story of T cell activation to AAV vector-encoded transgene products. Mol Ther **19:**16-27.

92.   **Meunier, P. C., B. J. Cooper, M. J. G. Appel, M. E. Lanieu, and D. O. Slauson.** 1985. Pathogenesis of canine parvovirus enteritis: sequential virus distribution and passive immunization studies. Vet. Pathol. **22:**617-624.

93.   **Miller, C. L., and D. J. Pintel.** 2002. Interaction between parvovirus NS2 protein and nuclear export factor Crm1 is important for viral egress from the nucleus of murine cells. J Virol **76:**3257-3266.

94.   **Mochizuki, M., M. Horiuchi, H. Hiragi, M. C. San Gabriel, N. Yasuda, and T. Uno.** 1996. Isolation of canine parvovirus from a cat manifesting clinical signs of feline panleukopenia. J Clin Microbiol **34:**2101-5.

95.   **Ned, R. M., W. Swat, and N. C. Andrews.** 2003. Transferrin receptor 1 is differentially required in lymphocyte development. Blood **102:**3711-8.

96.   **Nelson, C. D., E. Minkkinen, M. Bergkvist, K. Hoelzer, M. Fisher, B. Bothner, and C. R. Parrish.** 2008. Detecting small changes and additional peptides in the canine parvovirus capsid structure. J Virol **82:**10397-407.

97.   **Ng, R., L. Govindasamy, B. L. Gurda, R. McKenna, O. G. Kozyreva, R. J. Samulski, K. N. Parent, T. S. Baker, and M. Agbandje-McKenna.** Structural characterization of the dual glycan binding adeno-associated virus serotype 6. J Virol **84:**12945-57.

98.   **Nykky, J., J. E. Tuusa, S. Kirjavainen, M. Vuento, and L. Gilbert.** 2010. Mechanisms of cell death in canine parvovirus-infected cells provide intuitive insights to developing nanotools for medicine. Int J Nanomedicine **5:**417-28.

99.   **Oswald, W. B., T. W. Geisbert, K. J. Davis, J. B. Geisbert, N. J. Sullivan, P. B. Jahrling, P. W. Parren, and D. R. Burton.** 2007. Neutralizing antibody fails to impact the course of Ebola virus infection in monkeys. PLoS Pathog **3:**e9.

100.   **Pakkanen, K., S. Kirjavainen, A. R. Makela, N. Rintanen, C. Oker-Blom, T. O. Jalonen, and M. Vuento.** 2009. Parvovirus capsid disorders cholesterol-rich membranes. Biochem Biophys Res Commun **379:**562-6.

101.   **Palermo, L. M., S. L. Hafenstein, and C. R. Parrish.** 2006. Purified feline and canine transferrin receptors reveal complex interactions with the capsids of canine and feline parvoviruses that correspond to their host ranges. J. Virol. **80**.

102.   **Palermo, L. M., K. Hueffer, and C. R. Parrish.** 2003. Residues in the apical domain of the feline and canine transferrin receptors control host-specific binding and cell infection of canine and feline parvoviruses. J Virol **77:**8915-8923.

103.   **Parker, J. S., and C. R. Parrish.** 2000. Cellular uptake and infection by canine parvovirus involves rapid dynamin-regulated clathrin-mediated endocytosis, followed by slower intracellular trafficking. J Virol **74:**1919-1930.

104. **Parker, J. S. L., W. J. Murphy, D. Wang, S. J. O'Brien, and C. R. Parrish.** 2001. Canine and feline parvoviruses can use human or feline transferrin receptors to bind, enter, and infect cells. J. Virol. **75:**3896-3902.

105. **Parker, J. S. L., and C. R. Parrish.** 1997. Canine parvovirus host range is determined by the specific conformation of an additional region of the capsid. J. Virol. **71:**9214-9222.

106. **Parren, P. W., and D. R. Burton.** 2001. The antiviral activity of antibodies in vitro and in vivo. Adv Immunol **77:**195-262.

107. **Parrish, C. R.** 1990. Emergence, natural history, and variation of canine, mink, and feline parvoviruses. Adv Virus Res **38:**403-450.

108. **Parrish, C. R.** 1999. Host range relationships and the evolution of canine parvovirus. Vet Microbiol **69:**29-40.

109. **Parrish, C. R.** 1991. Mapping specific functions in the capsid structure of canine parvovirus and feline panleukopenia virus using infectious plasmid clones. Virology **183:**195-205.

110. **Parrish, C. R., C. Aquadro, M. L. Strassheim, J. F. Evermann, J.-Y. Sgro, and H. Mohammed.** 1991. Rapid antigenic-type replacement and DNA sequence evolution of canine parvovirus. J Virol **65:**6544-6552.

111. **Parrish, C. R., C. F. Aquadro, and L. E. Carmichael.** 1988. Canine host range and a specific epitope map along with variant sequences in the capsid protein gene of canine parvovirus and related feline, mink and raccoon parvoviruses. Virology **166:**293-307.

112. **Parrish, C. R., and L. E. Carmichael.** 1986. Characterization and recombination mapping of an antigenic and hostrange mutation of canine parvovirus. Virology **148:**121-132.

113. **Parrish, C. R., P. Have, W. J. Foreyt, J. F. Evermann, M. Senda, and L. E. Carmichael.** 1988. The global spread and replacement of canine parvovirus strains. J Gen Virol **69 (Pt 5):**1111-6.

114. **Parrish, C. R., and U. Truyen.** 1999. The evolution of parvoviruses. In: (Domingo, E., Webster, R.G., Holland, J.J., Picknett, T. Eds.), Origin and Evolution of Viruses, Academic Press, London. pp. 421-439.

115. **Pasquale, G. D., B. L. Davidson, C. S. Stein, I. Martins, D. Scudiero, A. Monks, and J. A. Chiorini.** 2003. Identification of PDGFR as a receptor for AAV-5 transduction. Nat Med **9:**1306-12.

116. **Pennick, K. E., M. A. Stevenson, K. S. Latimer, B. W. Ritchie, and C. R. Gregory.** 2005. Persistent viral shedding during asymptomatic Aleutian mink disease parvoviral infection in a ferret. J Vet Diagn Invest **17:**594-7.

117. **Pierson, T. C., D. H. Fremont, R. J. Kuhn, and M. S. Diamond.** 2008. Structural insights into the mechanisms of antibody-mediated neutralization of flavivirus infection: implications for vaccine development. Cell Host Microbe **4:**229-38.

118. **Pletcher, J. M., J. D. Toft, 2nd, R. M. Frey, and H. W. Casey.** 1979. Histopathologic evidence for parvovirus infection in dogs. J Am Vet Med Assoc **175:**825-8.

119. **Ponka, P., and C. N. Lok.** 1999. The transferrin receptor: role in health and disease. Int J Biochem Cell Biol **31:**1111-37.

120. **Qing, K., C. Mah, J. Hansen, S. Zhou, V. Dwarki, and A. Srivastava.** 1999. Human fibroblast growth factor receptor 1 is a co-receptor for infection by adeno-associated virus 2. Nat Med **5:**71-77.

121. **Reed, A. P., E. V. Jones, and T. J. Miller.** 1988. Nucleotide sequence and genome organization of canine parvovirus. J.Virol. **62:**266-276.

122. **Reguera, J., A. Carreira, L. Riolobos, J. M. Almendral, and M. G. Mateu.** 2004. Role of interfacial amino acid residues in assembly, stability, and conformation of a spherical virus capsid. Proc Natl Acad Sci U S A **101:**2724-9.

123. **Riolobos, L., J. Reguera, M. G. Mateu, and J. M. Almendral.** 2006. Nuclear transport of trimeric assembly intermediates exerts a morphogenetic control on the icosahedral parvovirus capsid. J Mol Biol **357:**1026-38.

124. **Ros, C., C. J. Burckhardt, and C. Kempf.** 2002. Cytoplasmic trafficking of minute virus of mice: low-pH requirement, routing to late endosomes, and proteasome interaction. J Virol **76:**12634-45.

125. **Ros, C., M. Gerber, and C. Kempf.** 2006. Conformational changes in the VP1-unique region of native human parvovirus B19 lead to exposure of internal sequences that play a role in virus neutralization and infectivity. Journal of virology **80:**12017-24.

126. **Samulski, R. J., Chang, L-S., Shenk, T.** 1989. Helper-free stocks of recombinant adeno-associated viruses: normal integration does not require viral gene expression. J.Virol. **63: 3822-3828**.

127. **Sanlioglu, S., P. K. Benson, J. Yang, E. M. Atkinson, T. Reynolds, and J. F. Engelhardt.** 2000. Endocytosis and nuclear trafficking of adeno-associated virus

type 2 are controlled by rac1 and phosphatidylinositol-3 kinase activation. J Virol **74:**9184-96.

128. **Seisenberger, G., M. U. Ried, T. Endress, H. Buning, M. Hallek, and C. Brauchle.** 2001. Real-time single-molecule imaging of the infection pathway of an adeno-associated virus. Science **294:**1929-32.

129. **Shackelton, L. A., C. R. Parrish, U. Truyen, and E. C. Holmes.** 2005. High rate of viral evolution associated with the emergence of carnivore parvovirus. Proc Natl Acad Sci U S A **102:**379-384.

130. **Sharma, R., and G. Saikumar.** 2010. Porcine parvovirus- and porcine circovirus 2-associated reproductive failure and neonatal mortality in crossbred Indian pigs. Trop Anim Health Prod **42:**515-22.

131. **Sieczkarski, S. B., and G. R. Whittaker.** 2005. Viral entry. Curr Top Microbiol Immunol **285:**1-23.

132. **Simpson, A. A., V. Chandrasekar, B. Hebert, G. M. Sullivan, M. G. Rossmann, and C. R. Parrish.** 2000. Host range and variability of calcium binding by surface loops in the capsids of canine and feline parvoviruses. J Mol Biol **300:**597-610.

133. **Smith, A. E., and A. Helenius.** 2004. How viruses enter animal cells. Science **304:**237-42.

134. **Smith-Arica, J. R., and J. S. Bartlett.** 2001. Gene therapy: recombinant adeno-associated virus vectors. Curr Cardiol Rep **3:**43-9.

135. **Sollner, T. H.** 2004. Intracellular and viral membrane fusion: a uniting mechanism. Curr Opin Cell Biol **16:**429-35.

136. **Sonntag, F., S. Bleker, B. Leuchs, R. Fischer, and J. A. Kleinschmidt.** 2006. Adeno-associated virus type 2 capsids with externalized VP1/VP2 trafficking domains are generated prior to passage through the cytoplasm and are maintained until uncoating occurs in the nucleus. Journal of virology **80:**11040-54.

137. **Srivastava, A.** 2001. Parvovirus vectors for human gene therapy. Curr Opin Mol Ther **3:**491-6.

138. **Stahnke, S., K. Lux, S. Uhrig, F. Kreppel, M. Hosel, O. Coutelle, M. Ogris, M. Hallek, and H. Buning.** Intrinsic phospholipase A2 activity of adeno-associated virus is involved in endosomal escape of incoming particles. Virology **409:**77-83.

139. **Steinel, A., C. R. Parrish, M. E. Bloom, and U. Truyen.** 2001. Parvovirus infections in wild carnivores. J Wildl Dis **37:**594-607.

140. **Strassheim, L. S., A. Gruenberg, P. Veijalainen, J.-Y. Sgro, and C. R. Parrish.** 1994. Two dominant neutralizing antigenic determinants of canine parvovirus are found on the threefold spike of the virus capsid. Virology **198:**175-184.

141. **Suikkanen, S., M. Antila, A. Jaatinen, M. Vihinen-Ranta, and M. Vuento.** 2003. Release of canine parvovirus from endocytic vesicles. Virology **316:**267-80.

142. **Suikkanen, S., K. Saajarvi, J. Hirsimaki, O. Valilehto, H. Reunanen, M. Vihinen-Ranta, and M. Vuento.** 2002. Role of recycling endosomes and lysosomes in dynein-dependent entry of canine parvovirus. J Virol **76:**4401-11.

143. **Summerford, C., J. S. Bartlett, and R. J. Samulski.** 1999. aVb5 integrin: a co-receptor for adeno-associated virus type 2 infection. Nat Med **5:**78-82.

144. **Sun, J. Y., V. Anand-Jawa, S. Chatterjee, and K. K. Wong.** 2003. Immune responses to adeno-associated virus and its recombinant vectors. Gene Ther **10:**964-76.

145. **Thomas, C. E., T. A. Storm, Z. Huang, and M. A. Kay.** 2004. Rapid uncoating of vector genomes is the key to efficient liver transduction with pseudotyped adeno-associated virus vectors. J Virol **78:**3110-22.

146. **Timpe, J. M., K. C. Verrill, and J. P. Trempe.** 2006. Effects of adeno-associated virus on adenovirus replication and gene expression during coinfection. J Virol **80:**7807-15.

147. **Tresnan, D. B., L. Southard, W. Weichert, J. Y. Sgro, and C. R. Parrish.** 1995. Analysis of the cell and erythrocyte binding activities of the dimple and canyon regions of the canine parvovirus capsid. Virology **211:**123-132.

148. **Truyen, U., M. Agbandje, and C. R. Parrish.** 1994. Characterization of the feline host range and a specific epitope of feline panleukopenia virus. Virology **200:**494-503.

149. **Truyen, U., J. F. Evermann, E. Vieler, and C. R. Parrish.** 1996. Evolution of canine parvovirus involved loss and gain of feline host range. Virology **215:**186-189.

150. **Truyen, U., and C. R. Parrish.** 1992. Canine and feline host ranges of canine parvovirus and feline panleukopenia virus: distinct host cell tropisms of each virus in vitro and in vivo. J Virol **66:**5399-5408.

151. **Tsao, J., M. S. Chapman, M. Agbandje, W. Keller, K. Smith, H. Wu, M. Luo, T. J. Smith, M. G. Rossmann, R. W. Compans, and C. R. Parrish.** 1991. The three-dimensional structure of canine parvovirus and its functional implications. Science **251:**1456-1464.

152. **Tullis, G. E., L. R. Burger, and D. J. Pintel.** 1993. The minor capsid protein VP1 of the autonomous parvovirus minute virus of mice is dispensible for encapsidation of progeny single stranded DNA but is required for infectivity. J. Virol. **67:**131-141.

153. **Tullis, G. E., L. R. Burger, and D. J. Pintel.** 1992. The trypsin-sensitive RVER domain in the capsid proteins of minute virus of mice is required for efficient cell binding and viral infection but not for proteolytic processing in vivo. Virology **191:**846-857.

154. **Van Vliet, K., V. Blouin, M. Agbandje-McKenna, and R. O. Snyder.** 2006. Proteolytic mapping of the adeno-associated virus capsid. Molecular Therapy **14:**809-21.

155. **Van Vliet, K. M., V. Blouin, N. Brument, M. Agbandje-McKenna, and R. O. Snyder.** 2008. The role of the adeno-associated virus capsid in gene transfer. Methods Mol Biol **437:**51-91.

156. **van Weert, A. W., K. W. Dunn, H. J. Gueze, F. R. Maxfield, and W. Stoorvogel.** 1995. Transport from late endosomes to lysosomes, but not sorting of integral membrane proteins in endosomes, depends on the vacuolar proton pump. J Cell Biol **130:**821-34.

157. **Vihinen-Ranta, M., L. Kakkola, A. Kalela, P. Vilja, and M. Vuento.** 1997. Characterization of a nuclear localization signal of canine parvovirus capsid proteins. Eur J Biochem **250:**389-394.

158. **Vihinen-Ranta, M., A. Kalela, P. Makinen, L. Kakkola, V. Marjomaki, and M. Vuento.** 1998. Intracellular route of canine parvovirus entry. J Virol **72:**802-806.

159. **Vihinen-Ranta, M., D. Wang, W. S. Weichert, and C. R. Parrish.** 2002. The VP1 N-terminal sequence of canine parvovirus affects nuclear transport of capsids and efficient cell infection. J Virol **76:**1884-91.

160. **Vihinen-Ranta, M., W. Yuan, and C. R. Parrish.** 2000. Cytoplasmic trafficking of the canine parvovirus capsid and its role in infection and nuclear transport. J Virol **74:**4853-4859.

161. **Vogt, M. R., B. Moesker, J. Goudsmit, M. Jongeneelen, S. K. Austin, T. Oliphant, S. Nelson, T. C. Pierson, J. Wilschut, M. Throsby, and M. S.**

Diamond. 2009. Human monoclonal antibodies against West Nile virus induced by natural infection neutralize at a postattachment step. J Virol **83:**6494-507.

162. **Walters, R. W., M. Agbandje-McKenna, V. D. Bowman, T. O. Moninger, N. H. Olson, M. Seiler, J. A. Chiorini, T. S. Baker, and J. Zabner.** 2004. Structure of adeno-associated virus serotype 5. J Virol **78:**3361-71.

163. **Walters, R. W., S. Yi, S. Keshavjee, K. E. Brown, M. J. Welsh, J. A. Chiorini, and J. Zabner.** 2001. Binding of adeno-associated virus type 5 to 2,3-linked sialic acid is required for gene transfer. J Biol Chem **2766:**20610-2061.

164. **Waner, T., A. Naveh, I. Wudovsky, and L. E. Carmichael.** 1996. Assessment of maternal antibody decay and response to canine parvovirus vaccination using a clinic-based enzyme-linked immunosorbent assay. J Vet Diagn Invest **8:**427-432.

165. **Wang, D., W. Yuan, I. Davis, and C. R. Parrish.** 1998. Nonstructural protein-2 and the replication of canine parvovirus. Virology **240:**273-81.

166. **Weichert, W. S., J. S. Parker, A. T. Wahid, S. F. Chang, E. Meier, and C. R. Parrish.** 1998. Assaying for structural variation in the parvovirus capsid and its role in infection. Virology **250:**106-17.

167. **Willwand, K., A. Q. Baldauf, L. Deleu, E. Mumtsidu, E. Costello, P. Beard, and J. Rommelaere.** 1997. The minute virus of mice (MVM) nonstructural protein NS1 induces nicking of MVM DNA at a unique site of the right-end telomere in both hairpin and duplex conformations in vitro. J Gen Virol **78:**2647-55.

168. **Wobus, C. E., B. Hugle-Dorr, A. Girod, G. Petersen, M. Hallek, and J. A. Kleinschmidt.** 2000. Monoclonal antibodies against the adeno-associated virus type 2 (AAV-2) capsid: epitope mapping and identification of capsid domains involved in AAV-2-cell interaction and neutralization of AAV-2 infection. J Virol **74:**9281-93.

169. **Xiao, W., N. Chirmule, S. C. Berta, B. McCullough, G. Gao, and J. M. Wilson.** 1999. Gene therapy vectors based on adeno-associated virus type 1. J Virol **73:**3994-4003.

170. **Xiao, W., K. H. Warrington, Jr., P. Hearing, J. Hughes, and N. Muzyczka.** 2002. Adenovirus-facilitated nuclear translocation of adeno-associated virus type 2. J Virol **76:**11505-17.

171. **Xiao, X., J. Li, and R. J. Samulski.** 1998. Production of high-titer recombinant adeno-associated virus vectors in the absence of helper adenovirus. J Virol **72:**2224-32.

172. **Xie, Q., W. Bu, S. Bhatia, J. Hare, T. Somasundaram, A. Azzi, and M. S. Chapman.** 2002. The atomic structure of adeno-associated virus (AAV-2), a vector for human gene therapy. Proc Natl Acad Sci U S A **99:**10405-10.

173. **Xie, Q., and M. S. Chapman.** 1996. Canine parvovirus capsid structure, analyzed at 2.9 Å resolution. J Mol Biol **264:**497-520.

174. **Yan, Z., R. Zak, G. W. Luxton, T. C. Ritchie, U. Bantel-Schaal, and J. F. Engelhardt.** 2002. Ubiquitination of both adeno-associated virus type 2 and 5 capsid proteins affects the transduction efficiency of recombinant vectors. J Virol **76:**2043-53.

175. **Yuan, W., and C. R. Parrish.** 2001. Canine parvovirus capsid assembly and differences in mammalian and insect cells. Virology **279:**546-557.

176. **Zabner, J., M. Seiler, R. Walters, R. M. Kotin, W. Fulgeras, B. L. Davidson, and J. A. Chiorini.** 2000. Adeno-associated virus type 5 (AAV5) but not AAV2 binds to the apical surfaces of airway epithelia and facilitates gene transfer. J Virol **74:**3852-3858.

177. **Zadori, Z., J. Szelei, M.-C. Lacoste, P. Raymond, M. Allaire, I. R. Nabi, and P. Tijssen.** 2001. A viral phospholipase A2 is required for parvovirus infectivity. Developmental Cell **1:**291-302.

178. **Zhong, L., W. Li, Y. Li, W. Zhao, J. Wu, B. Li, N. Maina, D. Bischof, K. Qing, K. A. Weigel-Kelley, I. Zolotukhin, K. H. Warrington, Jr., X. Li, W. B. Slayton, M. C. Yoder, and A. Srivastava.** 2006. Evaluation of primitive murine hematopoietic stem and progenitor cell transduction in vitro and in vivo by recombinant adeno-associated virus vector serotypes 1 through 5. Hum Gene Ther **17:**321-33.

179. **Zhong, L., W. Zhao, J. Wu, B. Li, S. Zolotukhin, L. Govindasamy, M. Agbandje-McKenna, and A. Srivastava.** 2007. A dual role of EGFR protein tyrosine kinase signaling in ubiquitination of AAV2 capsids and viral second-strand DNA synthesis. Mol Ther **15:**1323-30.

CHAPTER 2: EARLY STEPS IN CELLULAR INFECTION BY PARVOVIRUSES: HOST-SPECIFIC DIFFERENCES IN RECEPTOR BINDING BUT SIMILAR ENDOSOMAL TRAFFICKING

Modified from: **Harbison C.E., Lyi S.M., Weichert W.S., Parrish CR.** 2009. Early steps in cell infection by parvoviruses: host-specific differences in cell receptor binding but similar endosomal trafficking. J Virol. **83**(20): 10504-14. With permission.

2.1 Abstract

Canine parvovirus type 2 (CPV) and feline panleukopenia virus (FPV) are closely related parvoviruses that differ in their host ranges for cats and dogs. Both viruses bind their host transferrin receptor (TfR), enter cells by clathrin-mediated endocytosis, and traffic with that receptor through endosomal pathways. Infection by these viruses appears to be inefficient and slow, with low numbers of virions initiating replication only several hours after cellular entry. Species-specific binding to the TfR controls viral host range, and in this study FPV and different antigenic variants of CPV differed in the level of cell attachment, uptake, and infection in canine and feline cells. During infection, CPV particles initially bound and trafficked passively on the filopodia of canine cells, while they bound to the cell body of feline cells. That binding was specifically associated with the TfR as it was disrupted by the addition of anti-TfR antibodies. Capsids were taken up from the cell surface with different kinetics in canine and feline cells, but unlike the cycle with the cellular TfR ligand, transferrin, most capsids did not recycle back to the cell surface. The intracellular trafficking of fluorescently-labeled virus was examined and capsids were found to enter Rab5-, 7-, or 11-positive endosomal compartments within minutes of uptake. Constitutively active (CA) or dominant negative (DN) Rab mutants changed the intracellular distribution of capsids and affected the infectivity of virus in cells.

2.2 Introduction

Cellular infection by animal viruses involves a specific sequence of steps that deliver the virus and its genome from the cell surface to the compartment where replication can occur. For non-enveloped viruses, infection initiates with binding to a

specific viral receptor and uptake into the cell by receptor-mediated endocytosis. Various factors can control the process of viral uptake, including the signaling and endocytic properties of the receptor(s) bound by the virus, the affinity of the virus for the receptor, and the structural features of the interaction in different environments (36, 61). Receptors may be located on the cell body and/or may be displayed on the extended lamellipodia or filopodia that markedly increase the surface area of the cell. Viruses binding to filopodia can be either passively delivered to the cell body for endocytosis by dynamic movement of the entire structure or may be actively trafficked along the actin filaments that support the filopodia by retrograde actin transport or the action of myosin-2 motors (32, 57). Cross-linking and clustering of receptors by viral particles can influence the rate of endocytosis, and many viral receptors activate signaling pathways in this manner to alter the structure of the underlying cytoskeleton and enhance uptake (12, 30, 51). Once endocytosed, receptor-bound viruses are enclosed within vesicles and are trafficked within the endosomal pathways of the cell, where they may undergo structural alterations upon exposure to conditions such as low pH or proteases (36, 61). The specific receptor-mediated binding and entry pathways used by viruses often provide signals that trigger endosomal escape and allow the virus to establish infection.

Markers for variety of endosomal compartment have been used in studies of viral entry. For example, Rab proteins are monomeric small GTPases that regulate endosomal membrane trafficking, and specific Rab proteins are associated with individual endosomal compartments. Among the many Rab proteins that have been described, Rab5 is primarily associated with the early endosome and regulates trafficking through that compartment, Rab7 is associated with the late endosome, and

Rab11 is associated with the recycling endosome (14, 58). Tracking viral particles as they move through the endosomal system has been used to define the steps in the entry and infection processes of a variety of different viruses, and has revealed many of the common features and variant processes that are used (7-9, 33, 71).

Here we examine the uptake and infection of cells by parvovirus capsids, and compare some of the steps followed by capsids that differ in their receptor binding properties and host ranges. Feline panleukopenia virus (FPV) infects cats (50, 66), binds the transferrin receptor-1 (TfR) on feline cells, and uses that receptor for uptake and infection (27, 44). FPV does not bind the canine TfR, and does not infect dogs or cultured canine cells. Canine parvovirus type 2 (CPV) is a natural variant of FPV that emerged in 1978 after acquiring a small number of mutations that allow its capsid to bind the canine TfR (27). The original strain of CPV (CPV-2) spread worldwide in dogs during 1978, but some of the same mutations that gave it the canine host range rendered it unable to infect cats (66, 67). The original CPV-2 strains were replaced worldwide during 1979 and 1980 by a natural variant, CPV type-2a (CPV-2a), which contained an additional 4 to 5 changes in the VP2 coat protein (48, 49). Subsequently, the canine viruses have continued to evolve, and additional single mutations have been selected that further altered antigenic epitopes. In particular, strains altered at VP2 residue 426 are designated CPV-2b (Asn426Asp) and CPV-2c (Asp426Glu)(13, 48). CPV-2a and its variants are able to infect both dogs and cats, but show reduced binding to the feline TfR on cells and in vitro (27, 42). In addition, the affinity of binding to the canine TfR is much lower than that seen for the feline TfR (42).

The TfR is a type II membrane protein expressed in non-lipid raft regions of the

plasma membrane, and it facilitates iron uptake into cells by binding iron-loaded (holo) transferrin (Tf) at the neutral pH of the extracellular environment (2). TfR expression is tightly regulated and it is more highly expressed on dividing cells with high iron needs, which is advantageous for these viruses as they require cellular S phase for replication. The TfRs of mice and humans are also used as receptors for cell infection by other viruses, including the mouse mammary tumor virus and the New World hemorrhagic fever arenaviruses, respectively (52, 56).

The TfR is assembled as a homodimer on the surface of the cell, and each monomer of the ectodomain is composed of protease-like, apical, and helical domains, as well as a 30Å membrane-proximal stalk (5, 20, 31). The transmembrane domain mediates membrane insertion and influences some aspects of trafficking within the cell, while the short cytoplasmic domain contains a tyrosine-threonine-arginine-phenylalanine (YTRF) sequence that engages the clathrin-mediated endocytic machinery through adaptor protein-2 (AP-2) (53, 55). The TfR cytoplasmic sequence also includes one or two cysteines adjacent to the inner leaflet of the membrane that may be palmitoylated to influence the rate of receptor recycling, and contains sequences that control basolateral localization in polarized cells (41). In the normal pathway of TfR-mediated entry, the TfR-holoTf complex is transported into the endosomal system where low pH results in Tf conformational changes and iron release. A subset of the TfR-(iron free) apoTf complexes are rapidly recycled to the cell surface from the early endosome to release the apoTf, but a higher percentage passes through the perinuclear recycling endosome, remaining intracellular for a slightly longer period of time (21, 22, 24, 37, 38, 69, 70). The rate of uptake and the efficiency of TfR recycling

depend on the form of the ligand, and more than 97% of monomeric Tf recycles to the

cell surface within 10-30 minutes regardless of the intracellular pathway taken.

However, crosslinking TfRs with oligomeric Tf or antibodies causes the complexes to be

retained within endosomes for longer periods and a higher proportion to be trafficked to

late endosomes and lysosomes for degradation (35).

While holoTf binds the membrane proximal side of the feline and canine TfR

ectodomain (11), mutational analysis of the receptor has identified the importance of the

apical domain for binding FPV and CPV capsids (43). The feline and canine TfRs differ

in ~10% of their sequences, but the major difference controlling the CPV specific

binding is a unique glycosylation site in the apical domain of the canine TfR (43).

Alteration of the glycosylated Asn to Lys (the feline TfR residue) on the canine TfR

background allowed FPV to bind, and also greatly increased the affinity of binding by

CPV-2 and CPV-2a-related capsids (42).

CPV and FPV have small (25nm) non-enveloped icosahedral capsids that

package a single stranded DNA genome of ~5,120 bases (68). The particles are made

up of two overlapping proteins, VP1 and VP2, with 90% of the capsid protein being VP2.

VP1 contains a 143 residue amino (N)-terminal sequence that encodes phospholipase

A_2 (PLA-2) enzymatic activity, as well as basic amino acid motifs that play a role in

nuclear localization (72). The VP1 unique region becomes exposed during cell entry

without capsid disintegration, and the PLA-2 activity likely plays a role in endosomal

escape by modifying the endosomal membrane (19, 76).

Previous studies of cell entry by CPV, minute virus of mice (MVM), and various

adeno-associated viruses (AAVs) show that viral uptake primarily occurs through

clathrin-mediated endocytosis. However, when the AP-2 interacting sequences in the cytoplasmic tail of the feline TfR are mutated or deleted, the variant receptor still allows CPV infection at similar efficiency to wild type TfR (26). The intracellular pathways of viral entry and trafficking have been examined in cells fixed at various times after uptake followed by antibody staining for virus and cellular markers. Time courses examined were between one and six hours, and sequential steps of trafficking were suggested whereby the virus passed from the early endosomes to the recycling endosome, with localization in late endosomes and lysosomes only at later time-points (65). By specific anti-VP1 fluorescent antibody staining, VP1 N terminus release was only observed several hours after uptake, possibly in a low pH degradative compartment (64, 72). In addition, CPV capsids appeared to remain associated with the receptor for up to four hours after virus uptake, as antibodies against the TfR cytoplasmic tail microinjected into feline CRFK cells blocked infection in this time period (73). Neutralizing the low pH of the endosomal system with ammonium chloride or Bafilomycin A1 also blocked infection, although it is not clear whether this was due to direct effects on the capsid or to indirect, global alterations on the cellular endosomal system. Evidence has also been found to suggest that the capsid undergoes only minor structural rearrangement as it passes through the intracellular environment. When the X-ray crystal structures of capsids of CPV and FPV were determined at low pH, in the presence of EDTA, or following digestion by a panel of proteases, only small changes in the orientation of surface loops on the viral capsid were observed (40, 60).

Here we used microscopy to examine the dynamic steps of binding, uptake, and early trafficking by parvovirus capsids in live canine and feline cells. Labeled capsids

were seen to undergo rapid dissemination into multiple endosomal compartments within minutes of cellular attachment. Initial binding of CPV to canine cells involved filopodia, while in feline cells the virus bound primarily to receptors located on the cell body. In cells expressing green fluorescent protein (GFP)-conjugated Rab proteins to label different endosomal compartments, co-localization of viral particles with Rab5, 7, and 11-positive endosomes was readily observed, and virions gradually accumulated near the microtubule organizing center (MTOC) over 20-45 minutes. The distribution of intracellular viruses in feline cells was altered by expression of either constitutively active (CA) or dominant negative (DN) mutants of the Rab proteins. DN Rab5 and Rab7 and CA Rab5 inhibited infection, providing evidence for the importance of these compartments in the infectious pathway of parvoviruses.

2.3 Materials and methods

2.3a Cells and viruses

Feline Crandall-Rees feline kidney (CRFK) and Norden laboratory feline kidney (NLFK) cells, and canine A72 and Cf2Th cells, were grown in a 1:1 mixture of McCoy's 5A and Liebovitz L15 (MCC/L15) media containing 5% fetal bovine serum. Chinese hamster ovary (CHO)-derived cells lacking the hamster TfR (TRVb cells) (39) were grown in Ham's F12 medium containing 5% fetal bovine serum.

Viruses were derived from infectious plasmid clones of FPV (FPV-b), CPV-2 (CPV-d), and CPV-2b (CPV-39) strains (27, 47). Plasmids were transfected into NLFK cells and the viruses recovered titrated using $TCID_{50}$ assays (46). Virus capsids were concentrated by polyethylene glycol precipitation followed by sucrose gradient centrifugation, then dialyzed against either PBS or 20 mM Tris-HCl (pH 7.5) and stored

at 4ºC (1, 40).

2.3b Fluorescent markers and ligands, fluorescence microscopy, and intracellular localization

Rab5, Rab11, and Rab7 genes with green fluorescent protein (GFP) fused to the N-termini were obtained from Craig Roy, Yale University, or in some cases prepared by site-directed mutagenesis. Constitutively active mutants included Rab5-Q79L, Rab7-Q67L, Rab11-Q70V, and dominant negative mutants were Rab5-S34N, Rab7-T22N, and Rab11-S25N. Cells were transfected with plasmid DNA using Lipofectamine (Invitrogen, San Diego, CA), and 2 days later were seeded in culture dishes with coverslip inserts for imaging (MatTek, Ashland, MA).

Canine Tf (Sigma, St. Louis, MO) was iron loaded as previously described (4). Purified CPV capsids, FPV capsids, or canine Tf were labeled with Alexa-488, Alexa-594, or Alexa-647 dyes (Invitrogen) at 20% of the recommended concentrations for 30 minutes at 20°C (27). The labeled capsids or Tf were dialyzed against 0.2M phosphate buffered saline at pH 8.2, passed through a P10 gel filtration column (Millipore, Billerica, MA), and stored at 4°C. Capsids were examined by fluorescence microscopy to ensure single particle labeling, and images collected were analyzed with ImageJ software (US National Institutes of Health, Bethesda, MD).

2.3c Virus or Tf cell binding, uptake, and recycling

Cells were incubated at 37°C for five minutes with either labeled capsids or Tf, then the media was replaced with phenol-red free Dulbecco's Modified Eagle Medium (DMEM) and the cells were observed at various time points as indicated using a 37°C

100x-oil lens and time-lapse imaging. Images were collected with a Hamamatsu OrcaER CCD camera, with different labels collected sequentially as separate channels. Images were analyzed using SimplePCI software (Hamamatsu, Sewickley, PA). Co-localization of virions with endosomal markers was determined with ImageJ software, and particle tracking was performed using the ImageJ manual tracker plugin (Institut Curie, Orsay, Fr). Confocal images were obtained using a Zeiss LSM510 microscope, and images were prepared and analyzed using the Zeiss ZEN 2008 software.

As indicated, Alexa-488-labeled actin from rabbit muscle (Molecular Probes, Eugene, OR) was injected into cells at a concentration of 1 mg/ml using an Eppendorf injector and micromanipulator. Cells were incubated at 37°C for 60 minutes to allow actin diffusion and incorporation into cellular structures, then Alexa-594 labeled CPV-2 capsids were added and visualized as described above.

To determine the specific role of the TfR in virus or Tf binding to the cells, antibodies against the cytoplasmic tail or the ectodomain of the receptor were used. Antibody H68.4 (Zymed, South San Francisco, CA), recognizing the cytoplasmic tail of the TfR, was injected into cells using an Eppendorf microinjector and micromanipulator 30 minutes prior to incubating the cells with virus or Tf. Rabbit antibodies prepared against the extracellular domain of the receptor were prepared from peptide 559 to 571 of human TfR conjugated to Keyhole limpet hemocyanin as previously described, and were used for receptor visualization in this experiment (42).

The amount of cell-associated Alexa-488-labeled virus or Alexa-647-labeled Tf was quantified with a FACScalibur flow cytometer and Cell Quest software (Becton-Dickinson, San Jose, CA). Cells cultured in 10 cm_2 dishes overnight were incubated with

10 µg/ml labeled ligand for one hour at 37°C. After two washes in Hank's buffered saline solution without Mg^{2+} or Ca^{2+} (HBSS), cells were detached using 1mM Ethylenediaminetetraacetic acid (EDTA) in HBSS on ice, then fixed with 4% paraformaldehyde (PFA) in phosphate buffered saline (PBS) prior to analysis. One and two tailed Student's t tests were performed to assess the differences between the geometric mean fluorescence intensity levels (MFI) after background subtraction.

To examine the recycling of capsids or Tf, Alexa-488-labeled virus or Alexa-647-Tf was bound to CRFK or Cf2Th cells on ice for 30 minutes. The cells were washed and warmed to 37°C in fresh media and the relative amounts of cell-associated capsids or Tf determined at various times of incubation using flow cytometry as above.

2.3d Cell infection assays and relative infectivity

Fifty percent tissue culture infectious dose ($TCID_{50}$) titers were determined for freshly prepared stocks of the FPV, CPV-2, and CPV-2b strains of virus in CRFK and Cf2Th cells as previously described (46). The viral single stranded DNA in each inoculum was determined by quantitative polymerase chain reaction (qPCR) using a SYBRGreen-labeled probe (Applied Biosystems, Foster City, CA), and was standardized using known samples of the cloned CPV-2 genome. Student's t tests and paired t tests were used where indicated to examine the differences between the $logTCID_{50}$/genome for the different viruses.

2.3e Time course of infection

The rate of virus uptake was determined by measuring the infectivity in cells treated with neutralizing rabbit anti-CPV antiserum added at various times after

inoculation (45). Cells seeded at 2x 10^4 cells/cm^2 were incubated with virus inocula

diluted in DMEM with 0.1% BSA for 30 minutes on ice. The cells were cultured at 37°C

in growth media, and at the times indicated medium containing 1:1000 dilution of rabbit

anti-CPV serum was added. Cells were fixed after 24 hours with 4% PFA and stained

with an anti-NS1 antibody (CE10) (75) and an Alexa-488-labeled goat anti-mouse IgG

secondary antibody (Sigma).

2.4 Results

2.4a Cell binding levels

Purified full CPV-2, FPV, and CPV-2b capsids were labeled with Alexa dyes at a ratio of

five to 12 dye molecules per capsid. Microscopy analysis showed an even distribution of

apparently single particles with similar levels of labeling (Figures 2.1A and B), and the

capsids banded on sucrose gradients at the positions expected for full particles (results

not shown). In general the labeled capsids showed similar overall patterns of cell

binding and entry to those reported for unlabeled capsids examined after fixing and

antibody staining, but allowed superior spatial resolution of individual capsids (65).

Furthermore, the labeled capsids had similar levels of infectivity (data not shown). The

amount of labeled viruses binding to canine or feline cells depended on the specific

combination of virus strain and host cell used (Figure 2.1). All viruses bound and

entered feline cells (Figure 2.1C), though to different levels, and the level of cellular

association was similar to that seen for unlabeled viruses detected by antibody staining

(27). Although CPV-2 and CPV-2b both bound to canine cells, the level of cell-

associated CPV-2b observed was close to background levels, likely due to the low

affinity of this interaction (Figures 2.1D and H) (42). Feline cells bound and endocytosed

CPV-2 and CPV-2b capsids to 3.5- and 5 -fold higher levels, respectively, than canine

cells (Figures 2.1G and H). Comparisons between different viral strains showed that

CPV-2 capsids bound to ~10-fold higher levels than did CPV-2b in all cell lines tested

(Figures 2.1C, D, and I). In feline cells, FPV had an intermediate level of binding and

uptake compared to the two CPV strains (Figure 2.1C). These differences were not

related to the levels of TfR expression, as both the CRFK and Cf2Th cells bound

equivalent amounts of canine Tf, while the TfR-negative TRVb cells bound neither virus

nor Tf (Figures 2.1E and J).

Figure 2.1. Analysis of Alexa594-labeled CPV-2 full capsids by fluorescent microscopy. A and B) Diluted virus was sandwiched between 2 coverslips and imaged with a 100x oil lens. Panel B shows the fluorescence intensity associated with the particles shown in (A). C to E) Quantitative association of labeled capsids with canine or feline cells was determined by flow cytometry. The amount of FPV, CPV-2, or CPV-2b that was bound and taken up into (C) feline CRFK cells or (D) canine Cf2Th cells after 1 hour at 37°C. E) Canine Tf was incubated with canine and feline cells under the same conditions as in (C and D). Untransfected TRVb cells not expressing TfR were used as a negative control for all assays. F to H) The same data are represented to allow comparison between binding and uptake of (F) FPV, (G) CPV-2, and (H) CPV-2b capsids in feline or canine cells. I and J) The mean and standard deviation from three independent experiments of the background-subtracted median fluorescence intensities, showing binding and uptake levels of the three viruses or canine Tf. (*=p< 0.05); significant differences between groups.
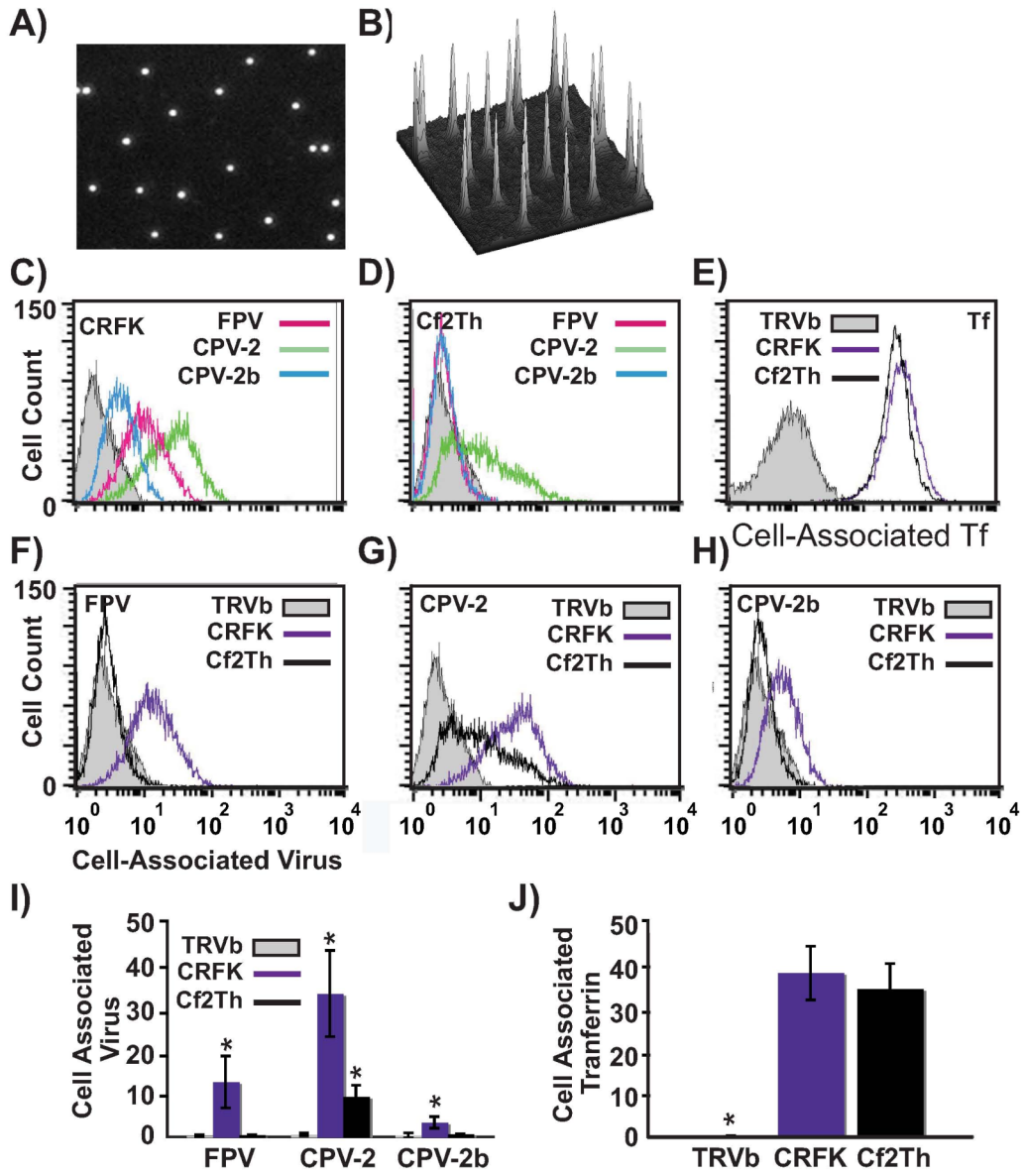
2.4b Infectivity of viruses in canine and feline cells

The relative infectivity of FPV, CPV-2 and CPV-2b, determined as log $TCID_{50}$/genome, varied depending on the species of cell line tested (Figure 2.2). Two canine (Cf2Th and A72) and two feline (NLFK and CRFK) cell lines were tested with two separately prepared inoculums of each virus, and similar patterns were seen for each host type. Data from one inoculum in one cell line per species is shown in Figure 2.2. CPV-2 had equal infectivity in canine and feline cells, while FPV and CPV-2b were significantly more infectious in feline than canine cells. About 1×10^5 virions per cell were needed to infect CRFK cells, with no significant differences in infectivity between the three viral strains. CPV-2 was up to 100-fold more infectious than CPV-2b on a per-genome basis in Cf2th canine cells, while FPV showed only background levels of infection in those cells.
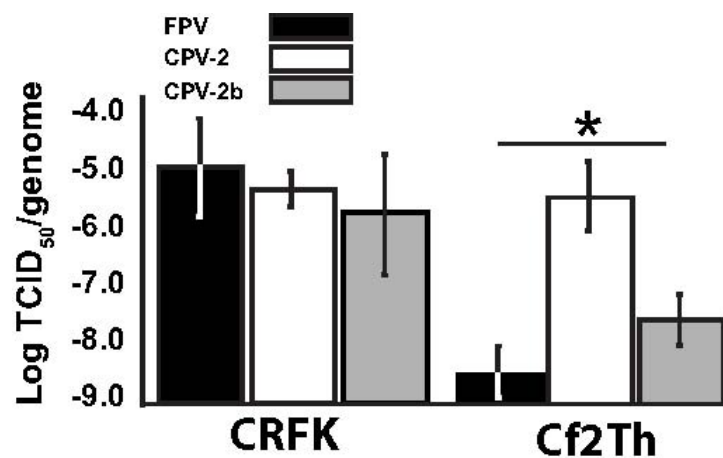
Figure 2.2. Relative infectivity of FPV, CPV-2, or CPV-2b in feline CRFK and canine Cf2Th cells. The mean log $TCID_{50}$/genome +/- 1 standard deviation from three independent experiments is shown (*=p< 0.05).

2.4c Uptake from the cell surface

In order to determine the rate of uptake from the surface of feline and canine cells, neutralizing antibodies were added to the extracellular medium at various times after virus addition, and the residual percentage of infection was compared to a control well with no antibody added. The infecting viruses were rapidly endocytosed into feline cells, and thus quickly acquired resistance to neutralization, with CPV-2 infection levels reaching 50% of control when the antibodies were added 10 minutes or more after virus addition. The uptake into canine cells was slower, taking 45 minutes to reach 50% protection of the virus (Figure 2.3).
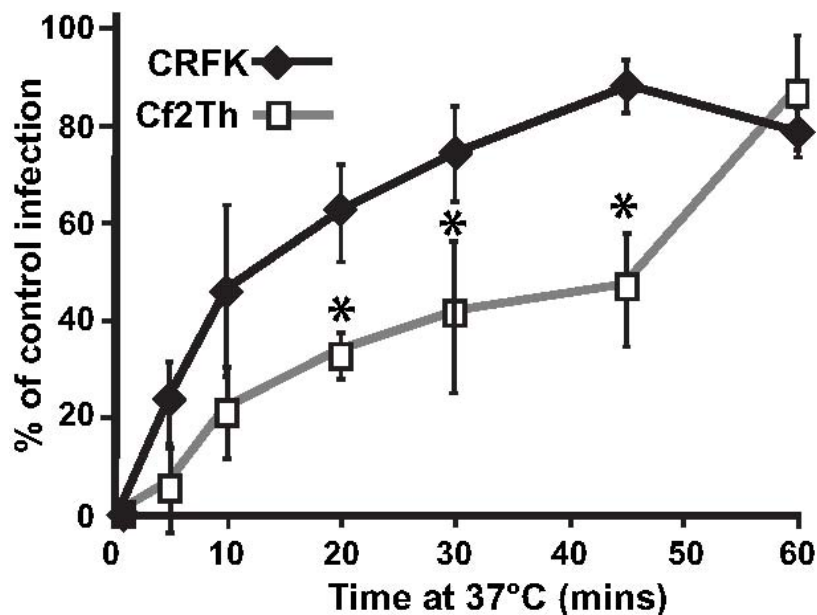
Figure 2.3. Kinetics of uptake and infection of CPV-2 in feline and canine cells. The percentage of infecting virus that resisted antibody neutralization at various times after virus binding to feline CRFK or canine Cf2th cells was compared to control infections where no antibody was added. (* = $p < 0.05$; significant differences between feline and canine cells).

Fluorescence microscopy was used to follow the capsids into cells, and a clear difference was seen in the surface distribution of labeled capsids on canine versus feline cells. When incubated with feline CRFK cells, CPV-2 (Figure 2.4A) and CPV-2b (data not shown) capsids bound and were taken up uniformly over the cell surface. In contrast, lower levels of CPV-2 or CPV-2b particles bound to canine cells, and during time points between five and 15 minutes at 37°C many capsids could be observed associating with filopodia rather than the main cell body (Figure 2.4B (CPV-2b data not shown)). Under the same conditions, Alexa-594-Tf bound evenly over both the feline and canine cells (Figures 2.4C and D), indicating that this pattern was not the result of altered receptor distribution.
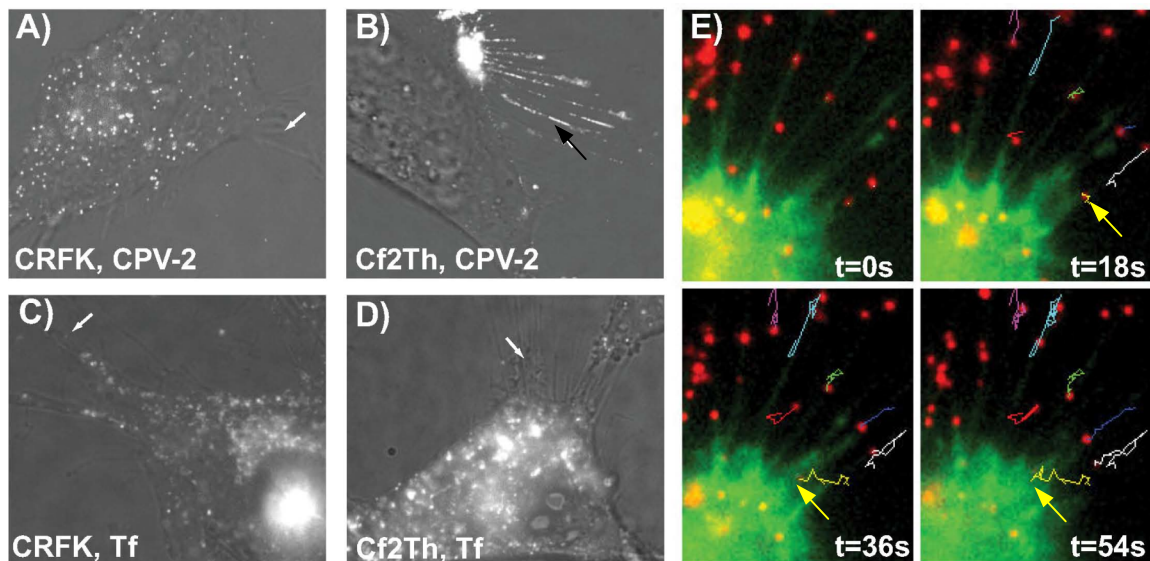
Figure 2.4. Association of CPV-2 with filopodia on canine cells. Alexa-594-labeled capsids were incubated with (A) feline or (B) canine cells for five minutes at 37°C then immediately observed. Alexa-594-Tf was also incubated with (C) feline and (D) canine cells under the same conditions. The white arrows highlight filopodia without virus or Tf bound, while the black arrow in (B) shows virus concentrating on the filopodia of canine cells. (E) Selected time-lapse frames 18 seconds apart showing CPV-2 particles (red) bound to filopodia of Cf2Th cells containing microinjected Alexa488-conjugated actin (green). The tracks show particle movement on the filopodia; the yellow arrow indicates one particle moving towards the cell at the same rate as filopodial retraction.

Alexa-488-labeled actin was microinjected into canine cells to highlight the cytoskeletal features of the filopodia. The CPV-2 particles bound to the filopodia of injected cells showed mostly random and bidirectional movement (Figure 2.4E), and did not move at the 1.8 to 3.2 μm/minute rate reported in other systems that engage the retrograde actin transport processes (32, 57). Nonetheless, capsids subsequently accumulated at the cell body, perhaps in association with filopodial retraction as this was directly observed in some cases (Figure 2.4E). Within about 10-20 minutes most virus was lost from the filopodia and became localized in intracellular vesicles.

The attachment of virus capsids to filopodia on canine cells was specifically controlled by the surface expression of the canine TfR. Either microinjection of an antibody recognizing the cytoplasmic sequence of the TfR (data not shown) or addition of an antibody against the ectodomain of the TfR to the medium (Figure 2.5), greatly reduced or eliminated the attachment of the virus (Figure 2.5B) to the filopodia and capsid accumulation in the cell cytoplasm compared to the untreated cells (Figure 2.5A). The same treatments reduced but did not eliminate the binding of labeled Tf to the cells (Figures 2.5D) compared to untreated cells (Figure 2.5C), and this result was inferred to be attributable to the greater affinity of Tf for the remaining accessible receptors on the cells.
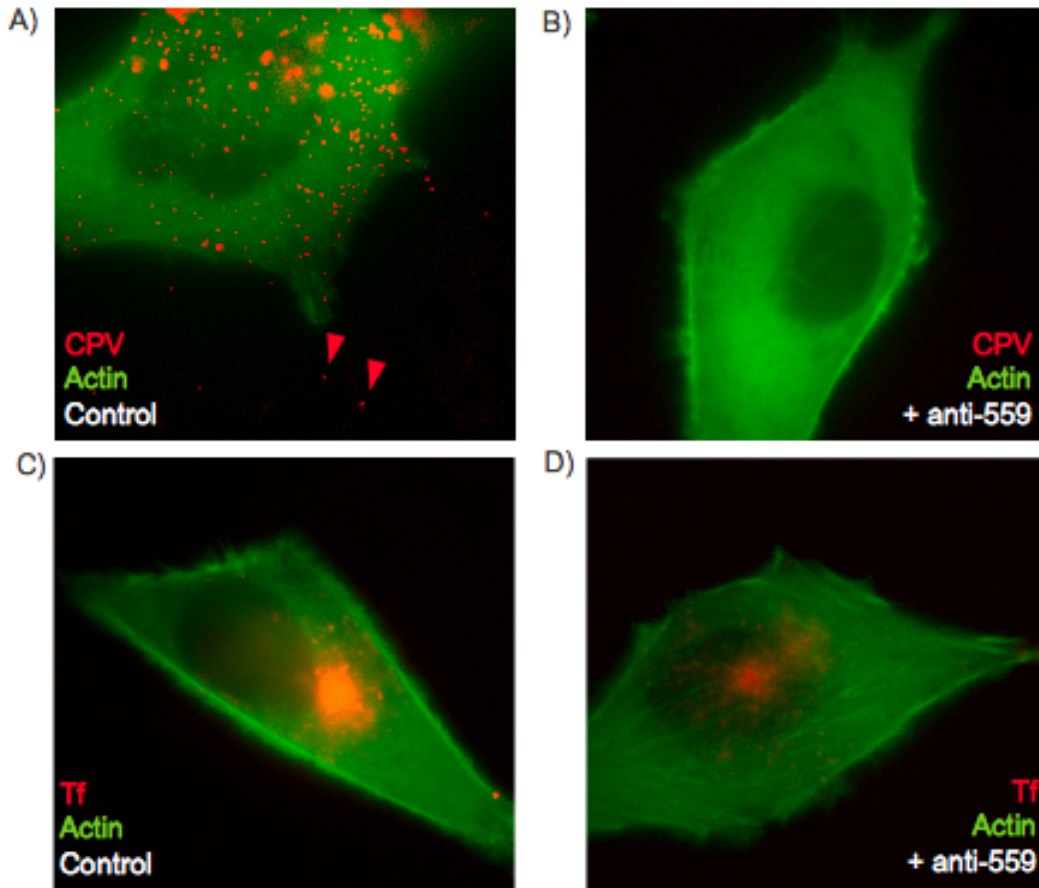
Figure 2.5. Specificity of virus binding to TfR on canine cell filopodia. CPV-2 capsids (A and B) or canine Tf (C and D) are bound and taken up into Cf2Th cells expressing actin-GFP. Addition of rabbit antibody against the TfR ectodomain to the extracellular medium reduces the binding and uptake of CPV-2 capsids (B) or canine Tf (D) to Cf2Th cells. Binding and uptake was performed under the same conditions for the antibody treated (B and D) and untreated cells (A and C). The arrowheads in (A) show individual viral particles binding to the filopodia.

2.4d Endosomal trafficking of Tf and viral capsids

To ensure that expression of the Rab-GFP constructs did not disrupt global endosomal trafficking patterns, we examined uptake and trafficking of Alexa-594-Tf and showed that it followed the endosomal pathways previously reported for the Tf-TfR complexe (63). Tf co-localized with vesicles positive for Rab5-GFP, a marker of the early endosome, within 10 minutes of uptake (Figure 2.6A) and with Rab11-GFP, a

marker of the recycling endosome, by 10 to 15 minutes (Figure 2.6B). Little Tf co-localized with Rab7-GFP, a marker of the late endosome (Figure 2.6C). Recycling in feline and canine cells also had similar dynamics to those described for Tf in human cells, with loss of cell-associated Tf within 20-30 minutes attributable to completion of recycling and release at the cell surface (Figures 2.6D and E) (10, 54). In contrast, the level of labeled virus associated with the cells decreased only slightly over 60 minutes of incubation, indicating either that capsids were retained within the recycling endosome compartment or were diverted into other intracellular pathway(s) (Figures 2.6D and E).

Soon after CPV-2 binding and uptake, particles were found within each of the three Rab-labeled endosomal compartments examined. Capsids co-localized and also showed co-movement with Rab5-GFP-labeled vesicles at the earliest time points imaged (5 minutes after uptake) (Figure 2.7A). At later times, the association with Rab5 decreased, although limited co-localization was still seen after one hour or more, particularly in cells showing high levels of Rab5-GFP overexpression (Figure 2.7B). Expressing the CA Rab5-GFP mutant resulted in the formation of large, ring-shaped, Rab5-positive vesicles within the cells. Virus particles accumulated in those vesicles, and were retained for prolonged periods (up to hours) after uptake. In some cases, particles were associated with the inner wall of the vesicles, while in others they appeared to be released into the lumen (Figure 2.7C). Trafficking patterns of the particles in canine Cf2Th cells expressing Rab5-GFP were similar to those seen in feline cells (Figures 2.7D and E).
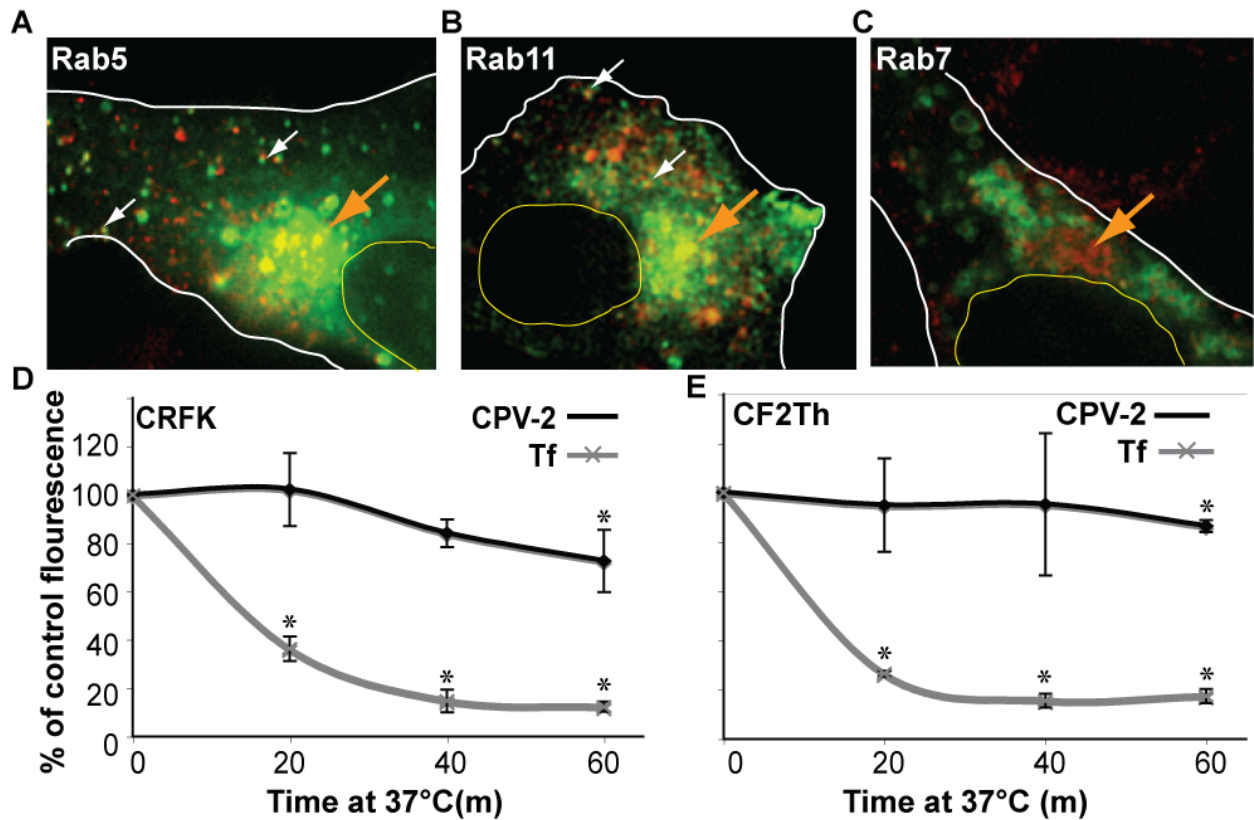
Figure 2.6. Intracellular trafficking of labeled Tf (red) in CRFK cells containing GFP-Rab proteins (green) labeling different endosomal compartments. Co-localization is shown with (A) Rab5 at 20 minutes and (B) Rab11 at 10 minutes after uptake but not with (C) Rab7 (27 minutes after inoculation shown). The large arrow highlights the perinuclear area, smaller vesicles showing co-localization are marked with small white arrows, and the cell body (white line) and nucleus (orange line) are outlined. Retention and/or recycling of capsids or Tf to the cell surface was measured in (D) CRFK or (E) Cf2Th cells by the decrease in the level of fluorescently labeled ligand over time. (*=$p<0.05$); significant differences in the relative level of cell-associated Tf vs. CPV-2.

Figure 2.7. The association of CPV-2 capsids with Rab5-GFP after endocytosis.
Time-lapse frames show the co-localization and co-movement of Alexa594-labeled
capsids with wild type Rab5-GFP in CRFK cells beginning at (A) 15 minutes and (B) 80
minutes after uptake, over the indicated intervals. C) CRFK cells expressing CA Rab5-
GFP contain large vesicles that accumulate CPV-2 capsids; an example time-lapse
series beginning 57 minutes after uptake is shown. (D and E) Rab5-GFP expressed in
(D) Cf2Th or (E) CRFK cells, 15 minutes after virus uptake. Tracks of co-localized
particles and vesicles are shown in A to C, while white arrows highlight co-localization in
D and E.
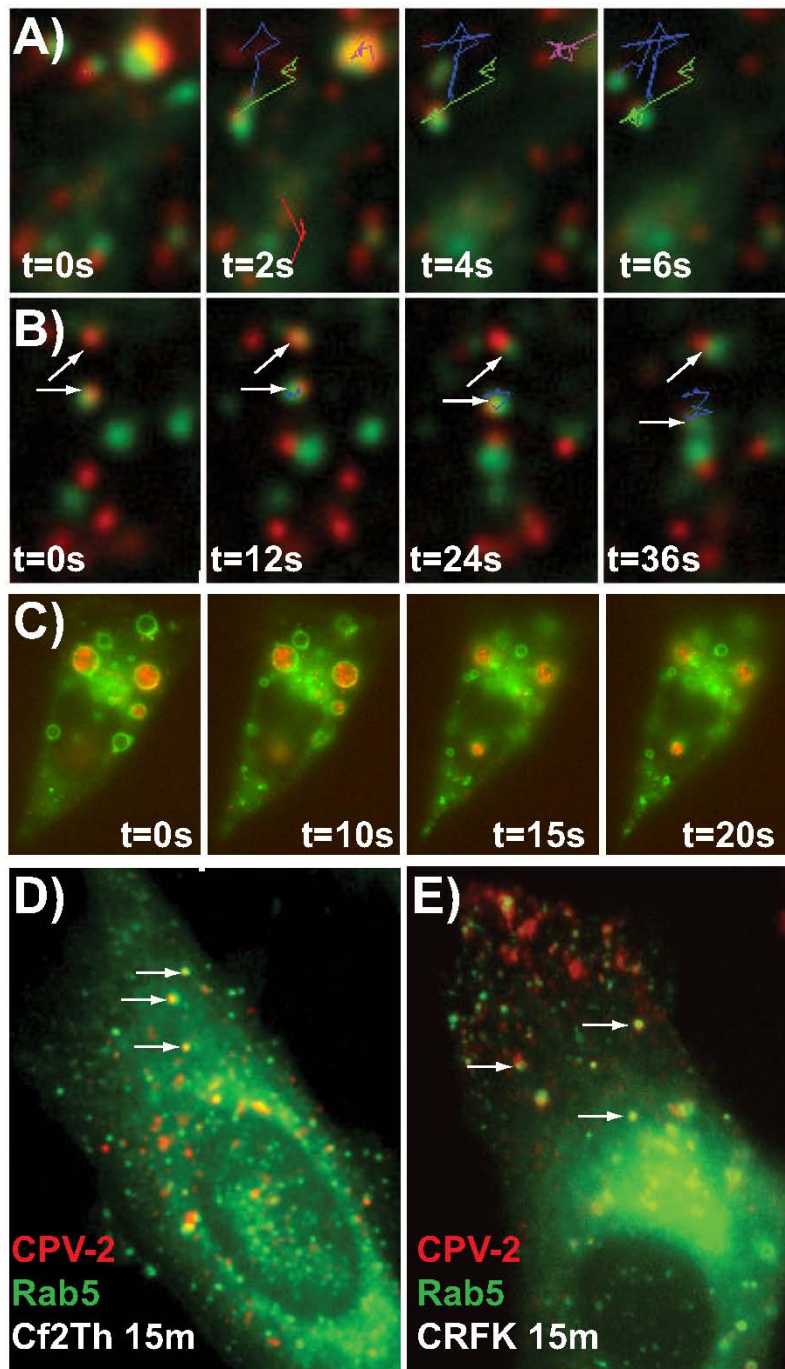
Within 15 to 20 minutes of uptake, virus particles both co-localized and co-moved with Rab11- and Rab7-GFP positive vesicles (Figures 2.8A and B). Movement rates of the virus-containing vesicles varied from stationary to very rapid, and in some cases could not be accurately tracked even at frame rate intervals of 0.2 seconds. Bidirectional movement, most likely on microtubules, was seen for virus-containing vesicles labeled with each of the Rab proteins examined. Within 30 to 45 minutes, the virus-containing vesicles accumulated in a perinuclear location near the microtubule organizing center. The perinuclear area has high concentrations of both Rab11 (Figures 2.8C and D) and Rab7 (Figures 2.8E and F) positive vesicles. In feline cells in particular, co-localization of capsids with particular markers in this section of the cell was difficult even by confocal microscopy (results not shown).
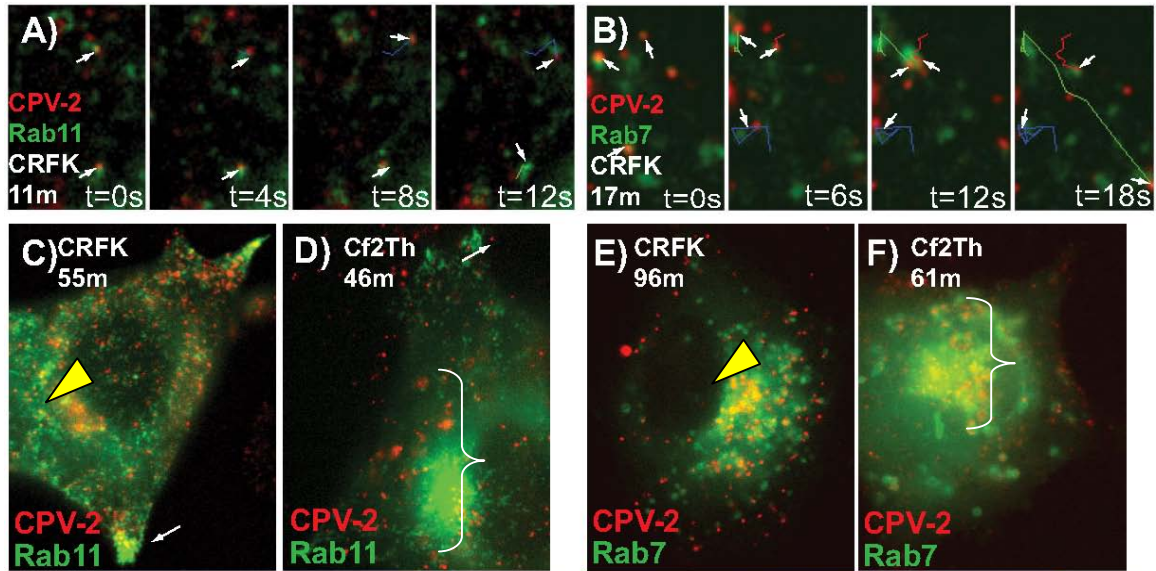
Figure 2.8. Association of CPV-2 particles with Rab11-GFP or Rab7-GFP-positive vesicles in cells after uptake. A and B) Time-lapse frames over indicated intervals of CPV-2 binding to feline CRFK cells expressing (A) Rab11-GFP beginning at 11 minutes and (B) Rab7-GFP beginning 17 minutes after uptake. Co-localization and co-movement of some particles with labeled vesicles are highlighted as individual tracks. C and D) Co-localization of virus with Rab11-GFP after uptake into (C) CRFK cells for 55 minutes or (D) Cf2th cells for 46 minutes after uptake. The white arrows highlight polar accumulations of Rab11-positive vesicles. The yellow arrowhead in C indicates the tight perinuclear accumulation of virus in feline cells, while the white bracket in D shows that this area is relatively more disperse in canine cells. E and F) Co-localization of virus with Rab7-GFP is observable after uptake into both (E) CRFK cells shown at 96 minutes, or (F) Cf2th cells shown at 61 minutes after uptake.

Although viruses rapidly dispersed to multiple compartments after uptake in both feline and canine cells, some differences were seen in the intracellular distribution of virions. First, the patterns of accumulation at the perinuclear area differed. CRFK cells showed a tight accumulation of perinuclear viral particles in vesicles (Figures 2.8C and E, arrowheads), while in Cf2Th cells they clustered more loosely and many endosomes appeared to contain several particles (Figures 2.8D and F, bracketed area). Furthermore, in canine cells co-localization of these particle groups with Rab7-positive vesicles could be more clearly identified than in feline cells.

The pattern of virus association with Rab11 also differed between the two cell types. Clusters of Rab11-positive vesicles were seen near the cell periphery of both cell types (white arrows in Figures 2.8C and D). However, localization of virus within those peripheral or polar vesicles was only seen in feline cells. These results suggest subtle differences in the endosomal trafficking of virions entering different cell types.

Expression of constitutively active (CA) Rab11 (Figure 2.8A) or Rab7 (Figure 2.9B) showed virus co-localization patterns similar to those seen for the wild type Rab proteins. However, as shown in Figure 2.7C, the CA Rab5 disrupted the accumulation of virus at the perinuclear area, and particles were retained within large ring-shaped vesicles. The DN Rab5 had variable effects on intracellular trafficking. Some cells appeared to have similar trafficking patterns as seen with wild-type Rab5, but most cells showed moderate disruption of the perinuclear virus concentration (Figure 2.9C). The DN Rab7 largely prevented perinuclear capsid accumulation, and the virus was displaced to large vesicles dispersed throughout the cell (Figure 2.9D). Finally, expression of DN Rab11 did not appreciably disrupt accumulation of the virus at the perinuclear area (Figure 2.9E), suggesting that virus becomes localized within the late endosome at this location. For CPV-2 capsids, these patterns were similar in both canine and feline cells (data for canine cells not shown). Capsid release into the cytoplasm or nucleus was not readily observed in these studies, and these steps likely represent further bottlenecks in the entry process of parvoviruses (17).
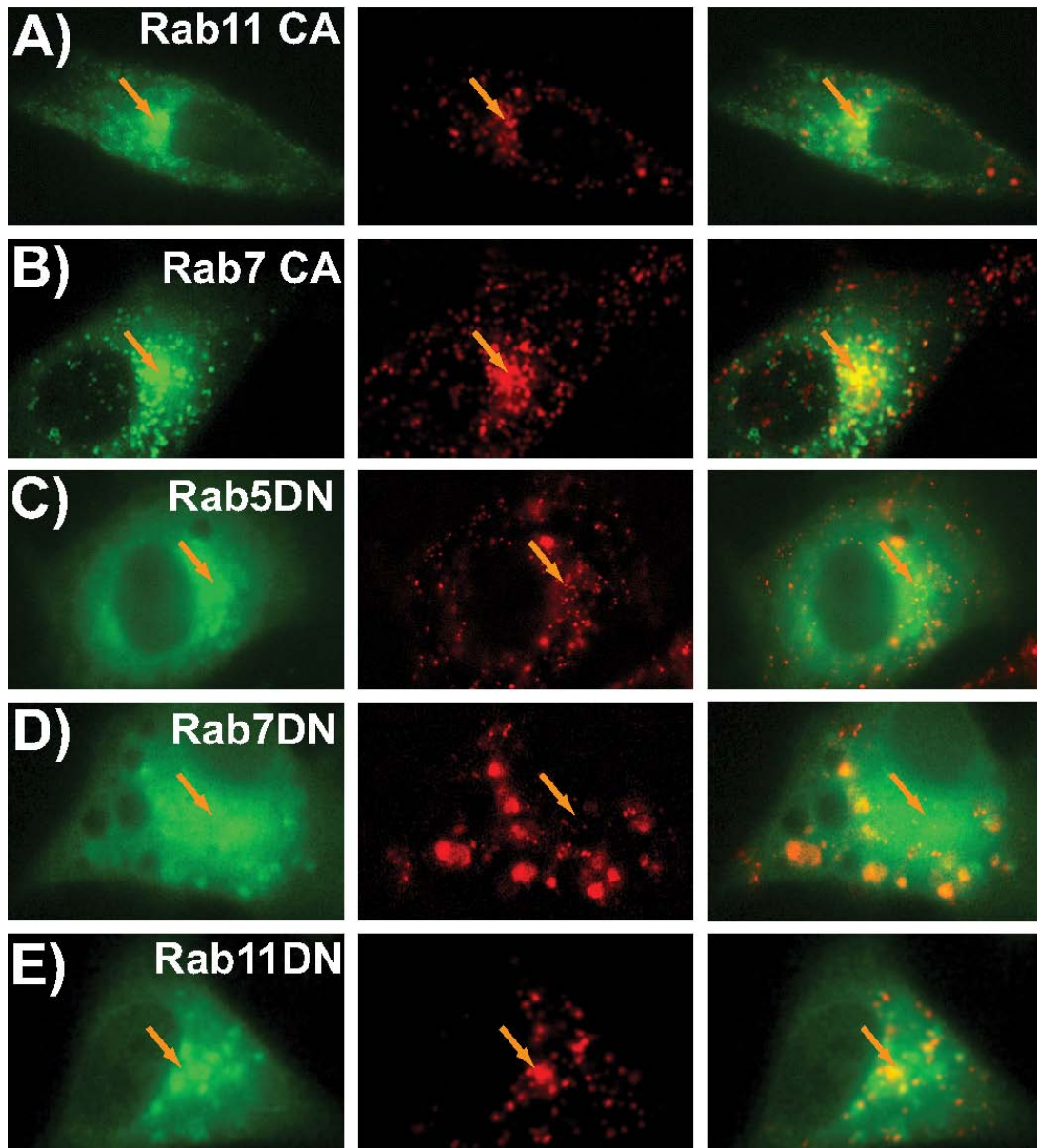
Figure 2.9. Distribution of CPV-2 particles in CRFK cells expressing CA or DN Rab-GFP mutants. The individual Rab-GFP (green) and CPV-2 (red) channels are shown as well as the merged image. A) CPV-2 capsids in cells expressing CA Rab11-GFP 35 minutes or (B) CA Rab7-GFP 39 minutes after uptake, showing similar behavior to wild-type CRFK cells with accumulation of virus capsids at the perinuclear area. C) DN Rab5-GFP at 43 minutes after uptake showing moderate disruption of the perinuclear virus concentration. D) DN Rab7-GFP (shown at 50 minutes after uptake) causes a substantial redistribution of virus-containing vesicles. E) Virus in cells expressing DN Rab11-GFP 59 minutes after uptake, showing that the virus maintains the ability to accumulate at the perinuclear area. Orange arrows highlight the perinuclear area in all cells.

Infection of cells expressing Rab-GFP proteins showed that the presence of wild-type, GFP tagged proteins had little effect on infection rates, except for Rab7 which moderately increased infection (Figure 2.10). Expression of CA and DN Rab11 or DN Rab7 did not significantly affect infection rates, whereas expressing DN or CA Rab5, or DN Rab7, mutants reduced infection by about 50% in the expressing cells.
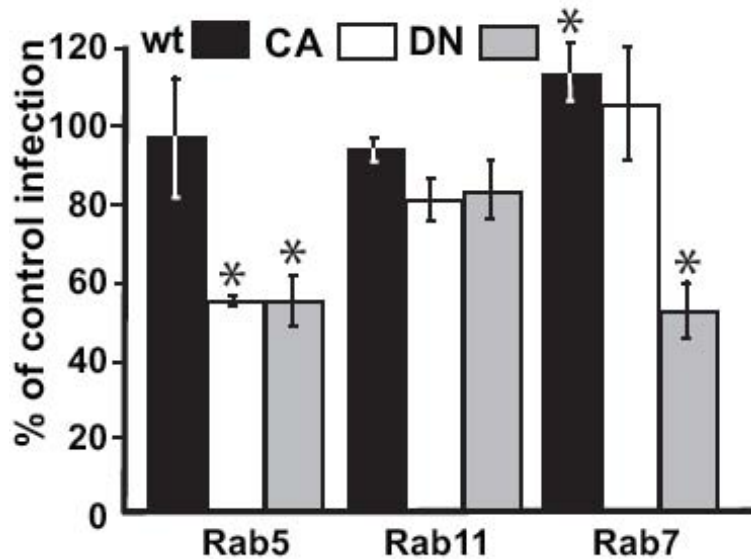
Figure 2.10. The effect of wild type (wt) and CA or DN mutant Rab5-, Rab11- and Rab7-GFP expression on FPV cell infection. Percentage of cells expressing mutant Rab-GFP proteins that became infected by FPV compared to infection rates of non-transfected cells are shown. (*=p<0.05).

2.5 Discussion

Here we examine the TfR-dependent binding, uptake, trafficking, and infection of cells by parvoviruses and show natural differences in the steps involved in feline and canine cells. Parvovirus infection is a complex process; the various parvoviruses that have been examined bind many different receptors and have been reported to follow a variety of different entry pathways with different dynamics (reviewed in 15 and 25). The

live-cell studies contained herein revealed the processes of CPV binding and entry when two distinct versions of the TfR were used. By using live cells and starting to image around five minutes after virus addition, our results illuminated a much more rapid and less linear process of endosomal trafficking than had been previously suggested. Virus particles taken up by the TfR were clearly identified in both recycling and late endosomes as early as 10 to 15 minutes after uptake. Although overexpression of the wild-type Rab proteins through transfection of GFP-conjugated constructs likely perturbed aspects of the endosomal system, the intracellular capsid distribution seen was generally similar to that of cells fixed and stained for endosomal markers, and infection rates in cells expressing those proteins was not reduced. Furthermore, the behavior of Tf in cells expressing wild-type Rab-GFP proteins has been examined in several studies and shows trafficking comparable to that seen in untransfected cells (29, 63). Even when the CA Rab5 is expressed, normal global endocytic trafficking patterns continue with some efficiency despite the generation of abnormal, large, Rab5-positive vesicles (10).

2.5a Binding and endocytosis

Although the levels of TfR expression in feline and canine cells were similar as detected by Tf or antibody binding, CPV capsids bound to canine cells at much lower levels due to their much lower affinity of binding. Furthermore, the infection efficiencies for canine cells differed between the naturally variant CPV strains. The CPV-2a/b variants first emerged in 1979, and these quickly replaced the original CPV-2 in dogs worldwide (48). These antigenically variant viruses differ in their ability to infect and replicate in cats (66), and in their binding properties to feline and canine cells or purified

TfRs *in vitro* (42). Despite these differences, these viruses were seen here to have similar surface and intracellular trafficking patterns.

CPV capsid endocytosis from the surface of canine cells was delayed compared to uptake into feline cells, and this is likely attributable to both the lower affinity of canine TfR binding and the time spent interacting with filopodia before endocytosis. Filopodia are dynamic structures that contain actin bundles covered in membrane and are prominent at the leading edges of mobile cells (28). In tissue culture cells, they present a large surface area and would therefore be of particular benefit for low-affinity binding interactions. The filopodial association observed was not a result of differences in receptor distribution, as labeled canine Tf bound evenly over these cells. Binding and cellular uptake of CPV was confirmed to be specifically associated with the TfR as it was inhibited by the addition of anti-TfR antibodies against either the cytoplasmic tail or the ectodomain (Figure 2.4). These antibodies cross-link the receptor and prevent normal patterns of trafficking and recycling such that they greatly reduce TfR expression on the cell surface (44, 73). Preferential binding of capsids to filopodia has been reported for other viruses, including retroviruses, papillomaviruses, and adeno-associated viruses, and these are actively trafficked to the cell body by retrograde actin flow and/or myosin II acting on actin filaments (3, 32, 57). No consistent directional movement was seen for CPV particles on the filopodia of canine cells, but the bound virions accumulated at the base of these structures and entered the cells, at least in part due to the normal dynamic movement of the filopodia. We saw no evidence that CPV capsids induced the formation of filopodia or modified their behavior (62).

Binding and entry via the cell surface or filopodia allowed similar efficiencies of CPV-2 infection of both feline and canine cells, while lower CPV-2b infection rates were seen in the canine cells. Nonetheless, the efficient endocytosis of viral capsids by the TfR allowed productive entry even for these low-affinity interactions. In previous studies, TfR binding has been shown to provide a structural interaction necessary for infection as replacement of the TfR ectodomain with binding domains of antiviral antibodies allowed attachment and uptake of virus but not infection (26).

2.5b Endosomal trafficking

At the earliest time-points imaged, labeled capsids co-localized with Rab5-positive vesicles. Early endosomes are important in the initial sorting of many cargo molecules into their correct endosomal pathways, and this process depends on both the properties of the ligand and receptor (29, 59). The CA form of Rab5 induces large, ring-like vesicles in cells (10, 16), and a high proportion of the CPV particles in this study were observed to enter these expanded vesicles and remain there for extended periods of one hour or more (Figure 2.7C). Many of these particles remained attached to the wall of the vesicle, most likely due to continued association with the TfR. This observation is in accordance with models showing prolonged receptor interactions and slow intracellular trafficking, and was also supported by experiments where infection was blocked by microinjection of antibodies against the cytoplasmic tail of the TfR up to four hours after inoculation (44). The DN Rab5 also disrupted normal trafficking of the virus to the perinuclear region in many cells, again suggesting that the early endosome is required for correct endosomal trafficking. Reduced infectivity was seen in cells expressing either mutant Rab5 protein.

Virus capsids were localized with both Rab11- and Rab7-positive vesicles by 15 minutes of uptake, displaying a more rapid and complex virus trafficking pattern than had been previously suggested (64, 65). This trafficking was also different from that reported for monomeric Tf. The multivalent icosahedral virus interacting with the dimeric TfR could potentially result in cross-linked TfR-capsid complexes, which would be at least partly diverted into the degradative pathway based on the results of previous studies (35). Even with limited cross-linking, the large size of the virus capsid alone may alter trafficking within the tubular-vesicular endosomal sorting structures (6, 59).

Parvoviruses have been suggested to escape from the endosome along the degradative pathway (18, 34), and this was supported by the finding that expression of DN Rab7-GFP significantly decreased infection. Because the viruses require cell division for genome replication, expression of DN Rab proteins may have globally disrupted the intracellular environment to indirectly inhibit replication. However, the mutants that disrupted the accumulation of virus at the perinuclear area (DN Rab5 and Rab7, but not DN Rab11) showed the largest decreases in infection rates, suggesting a role for this specific trafficking pathway in infection.

The entry of viruses into cells by receptor-mediated endocytosis can involve a variety of pathways, and even within the parvovirus family receptors of many types are used for functional entry. These studies show that these viruses can efficiently use canine and feline TfRs with very different affinities of binding, and can initially follow different routes of uptake from the surface into feline and canine cells that then converge on the same vesicular compartments. This shows that the infection process can accommodate significant flexibility. In the case of CPV-2, binding to the canine TfR

92

resulted in the host range shift from cats to dogs, and subsequent evolution further

modified host range and TfR binding properties. By examining the details of the initial

cellular uptake and trafficking events, we further elucidate the essential properties of the

capsid-receptor interaction and the entry pathways required for cell infection.

2.6 Acknowledgements

2.7 References

1. **Agbandje, M., R. McKenna, M. G. Rossmann, M. L. Strassheim, and C. R. Parrish.** 1993. Structure determination of feline panleukopenia virus empty particles. Proteins **16:** 155-171.

2. **Aisen, P.** 2004. Transferrin receptor 1. Int. J. Biochem. Cell Biol. **36:**2137-2143.

3. **Bantel-Schaal, U., I. Braspenning-Wesch, and J. Kartenbeck.** 2009. Adeno-associated virus type 5 exploits two different entry pathways in human embryo fibroblasts. J. Gen. Virol. **90:**317-322.

4. **Bates, G. W., and M. R. Schlabach.** 1973. The reaction of ferric salts with transferrin. J. Biol. Chem. **248:**3228-3232.

5. **Bennett, M. J., J. A. Lebron, and P. J. Bjorkman.** 2000. Crystal structure of the hereditary haemochromatosis protein HFE complexed with transferrin receptor. Nature **403:**46-53.

6. **Bishop, N. E.** 2003. Dynamics of endosomal sorting. Int. Rev. Cytol. **232:**1-57.

7. **Brandenburg, B., L. Y. Lee, M. Lakadamyali, M. J. Rust, X. Zhuang, and J.M. Hogle.** 2007. Imaging Poliovirus Entry in Live Cells. PLoS Biol. **5:**e183.

8. **Brandenburg, B., and X. Zhuang.** 2007. Virus trafficking - learning from single-virus tracking. Nat. Rev. Microbiol. **5:**197-208.

9. **Campbell, E. M., and T. J. Hope.** 2008. Live cell imaging of the HIV-1 life cycle. Trends Microbiol. **16:**580-587.

10. **Ceresa, B. P., M. Lotscher, and S. L. Schmid.** 2001. Receptor and membrane recycling can occur with unaltered efficiency despite dramatic Rab5(q79l)-induced changes in endosome geometry. J. Biol. Chem. **276:**9649-9654.

11. **Cheng, Y., O. Zak, P. Aisen, S. C. Harrison, and T. Walz.** 2004. Structure of the human transferrin receptor-transferrin complex. Cell **116:**565-576.

12. **Coyne, C. B., and J. M. Bergelson.** 2006. Virus-induced Abl and Fyn kinase signals permit coxsackievirus entry through epithelial tight junctions. Cell **124:**119-131.

13. **Decaro, N., C. Desario, A. Parisi, V. Martella, A. Lorusso, A. Miccolupo, V. Mari, M. L. Colaianni, A. Cavalli, L. Di Trani, and C. Buonavoglia.** 2009. Genetic analysis of canine parvovirus type 2c. Virology **385:** 5-10.

14. **Del Conte-Zerial, P., L. Brusch, J. C. Rink, C. Collinet, Y. Kalaidzidis, M. Zerial, and A. Deutsch.** 2008. Membrane identity and GTPase cascades regulated by toggle and cut-out switches. Mol. Syst. Biol. **4:**206.

15. **Ding, W., L. Zhang, Z. Yan, and J. F. Engelhardt.** 2005. Intracellular trafficking of adeno-associated viral vectors. Gene Ther **12:**873-80.

16. **Dinneen, J. L., and B. P. Ceresa.** 2004. Continual expression of Rab5(Q79L) causes a ligand-independent EGFR internalization and diminishes EGFR activity. Traffic **5:**606-615.

17. **Ellenberg, J., E. D. Siggia, J. E. Moreira, C. L. Smith, J. F. Presley, H. J. Worman, and J. Lippincott-Schwartz.** 1997. Nuclear membrane dynamics and reassembly in living cells: targeting of an inner nuclear membrane protein in interphase and mitosis. J. Cell Biol. **138:**1193-1206.

18. **Farr, G. A., S. F. Cotmore, and P. Tattersall.** 2006. VP2 cleavage and the leucine ring at the base of the fivefold cylinder control pH-dependent externalization of both the VP1 N terminus and the genome of minute virus of mice. J. Virol. **80:**161-171.

19. **Farr, G. A., L. G. Zhang, and P. Tattersall.** 2005. Parvoviral virions deploy a capsid-tethered lipolytic enzyme to breach the endosomal membrane during cell entry. Proc. Natl. Acad. Sci. USA **102:**17148-17153.

20. **Fuchs, H., U. Lucken, R. Tauber, A. Engel, and R. Gessner.** 1998. Structural model of phospholipid-reconstituted human transferrin receptor derived by electron microscopy. Structure **6:**1235-1243.

21. **Gagescu, R., N. Demaurex, R. G. Parton, W. Hunziker, L. A. Huber, and J. Gruenberg.** 2000. The recycling endosome of Madin-Darby canine kidney cells

is a mildly acidic compartment rich in raft components. Mol. Biol. Cell **11:**2775-2791.

22.   **Giannetti, A. M., P. M. Snow, O. Zak, and P. J. Bjorkman.** 2003. Mechanism for multiple ligand recognition by the human transferrin receptor. PLoS Biol. **1:**E51.

23.   **Hafenstein, S., L. M. Palermo, V. A. Kostyuchenko, C. Xiao, M. C. Morais, C. D. Nelson, V.D. Bowman, A. J. Battisti, P. R. Chipman, C. R. Parrish, and M. G. Rossmann.** 2007. Asymmetric binding of transferrin receptor to parvovirus capsids. Proc. Natl. Acad. Sci. USA **104:**6585-6589.

24.   **Hao, M., and F. R. Maxfield.** 2000. Characterization of rapid membrane internalization and recycling. J. Biol. Chem. **275:**15279-15286.

25.   **Harbison, C. E., J. A. Chiorini, and C. R. Parrish.** 2008. The parvovirus capsid odyssey: from the cell surface to the nucleus. Trends Microbiol. **16:**208-214.

26.   **Hueffer, K., L. M. Palermo, and C. R. Parrish.** 2004. Parvovirus infection of cells by using variants of the feline transferrin receptor altering clathrin-mediated endocytosis, membrane domain localization, and capsid-binding domains. J. Virol. **78:**5601-56011.

27.   **Hueffer, K., J. S. Parker, W. S. Weichert, R. E. Geisel, J. Y. Sgro, and C. R. Parrish.** 2003. The natural host range shift and subsequent evolution of canine parvovirus resulted from virus-specific binding to the canine transferrin receptor. J. Virol. **77:**1718-1726.

28.   **Kaksonen, M., C. P. Toret, and D. G. Drubin.** 2006. Harnessing actin dynamics for clathrin-mediated endocytosis. Nat. Rev. Mol. Cell Biol. **7:**404-14.

29.   **Lakadamyali, M., M. J. Rust, and X. Zhuang.** 2006. Ligands for clathrin-mediated endocytosis are differentially sorted into distinct populations of early endosomes. Cell **124:**997-1009.

30.   **Lau, C., X. Wang, L. Song, M. North, S. Wiehler, D. Proud, and C. W. Chow.** 2008. Syk associates with clathrin and mediates phosphatidylinositol 3-kinase activation during human rhinovirus internalization. J. Immunol. **180:**870-880.

31.   **Lawrence, C. M., S. Ray, M. Babyonyshev, R. Galluser, D. W. Borhani, and S. C. Harrison.** 1999. Crystal structure of the ectodomain of human transferrin receptor. Science **286:**779-782.

32.   **Lehmann, M. J., N. M. Sherer, C. B. Marks, M. Pypaert, and W. Mothes.** 2005. Actin- and myosin-driven movement of viruses along filopodia precedes their entry into cells. J. Cell Biol. **170:**317-325.

33. **Lux, K., N. Goerlitz, S. Schlemminger, L. Perabo, D. Goldnau, J. Endell, K. Leike, D. M. Kofler, S. Finke, M. Hallek, and H. Buning.** 2005. Green fluorescent protein-tagged adeno-associated virus particles allow the study of cytosolic and nuclear trafficking. J. Virol. **79:**11776-11787.

34. **Mani, B., C. Baltzer, N. Valle, J. M. Almendral, C. Kempf, and C. Ros.** 2006. Low pH-dependent endosomal processing of the incoming parvovirus minute virus of mice virion leads to externalization of the VP1 N-terminal sequence (N-VP1), N-VP2 cleavage, and uncoating of the full-length genome. J. Virol. **80:**1015-1024.

35. **Marsh, E. W., P. L. Leopold, N. L. Jones, and F. R. Maxfield.** 1995. Oligomerized transferrin receptors are selectively retained by a lumenal sorting signal in a long-lived endocytic recycling compartment. J. Cell Biol. **129:**1509-1522.

36. **Marsh, M., and A. Helenius.** 2006. Virus entry: open sesame. Cell **124:**729-40.

37. **Maxfield, F. R., and T. E. McGraw.** 2004. Endocytic recycling. Nat. Rev. Mol. Cell Biol. **5:**121-132.

38. **McCaffrey, M. W., A. Bielli, G. Cantalupo, S. Mora, V. Roberti, M. Santillo, F. Drummond, and C. Bucci.** 2001. Rab4 affects both recycling and degradative endosomal trafficking. FEBS Lett. **495:**21-30.

39. **McGraw, T. E., L. Greenfield, and F. R. Maxfield.** 1987. Functional expression of the human transferrin receptor cDNA in Chinese hamster ovary cells deficient in endogenous transferrin receptor. J. Cell Biol. **105:**207-214.

40. **Nelson, C. D., E. Minkkinen, M. Bergkvist, K. Hoelzer, M. Fisher, B. Bothner, and C. R. Parrish.** 2008. Detecting small changes and additional peptides in the canine parvovirus capsid structure. J. Virol. **82:**10397-407.

41. **Odorizzi, G., A. Pearse, D. Domingo, I. S. Trowbridge, and C. R. Hopkins.** 1996. Apical and basolateral endosomes of MDCK cells are interconnected and contain a polarized sorting mechanism. J. Cell Biol. **135:**139-152.

42. **Palermo, L. M., S. L. Hafenstein, and C. R. Parrish.** 2006. Purified feline and canine transferrin receptors reveal complex interactions with the capsids of canine and feline parvoviruses that correspond to their host ranges. J. Virol. **80:**8482-8492.

43. **Palermo, L. M., K. Hueffer, and C. R. Parrish.** 2003. Residues in the apical domain of the feline and canine transferrin receptors control host-specific binding and cell infection of canine and feline parvoviruses. J. Virol. **77:**8915-8923.

44. **Parker, J. S., W. J. Murphy, D. Wang, S. J. O'Brien, and C. R. Parrish.** 2001. Canine and feline parvoviruses can use human or feline transferrin receptors to bind, enter, and infect cells. J. Virol. **75:**3896-902.

45. **Parker, J. S., and C. R. Parrish.** 2000. Cellular uptake and infection by canine parvovirus involves rapid dynamin-regulated clathrin-mediated endocytosis, followed by slower intracellular trafficking. J. Virol. **74:**1919-1930.

46. **Parker, J. S. L., and C. R. Parrish.** 1997. Canine parvovirus host range is determined by the specific conformation of an additional region of the capsid. J. Virol. **71:**9214-9222.

47. **Parrish, C. R.** 1991. Mapping specific functions in the capsid structure of canine parvovirus and feline panleukopenia virus using infectious plasmid clones. Virology **183:**195-205.

48. **Parrish, C. R., C. Aquadro, M. L. Strassheim, J. F. Evermann, J.-Y. Sgro, and H. Mohammed.** 1991. Rapid antigenic-type replacement and DNA sequence evolution of canine parvovirus. J. Virol. **65:**6544-6552.

49. **Parrish, C. R., P. Have, W. J. Foreyt, J. F. Evermann, M. Senda, and L. E. Carmichael.**1988. The global spread and replacement of canine parvovirus strains. J. Gen. Virol. **69:**1111-1116.

50. **Parrish, C. R., and Y. Kawaoka.** 2005. The origins of new pandemic viruses: the acquisition of new host ranges by canine parvovirus and influenza A viruses. Annu. Rev. Microbiol. **59:**553-586.

51. **Pietiainen, V., V. Marjomaki, P. Upla, L. Pelkmans, A. Helenius, and T. Hyypia.** 2004. Echovirus 1 endocytosis into caveosomes requires lipid rafts, dynamin II, and signaling events. Mol. Biol. Cell. **15:**4911-4925.

52. **Radoshitzky, S. R., J. Abraham, C. F. Spiropoulou, J. H. Kuhn, D. Nguyen, W. Li, J. Nagel, P. J. Schmidt, J. H. Nunberg, N. C. Andrews, M. Farzan, and H. Choe.** 2007. Transferrin receptor 1 is a cellular receptor for New World haemorrhagic fever arenaviruses. Nature **446:**92-96.

53. **Rappoport, J. Z.** 2008. Focusing on clathrin-mediated endocytosis. Biochem. J. **412:**415-423.

54. **Ren, M., G. Xu, J. Zeng, C. De Lemos-Chiarandini, M. Adesnik, and D. D. Sabatini.** 1998. Hydrolysis of GTP on rab11 is required for the direct delivery of transferrin from the pericentriolar recycling compartment to the cell surface but not from sorting endosomes. Proc. Natl. Acad. Sci. USA **95:**6187-192.

55. **Robinson, M. S.** 2004. Adaptable adaptors for coated vesicles. Trends Cell Biol. **14:**167-174.

56. **Ross, S. R., J. J. Schofield, C. J. Farr, and M. Bucan.** 2002. Mouse transferrin receptor 1 is the cell entry receptor for mouse mammary tumor virus. Proc. Natl. Acad. Sci. USA **99:**12386-12390.

57. **Schelhaas, M., H. Ewers, M. L. Rajamaki, P. M. Day, J. T. Schiller, and A. Helenius.** 2008. Human papillomavirus type 16 entry: retrograde cell surface transport along actin-rich protrusions. PLoS Pathog. **4:**e1000148.

58. **Seaman, M. N.** 2008. Endosome protein sorting: motifs and machinery. Cell. Mol. Life Sci. **65:**2842-2858.

59. **Sharma, M., F. Pampinella, C. Nemes, M. Benharouga, J. So, K. Du, K. G. Bache, B. Papsin, N. Zerangue, H. Stenmark, and G. L. Lukacs.** 2004. Misfolding diverts CFTR from recycling to degradation: quality control at early endosomes. J. Cell Biol. **164:**923-933.

60. **Simpson, A. A., V. Chandrasekar, B. Hebert, G. M. Sullivan, M. G. Rossmann, and C. R. Parrish.** 2000. Host range and variability of calcium binding by surface loops in the capsids of canine and feline parvoviruses. J. Mol. Biol. **300:**597-610.

61. **Smith, A. E., and A. Helenius.** 2004. How viruses enter animal cells. Science **304:**237-242.

62. **Smith, J. L., D. S. Lidke, and M. A. Ozbun.** 2008. Virus activated filopodia promote human papillomavirus type 31 uptake from the extracellular matrix. Virology **381:**16-21.

63. **Sonnichsen, B., S. De Renzis, E. Nielsen, J. Rietdorf, and M. Zerial.** 2000. Distinct membrane domains on endosomes in the recycling pathway visualized by multicolor imaging of Rab4, Rab5, and Rab11. J. Cell Biol. **149:**901-914.

64. **Suikkanen, S., M. Antila, A. Jaatinen, M. Vihinen-Ranta, and M. Vuento.** 2003. Release of canine parvovirus from endocytic vesicles. Virology **316:**267-280.

65. **Suikkanen, S., K. Saajarvi, J. Hirsimaki, O. Valilehto, H. Reunanen, M. Vihinen-Ranta, and M. Vuento.** 2002. Role of recycling endosomes and lysosomes in dynein-dependent entry of canine parvovirus. J. Virol. **76:**4401-4411.

66. **Truyen, U., A. Gruenberg, S. F. Chang, B. Obermaier, P. Veijalainen, and C. R. Parrish.** 1995. Evolution of the feline-subgroup parvoviruses and the control of canine host range in vivo. J. Virol. **69:**4702-4710.

67. **Truyen, U., and C. R. Parrish.** 1992. Canine and feline host ranges of canine parvovirus and feline panleukopenia virus: distinct host cell tropisms of each virus in vitro and in vivo. J. Virol. **66:**5399-5408.

68. **Tsao, J., M. S. Chapman, M. Agbandje, W. Keller, K. Smith, H. Wu, M. Luo, T. J. Smith, M. G. Rossmann, R. W. Compans, and C. R. Parrish.** 1991. The three-dimensional structure of canine parvovirus and its functional implications. Science **251:**1456-1464.

69. **Van Dam, E. M., and W. Stoorvogel.** 2002. Dynamin-dependent transferrin receptor recycling by endosome-derived clathrin-coated vesicles. Mol. Biol. Cell. **13:**169-182.

70. **Van Dam, E. M., T. Ten Broeke, K. Jansen, P. Spijkers, and W. Stoorvogel.** 2002. Endocytosed transferrin receptors recycle via distinct dynamin and phosphatidylinositol 3-kinasedependent pathways. J. Biol. Chem. **277:**48876-83.

71. **Van der Schaar, H. M., M. J. Rust, C. Chen, H. van der Ende-Metselaar, J. Wilschut, X. Zhuang, and J. M. Smit.** 2008. Dissecting the cell entry pathway of dengue virus by single particle tracking in living cells. PLoS Pathog. **4:**e1000244.

72. **Vihinen-Ranta, M., D. Wang, W. S. Weichert, and C. R. Parrish.** 2002. The VP1 N-terminal sequence of canine parvovirus affects nuclear transport of capsids and efficient cell infection. J. Virol. **76:**1884-1891.

73. **Vihinen-Ranta, M., W. Yuan, and C. R. Parrish.** 2000. Cytoplasmic trafficking of the canine parvovirus capsid and its role in infection and nuclear transport. J Virol. **74:**4853-4859.

74. **White, S., K. Miller, C. Hopkins, and I. S. Trowbridge.** 1992. Monoclonal antibodies against defined epitopes of the human transferrin receptor cytoplasmic tail. Biochim. Biophys. Acta. **1136:**28-34.

75. **Yeung, D. E., G. W. Brown, P. Tam, R. H. Russnak, G. Wilson, I. Clark-Lewis, and C. R. Astell.** 1991. Monoclonal antibodies to major nonstructural nuclear protein of minute virus of mice. Virology **181:**35-45.

76. **Zadori, Z., J. Szelei, M.C. Lacoste, P. Raymond, M. Allaire, I. R. Nabi, and P. Tijssen.** 2001. A viral phospholipase A2 is required for parvovirus infectivity. Developmental Cell **1:**291-302.

CHAPTER 3: ENDOCYTOSIS OF CANINE AND FELINE PARVOVIRUSES: ALTERING RECEPTOR TRANSMEMBRANE AND CYTOPLASMIC SEQUENCES TO SHOW REQUIREMENTS FOR INFECTION.

3.1 Abstract

Canine and feline parvovirus (CPV and FPV) capsids bind the transferrin receptor type 1 (TfR) on the surface of host cells, are taken up by clathrin-mediated endocytosis, and are trafficked within the endosomal pathways of the cell leading to infection. The specific endocytic requirements for parvoviral infection were examined using variant receptors prepared from the feline TfR ectodomain joined to transmembrane and cytoplasmic sequences from other type II transmembrane proteins. Despite being expressed at the cell surface and able to bind transferrin (Tf), the chimeras with cytoplasmic and transmembrane domains from influenza neuraminidase (FluNA), Newcastle disease virus hemagglutinin neuraminidase (NDVHN), and parainfluenza 4a HN (PI4aHN) allowed little infection when compared to the wild type TfR. Chimeras with the cellular proteins asialoglycoprotein receptor 1 (Asialo) and Fcε receptor 2 (CD23) allowed approximately 50% of wild type infection levels. The mutant TfRs were associated with alterations in expression and uptake from the cell surface, and there was no specific requirement for the cytoplasmic tail to contain sequences for interaction with the clathrin endocytic machinery.

3.2 Introduction

The viral receptor plays many roles in the infection process of non-enveloped viruses. Binding to a specific protein or carbohydrate moiety tethers the virus to the cell surface and may initiate one or more events including receptor clustering, binding to additional receptors, structural changes in the virus capsid, activation of cell signaling pathways, and endocytosis (10, 29, 41, 57). Hijacking cellular endocytic pathways

allows the virus to rapidly gain entry into the cell, and viruses may use one or more

cellular mechanisms for uptake from the cell surface. Many viruses, such as Ebola

virus, influenza virus, and parvoviruses, interact with the clathrin endocytic machinery

through their receptors (8, 11, 13, 38). The viruses can either recruit clathrin machinery

to the binding site via the clustering of receptors, or may migrate on the surface of the

cell and engage forming or pre-formed clathrin pits. Other viruses utilize caveolae for

entry, such as the polyomavirus simian virus 40 (SV40), or may bind to a variety of cell

surface molecules for entry via less well-characterized pathways (2). Uptake by

macropinocytosis (Vaccinia virus), cholesterol-dependent entry (Polyomavirus), and

non-clathrin, non-caveolar uptake processes (Murine Norovirus-1), as well as non-

specific membrane recycling have all been described for different viruses (16, 36, 37,

50, 51).

   After uptake, viral particles may be routed through pathways that provide signals

for infection, such as exposure to low pH or proteases. While there is some overlap

between these pathways, cytoplasmic sorting signals can direct ligands to specific

destinations within the cell (26, 45). Trafficking time within the vesicular system can vary

from minutes to hours before the infecting particles leave the endosomes to enter the

cytoplasm, with most DNA viruses further trafficking to the nucleus. Viruses utilizing

clathrin-mediated endocytosis may be trafficked to low pH compartments such as the

early and late endosomes where the pH signal alone or in concert with the action of

cellular factors provides triggers for endosomal escape (12, 59). Intracellular trafficking

following caveolar uptake delivers ligands to the endoplasmic reticulum and/or Golgi

complex, and viruses have evolved various mechanisms of escape from these compartments (42, 60).

We are studying the cellular infection process of two closely related parvoviruses with distinct receptor binding and host range properties. The canine and feline parvoviruses are small non-enveloped particles with T=1 icosahedral symmetry and a single stranded DNA genome of about five kb (27). Canine parvovirus (CPV) emerged in 1978 as a host range variant of feline panleukopenia virus (FPV) through the acquisition of a small number of mutations that allowed it to bind the canine cellular receptor, the transferrin receptor type 1 (TfR) (25). The original CPV, designated CPV type-2 (CPV-2), was rapidly replaced in the wild by antigenic and host range variants designated CPV type-2a, 2b, and 2c (e.g. CPV-2a) (49). All of these strains share above 95% identity in capsid sequence, but differ in host range, antigenicity, and other properties. Capsids are assembled from a combination of 90% VP2 and 10% VP1 viral proteins, which share the same C-terminal sequence. The N-terminal VP1 unique sequence becomes exposed during viral entry, is required for infection, and contains sequences with phospholipase A_2 (PLA-2) and nuclear targeting activity (19, 63). The PLA-2 may modify endosomal membranes to facilitate release into the cytoplasm, and the nuclear localization sequences may mediate capsid passage past the nuclear envelope. However, the mechanism underlying both of these entry steps is still poorly understood (62).

The TfR is a type II membrane protein that is expressed as a homodimer on the cell surface (14). The ectodomain is comprised of protease-like, apical, and helical domains, while the cytoplasmic domain contains a Tyr-Thr-Arg-Phe (YTRF) sequence

that mediates endocytosis through clathrin-coated pits (6, 9, 30). The length and specific sequence of the transmembrane domain mediates its insertion in non-lipid raft areas of the plasma membrane. The normal intracellular TfR trafficking pathway routes 97% of internalized receptors through the early endosome to the recycling endosome and back to the surface within 15 to 20 minutes (55, 58, 61). In studies with experimentally oligomerized Tf, the receptor is retained for much longer periods within endosomes and a higher percentage is trafficked to the late endosomes and lysosomes where it is degraded (32).

The roles, routes, and kinetics of specific receptor-mediated endocytic pathways in cell infection have only been partially defined for CPV. The CPV capsid interacts with the TfR apical domain at a raised region on the capsid surrounding the threefold axis of icosahedral symmetry, designated the threefold spike (44). Residue changes in this domain influence viral binding such that only CPV can interact with the canine TfR to infect canine cells, though different strains vary in their binding affinity (20, 23, 25). Virus binding does not compete with transferrin uptake, which interacts with the membrane-proximal portion of TfR (17). The TfR provides specific structural interactions with the capsid that allow cell infection, as viral binding to sialic acids or artificial receptors prepared from antibody binding domains fused to the TfR transmembrane and cytoplasmic sequences allows viral endocytosis but not completion of the replication cycle (24).

CPV capsids, like Tf, are rapidly taken up by clathrin-mediated endocytosis (22, 46). However, infection kinetics in feline cells are very slow, as cytoplasmic microinjection of antibodies against either the cytoplasmic tail of the TfR or the capsid

can block infection when added four or eight hours after uptake, respectively (63). By immunofluorescence microscopy, capsids can be found co-localized with several endosomal compartments within minutes, rapidly associating with markers of the early, recycling, and late endosomes (22). The markers utilized in these studies include a variety of Rab adaptor proteins, which function to regulate endosomal trafficking within the cell (43, 64). Specific Rab proteins mark generally distinct cellular compartments including Rab5 in the early endosome, Rab7 in the late endosome, and Rab11 in the perinuclear recycling endosome (34, 39). Structural changes in the capsid, such as the release of the VP1 unique sequence, occur within one or more of these compartments during the trafficking process and are required for infection. However, the controlling factors that determine the rate and direction of viral capsid trafficking within the endosome and how those factors affect the success of the infection are still not well understood.

We previously examined infection in cells expressing mutant feline TfRs expected to have reduced interaction with the clathrin-mediated endocytic machinery and a chimeric TfR with the transmembrane and cytoplasmic sequences replaced with those from the influenza virus neuraminidase protein (FluNA-TfR) (24). In this study the clathrin-interaction sequence mutants still allowed efficient virus infection, although the FluNA-TfR chimera did not. This suggested that while clathrin-mediated endocytosis is dispensable, the properties of the plasma membrane or the subsequent trafficking pathways of the capsids are important for cellular infection by these parvoviruses.

Here we further examine the functional steps leading to infection by comparing the functionality of the feline TfR ectodomain fused to transmembrane and cytoplasmic

tails from several other viral and cellular-origin proteins with differences in reported membrane association and trafficking properties. This approach to evaluating the specific requirements for endocytic uptake has been validated in other studies (18). For example, in cells expressing wild-type nectin 1 as a cellular receptor, herpes simplex virus (HSV) fuses with the plasma membrane soon after receptor binding and does not require exposure to intracellular signals to trigger this event. Chimeric receptors fusing the extracellular domain of the cellular receptor Nectin 1 to the epidermal growth factor receptor or to a glycosylphosphatidylinositol (GPI) anchor were successful in retargeting the virus to be either taken up into the endosomal system through clathrin-mediated endocytosis or via lipid raft domains of the plasma membrane, respectively. HSV entry, membrane fusion, and infection did not require any specific transmembrane or cytoplasmic sequences to be present in the cellular receptor, as long as the structural interaction of the virus with the extracellular domain remained intact (18).

In the present study, chimeric TfRs with the transmembrane and cytoplasmic domains replaced with those from other type II membrane proteins were tested by expression on hamster cells lacking the endogenous TfR (TRVb cells). Most receptors were expressed as functional proteins on the cell surface, but the chimeras containing sequences from viral glycoproteins were inefficient at infection. The localization of the virus with intracellular markers showed that endocytosed capsids could be found in multiple endosomal locations, and that there was not a single defined pathway of entry.

Table 3.1. The cytoplasmic and transmembrane sequences of the mutant or chimeric feline TfRs tested in this study. The source of each sequence is given along with the amino acid sequence in single letter code. The predicted transmembrane sequences are underlined, and sequences with predicted functionality are indicated in bold. The first few amino acids of the shared ectodomain from the feline TfR are indicated in italics.

FelTfR	Wild-type feline TfR, Genbank AF276984.1 SwissProt Q9MYZ3	MMDQARSAFSTLFGGEPLS**YTRF**SLA RQVDGDNSHVEMKLAADEEENVDNN MRDNGASVTKPKRFNGFIC<u>YGTIAIILF FLIGFMIGYLG</u>YCKRVEAK
FelTfR-Δ3-32	Feline TfR, cytoplasmic residues 3-32 deleted	MMHVEMKLAADEEENVDNNMRDNG ASVTKPKRFNGFIC<u>YGTIAIILFFLIGFM IGYLG</u>YCKRVEAK
FelTfR-ATAA	Feline TfR, YTRF residues 20-24 mutated to ATAA	MMDQARSAFSTLFGGEPLS**ATAA**SL ARQVDGDNSHVEMKLAADEEENVDN NMRDNGASVTKPKRFNGFIC<u>YGTIAII LFFLIGFMIGYLG</u>YCKRVEAK
Asialo-FelTfR	Asialoglycoprotein receptor I Genbank BAB83508.1 SwissProt P07306	MTKEYQDLQHLDNEESDHHQLRKGP PPPQP**LL**QRLCSGPR<u>LLLLLSLGLSLLL LVVVCVIGSQNSQ</u>*RVEAK*
CD23-FelTfR	FC Epsilon receptor 2 Genbank M15059 SwissProt P06734	MEEGQ**YSEI**EELPRRRCCRRG<u>TQIVL LGLVTAALWAGLLTLLLLWHW</u>DTTQR VEAK
Ii-FelTfR	Invariant chain Genbank CAA25192.1 SwissProt P04233	MHRRRSRSCREDQKPVMDDQRD**LIS** NNEQLP**ML**GRRPGAPESKCSRG<u>ALY TGFSILVTLLLAGQATTAYFLYQQ</u>*RVE AK*
PI4aHN-FelTfR	Parainfluenza 4a hemagglutinin neuraminidase EMBL AAA46799.1 SwissProt P21526	MQDSHGNTQILNQANSMVKRTWR**LL** FR<u>IATLILLVSIFVLSLIIVLQSTPG</u>*RVEA K*
FluNA-FelTfR	Influenza neuraminidase Genbank AAA91326.1 SwissProt P03470	MNPNQK<u>IITIGSICMV**VGIIS**LILQIGNIIS IWIS</u>*RVEAK*
NDVHN-FelTfR	Newcastle disease virus hemagglutinin neuraminidase Genbank AAA46670.1 SwissProt P12554	MNRAVCQVALENDEREAKNTWRLVF R<u>IAILLLTVMTLAISAAALAYSI</u>*RVEAK*
SV5HN-FelTfR	Simian virus 5 hemagglutinin neuraminidase Genbank AAB21114.1 SwissProt P04850	MVAEDAPVRATCRVLFR<u>TTTLIFLCTL LALSISILY**E**</u>SLITQKQIMSQDVI*EAK*

3.3 Materials and methods

3.3a Cells and viruses

Chinese hamster ovary (CHO)-derived cells lacking the hamster TfR (TRVb cells) (35) were grown in Ham's F12 medium containing 5% fetal bovine serum. Norden Laboratory feline kidney (NLFK) cells were grown in a 1:1 mixture of McCoy's 5A and Liebovitz L15 media with 5% fetal bovine serum.

Parvoviruses were derived from infectious plasmid clones of FPV (FPV-b), CPV-2 (CPV-d), and CPV-2b (CPV-39) strains (25, 48). Plasmids were transfected into NLFK cells, and the viruses were titered using tissue culture infectious dose ($TCID_{50}$) assays (47). Virus capsids were concentrated by polyethylene glycol precipitation followed by sucrose gradient centrifugation, then dialyzed against either PBS or 20 mM Tris-HCl (pH 7.5) and stored at 4ºC (1).

3.3b TfR clones and mutants

TfR clones prepared from the feline TfR (Genbank AF276984) are listed in Table 3.1. New chimeric receptors constructed in this study used the transmembrane and cytoplasmic sequences from the cellular proteins asialoglycoprotein receptor-1 (Asialo-TfR) (Genbank BAB83508.1), the Fc-epsilon receptor-2 (CD23-TfR)(Genbank M15059), and the MHC class II invariant chain (Ii-TfR) (Genbank CAA25192.1). Viral-derived chimeras utilized the cytoplasmic and transmembrane sequences of the HN protein from simian virus 5 (SV5HN-TfR) (Genbank AAB21114.1), Newcastle disease virus (NDVHN-TfR) (Genbank AAA46670.1), and parainfluenza virus 4a (PI4aHN-TfR) (EMBL AAA46799.1). The alternative cytoplasmic and TM sequences were synthesized

and cloned in place of the equivalent feline TfR sequence in the mammalian cell expression vector pcDNA3.1(-) (Invitrogen, Carlsbad, CA). Other previously described mutant TfRs contained influenza neuraminidase sequences (NA-TfR), or were based upon the FelTfR with the sequence between residues two and 32 deleted (FelTfRΔ3-32) or with the cytoplasmic YTRF sequence mutated to ATAA (FelTfR-ATAA) (24). Following conformation of correct sequence replacement, the plasmids were transfected into TRVb cells using Lipofectamine according to manufacturer's instructions (Invitrogen).

3.3c Fluorescent labeling of virus or Tf

As previously described, canine Tf (Sigma Aldrich, St. Louis, MO) was iron loaded, and purified CPV capsids, FPV capsids, or canine Tf were labeled with Alexa488 (Invitrogen) (4, 5, 22, 25). Dyes were used to label viruses at 20% of the recommended concentrations, and after labeling the capsids were separated from free dye by a PD10 desalting column (GE Healthcare, Waukesha, WA) and dialysis against 0.2M phosphate buffered saline (PBS) at pH 8.2.

3.3d Determining TfR expression levels and Tf uptake

To detect receptor expression, TRVb cells transiently transfected with the variant TfR constructs were seeded onto coverslips, fixed with 4% paraformaldehyde (PFA) for 20 minutes, then incubated with an anti-TfR ectodomain monoclonal antibody (T4F3) diluted in permeabilization buffer (PBS containing 1% BSA and 0.1% Triton X-100). Bound IgG was detected with a goat anti-mouse IgG-Alexa 488-labeled secondary antibody (Sigma). Receptor expression was quantified using a FACScalibur flow cytometer (Becton-Dickinson, San Jose, Calif.).

To examine virus and Tf uptake, transfected cells were incubated in solution at 37°C with either 10 µg/ml of purified Alexa488-labeled CPV-2 virus capsids or Alexa488-labeled Tf diluted in Dulbecco's Modified Eagle medium (DMEM) containing 0.1% bovine serum albumin (BSA) for times ranging from 15 seconds to 60 minutes. Cells were washed three times in ice-cold medium prior to quantification of cell-associated virus or Tf using flow cytometry as above.

3.3e Cell infection assays

To measure viral infection rates, cells transfected with the variant TfRs were incubated with FPV, CPV-2, or CPV-2b inocula at a MOI of 5 for one hour, then washed and incubated at 37°C for a further 48 hours. Prior to fixation with 4% PFA, the cells were incubated with Alexa 488-labeled Tf for 30 minutes to score for receptor expression. After fixation and washing in PBS, cells were permeabilized with 0.1% Triton X-100 and further stained for receptor expression using the T4F3 antibody as above. Infected cells were identified by immunostaining with an Alexa 594-conjugated monoclonal antibody (CE-10) against nonstructural protein-1 (66). The proportion of infected cells was determined as the percentage of the TfR-expressing cells that became infected and expressed the NS1 protein. Student t tests were used to determine the significance of differences in infection rates.

3.3f Membrane localization

The membrane association of the receptors was tested by resistance to cold detergent extraction similar to the method previously described (24). The extracted and detergent resistant fractions were tested for the presence of the TfR or caveolin-1 by

Western blot, using an anti-TfR antibody (U1D4) or anti-caveolin antibody (Sigma) and a horseradish peroxidase-conjugated secondary antibody.

3.3g Fluorescence microscopy

Markers tested in these studies included the previously described GFP-labeled Rab5, Rab11, and Rab7 as markers of the early, recycling, and late endosomal compartments, respectively (22). To determine viral uptake using the variant TfRs, TRVb cells cotransfected with the different receptor constructs and one of these markers were incubated with labeled virus or Tf for 5 min at 37°C. After washing with warm phenol-red free DMEM, time lapse images were obtained at the times indicated with a 37°C 100× oil lens. Separate channels were collected sequentially using a Hamamatsu OrcaER CCD camera. Image analysis was performed using SimplePCI (Hamamatsu, Sewickley, PA) and ImageJ software (US National Institutes of Health, Bethesda, MD), including the ImageJ manual tracker plugin for detecting virus-vesicle co-movement (Institut Curie, Orsay, Fr).

3.4 Results

3.4a Construction of receptor chimeras

We prepared a series of chimeric TfRs containing the cytoplasmic and transmembrane sequences from a variety of type II membrane proteins fused to the stalk and ectodomain of the feline TfR (Table 3.1), with the junction site within a few residues of the transmembrane-ectodomain boundary. Chimeras included sequences from cellular proteins including the asialoglycoprotein receptor (Asialo-TfR), the low affinity Fc fragment of IgE receptor II (CD23-TfR), and the invariant chain (Ii-TfR). Other

chimeras were prepared with cytoplasmic and transmembrane sequences of type II hemagglutinin neuraminidase (HN) proteins from paramyxoviruses including simian virus 5 (SV5HN-TfR), Newcastle disease virus (NDVHN-TfR), and parainfluenza virus 4a (PI4aHN-TfR). One chimera with the transmembrane and cytoplasmic domain replaced with that from the influenza NA protein (FluNA-TfR) has been previously described (24). Two clones used as controls in these studies have also been previously described, and include mutants of the feline TfR whose altered cytoplasmic sequences were expected to disrupt the association with adaptor protein 2 (AP-2) and clathrin-mediated endocytosis (FelTfR-Δ3-32, FelTfR-ATAA) (24, 44). Several of these chimeras contain sequences which, at least in the context of native protein, lead to interaction with the clathrin endocytic machinery (Figure 3.1). These motifs include tyrosine-containing motifs such as YXXΦ, where X is any amino acid and Φ is any bulky, hydrophobic amino acid, and were present in the wild-type FelTfR and CD23-TfR chimeras. Alternate clathrin-interacting motifs include a dileucine (LL) patch in Asialo-TfR and PI4aHN-TfR and an unusual extracellular glutamic acid motif proposed to be functional in the SV5HN-TfR. Other sequences with functionality in their native proteins include a "LI...ML" motif for lysosomal targeting in Ii-TfR, and a transmembrane "VGIIS" sequence for targeting to lipid raft domains within the plasma membrane in FluNA-TfR. The NDVHN-TfR cytoplasmic and transmembrane domains contained no known motifs.
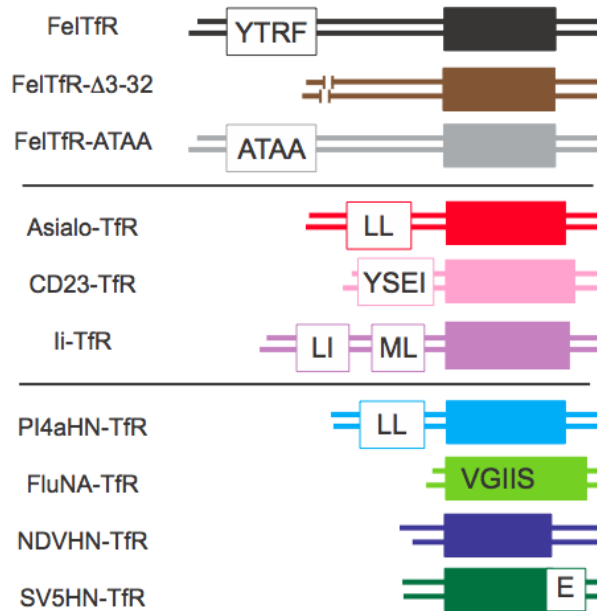
Figure 3.1. Diagrammatic representation of the variant TfR clones highlighting features with predicted functionality. The receptors are grouped by sequence origin, with feline TfR mutants in neutral colors, chimeras with cytoplasmic tails from cellular proteins in reds and purples, and chimeras with tails from viral proteins in blues and greens. Highlighted in boxes are sequences involved in clathrin-mediated endocytosis (tyrosine-containing motifs, dileucine sequence, and an extracellular glutamic acid), lysosomal targeting (LI...ML), and segregation into lipid raft domains (VGIIS). The length of the cytoplasmic and transmembrane domains is drawn approximately to scale.

3.4b Expression of cloned receptors

Cells transiently transfected with the variant receptor constructs were stained with a monoclonal antibody against the TfR ectodomain (an area conserved between the mutants) to determine whether the clones could be expressed as intact proteins within the cell. The Ii-TfR and SV5HN-TfR chimeras showed less than five percent of cells expressing only low levels of receptor and were excluded from further analysis (data not shown). Of the remaining receptors, most mutant and chimeric receptors expressed equivalent levels of TfR to wild-type FelTfR in TRVb cells (Figure 3.2). Only the FluNA-TfR had significantly lower expression than the wild-type receptor (~22%).

However, the expression level of FluNA-TfR was comparable to that seen in wild-type

feline NLFK cells (Figure 3.2B), indicating that most receptor constructs are actually

significantly overexpressed. By microscopy, the distribution of the transfected wild type

FelTfR receptor throughout the cell (Figure 3.2C) was comparable to that of NLFK cells

(Figure 3.2D), and the receptors had a patchy distribution consistent with their

localization on endosomal membranes and the cell surface.
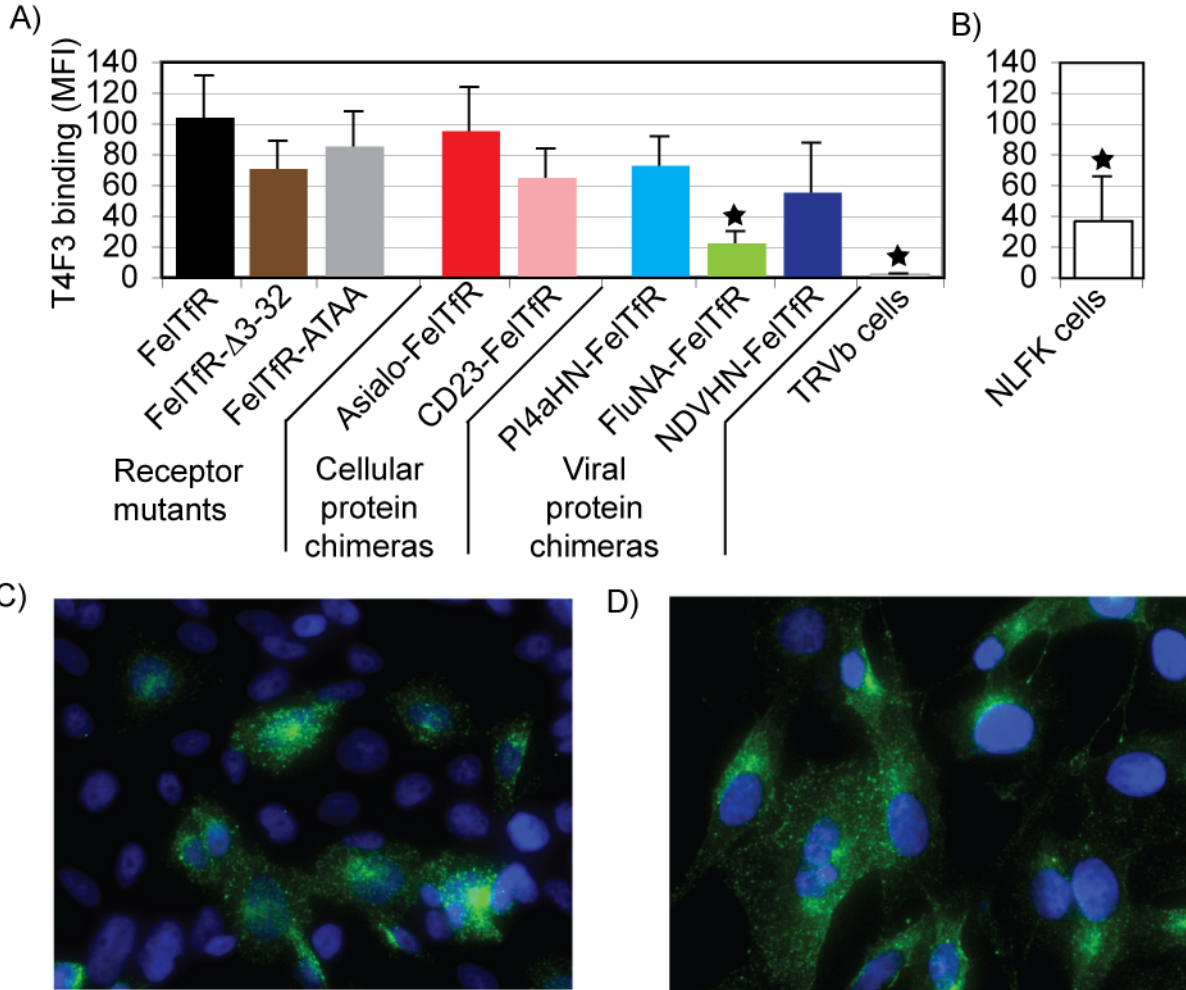
Figure 3.2. Cellular expression of the different TfR mutants after transfection into TRVb cells. A) Expression of the wild-type and mutant receptors in permeabilized TRVb cells was quantified using an anti-TfR ectodomain antibody and an Alexa-488 conjugated secondary antibody. Expression level as determined by flow cytometry in three independent experiments is shown as raw mean fluorescence intensity (MFI) of the transfected population or of the whole population for untransfected TRVb cells; receptors with significantly lower expression than wild-type FelTfR in TRVb cells are indicated ($p<0.05$). B) Expression level of the TfR in wild-type NLFK feline cells, as described in (A). Fluorescence microscopy showing the expression pattern of the TfR in permeabilized (C) TRVb cells expressing wild type FelTfR or (D) NLFK cells as indicated, detected using a monoclonal antibody raised against the TfR ectodomain.

3.4c Infection by parvoviruses in cells expressing variant TfRs

The receptor mutants were tested for their ability to mediate parvovirus infection in transiently transfected cells. The data for FPV infection are shown in Figure 3.3, as it has the highest levels of infection and is the easiest to interpret differences, though the infectivity patterns were similar for CPV-2 and CPV-2b inocula (data not shown). The wild-type FelTfR and the two clathrin motif mutants (FelTfR-ATAA, FelTfR-Δ3-32) (Figure 3.3A) mediated infection levels similar to that of untransfected, wild-type NLFK feline cells (Figure 3.3B), with approximately 25-30% of transfected cells becoming infected. The chimeric receptors with cytoplasmic tails from cellular receptors (Asialo-TfR, CD23-TfR) mediated significantly lower levels than wild-type but retained approximately 15% infection rates of transfected cells. Finally, consistently very low levels of infection were obtained using the viral protein-TfR chimeras (FluNA-TfR, PI4aHN-TfR, and NDVHN-TfR), which showed 0-5% infection of transfected cells (Figure 3.3A).

Figure 3.3. FPV infection of TRVb cells expressing the wild type or mutant feline TfRs or wild-type feline cells. A) Cells were transfected with plasmids expressing the variant TfRs, incubated for two days, and then were re-seeded for 24 hours and inoculated with five $TCID_{50}$ units of FPV. After 48 hours, receptor expression was detected with Alexa-488 labeled canine Tf and staining with an anti-TfR extracellular domain monoclonal antibody. The percentage of infected cells was determined by staining with an Alexa-594 conjugated anti-NS1 viral protein antibody. Results of at least three independent experiments are shown as the infected percentage of transfected cells, or the total percentage of TRVb cells that expressed viral antigen, and significantly different groups are indicated by the symbols above each column ($p<0.05$). B) Infection of wild-type NLFK feline cells, performed as described in (A). C) Example images of infection in TRVb cells transfected with (C) wild-type FelTfR or (D) NDVHN-TfR. Cells expressing the TfRs are shown in green, and infected cells have red nuclei due to the presence of viral NS1 antigen (white arrow in (C)). Red arrows in (C) and (D) depict transfected but uninfected cells, and the yellow boxes indicate nuclei of untransfected cells stained with DAPI (blue).

A)

B)

C) FelTfR

D) NDVHN-TfR

118
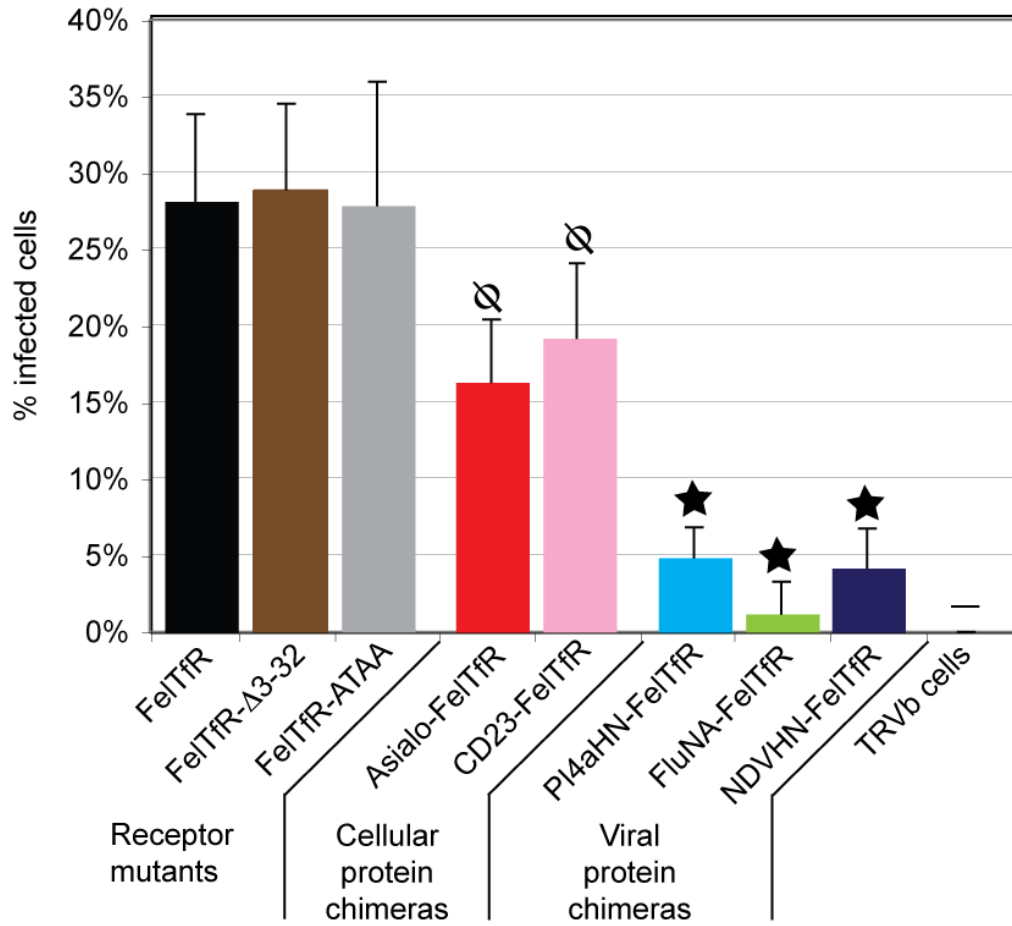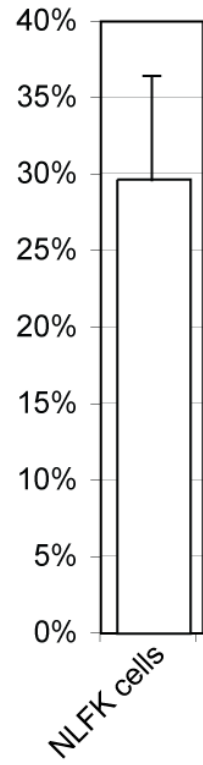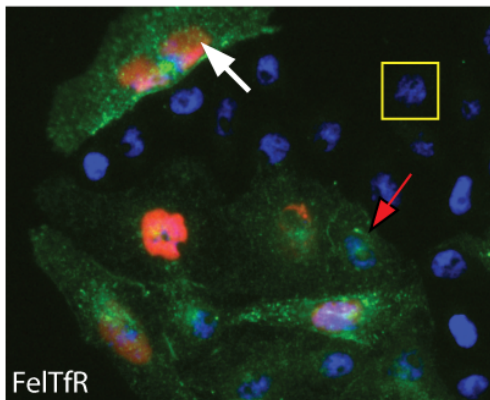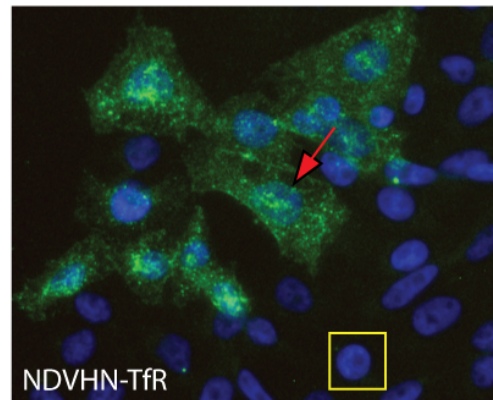
3.4d Determining the functionality of variant receptors for binding Tf and CPV

Binding and uptake of fluorescently labeled canine Tf or CPV capsids were used to assess functionality of the receptors for binding and endocytosis of these ligands (Figure 3.4). The mutant receptors showed variable levels of Tf uptake that in most cases was 50-60% of wild-type (Figure 3.4A). Only Asialo-TfR retained equivalent levels of Tf uptake to the wild-type FelTfR, while NDVHN-TfR and FluNA-TfR had the lowest levels of transferrin uptake, both less than 40% of wild-type. All the variant receptors allowed CPV binding and uptake at levels comparable to wild-type, except for NDVHN-TfR that bound ~50% and FluNA-TfR that bound ~20% of wild-type level (Figure 3.4B).
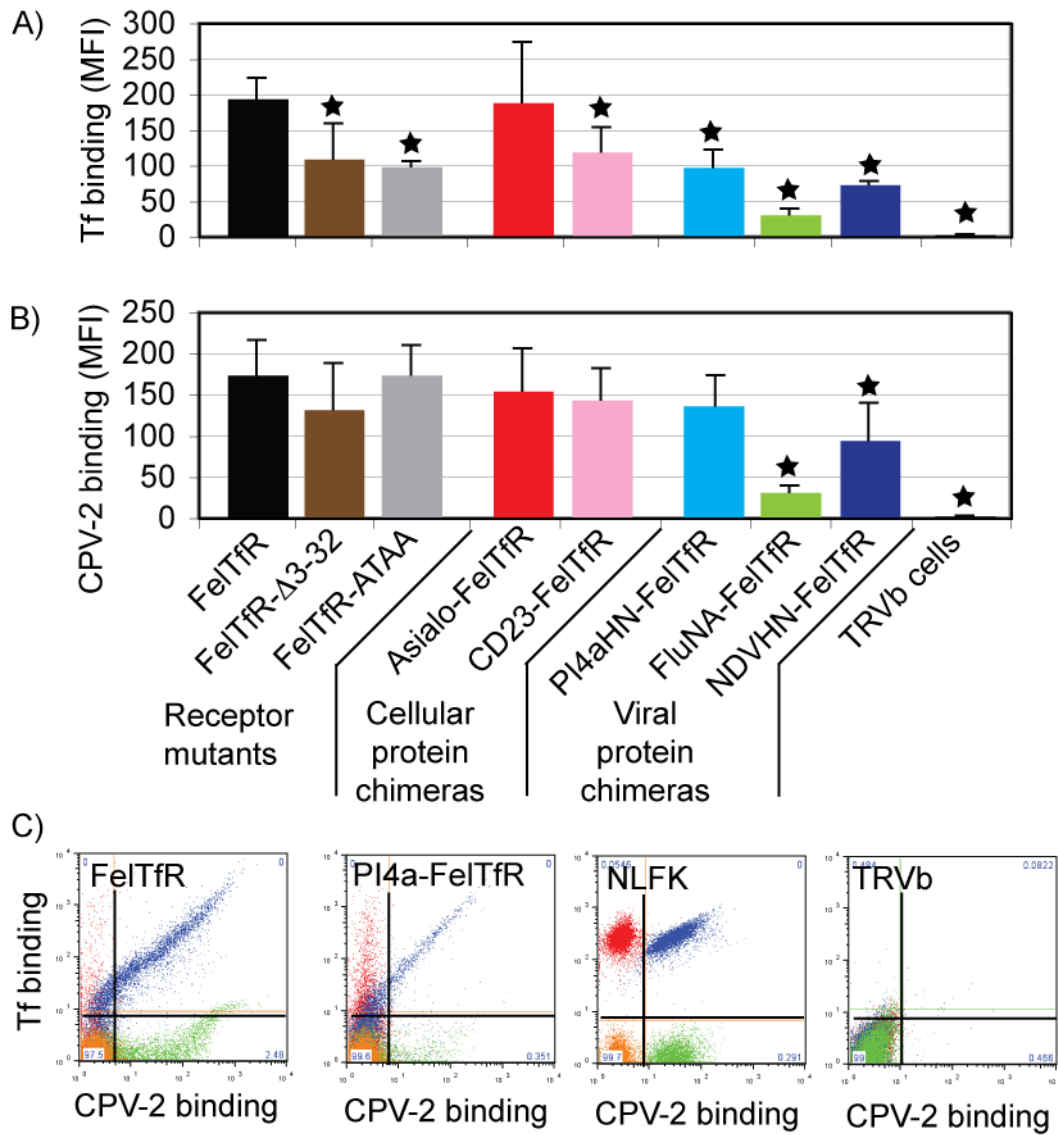
Figure 3.4. Functionality of mutant receptors for binding and uptake of Tf or CPV-2. Transiently transfected TRVb cells expressing the various receptors were incubated for one hour at 37°C with 10 mg/mL Alexa-488 labeled (A) canine Tf or (B) CPV-2, then washed extensively. Cell-associated fluorescence was detected using flow cytometry. The mean fluorescence intensity (MFI) of ligand binding to the transfected population or the complete population of untransfected TRVb cells, measured in at least 3 independent experiments, is shown. Receptors binding significantly less ligand than the wild-type receptor are indicated ($p < 0.05$). C) Example flow cytometry plots showing the binding levels of TRVb cells transfected two of the variant TfRs, as well as untransfected NLFK (positive control) and TRVb (negative control) cells. Cells were incubated with Alexa488-CPV-2 or Cy5-Tf alone (green and red data, respectively) or together (blue data). Control cells with no ligand added are shown in orange.

To further examine the endocytic defects in cells expressing the variant receptors, the kinetics of Tf uptake were examined by binding for short periods of time ranging from 15 seconds to 20 minutes (Figure 3.5). Most of the receptors showed slower uptake kinetics than wild-type, except for Asialo-TfR. The viral chimeras that allowed the lowest levels of infection (FluNA-TfR, NDVHN-TfR, PI4aHN-TfR) also had the slowest rates of accumulation as determined by the slope of the curve in different segments. Furthermore, after binding for 10 and 20 minutes, these three chimeras had attained only 20% of wild type association levels.
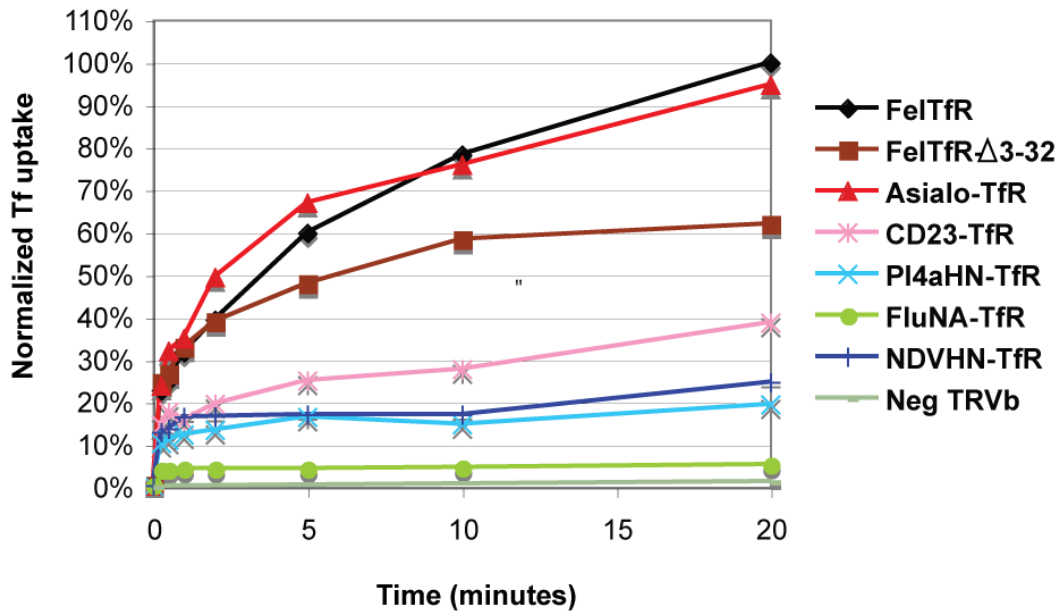
Figure 3.5. Kinetics of canine Tf uptake into cells expressing the variant feline TfRs. Cells were incubated with Alexa-488-labeled canine Tf at 37°C for the indicated times, then were rapidly diluted in ice-cold media to stop further endocytosis. Cells were washed, and cell-associated Tf was quantified using flow cytometry. Graphs indicate the mean fluorescence intensity of the transfected population at each time point normalized to maximum binding to wild-type FelTfR.

3.4e Differences in membrane localization of variant TfRs

Cold detergent extraction was used to determine the localization of a subset of receptors to lipid raft areas of the plasma membrane (Figure 3.6). The wild-type FelTfR,

Asialo-TfR, and PI4aHN-TfR primarily segregated to the non-lipid raft associated, detergent extracted fraction, while only FluNA-TfR stayed associated with the lipid raft membrane subdomains in the detergent resistant fraction as has been previously shown (24). Western blotting for caveolin-1 was used as a positive control for a protein expected to associate to lipid rafts, and as expected showed ~50% association with detergent resistant membranes (data not shown).
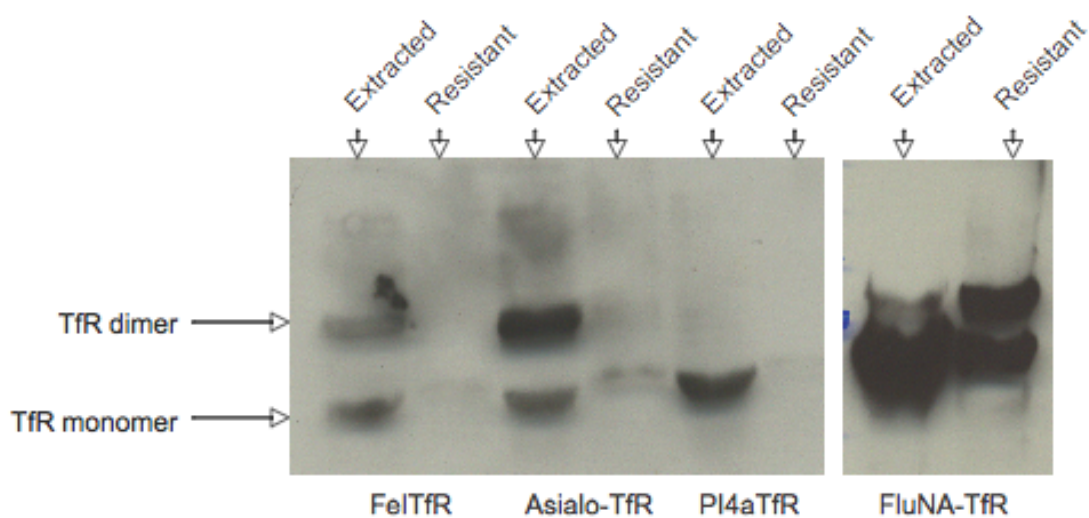
Figure 3.6. Association of a subset of the chimeric TfRs with detergent insoluble membranes. The results show Western blots of the cold detergent resistant and extracted fractions from cells expressing the wild-type or mutant TfRs. The blots were probed with an anti-TfR monoclonal antibody and a horseradish peroxidase-conjugated secondary antibody. Not shown are blots stained with an anti-caveolin antibody showing ~50% of this protein localizing to the detergent resistant fraction.

3.4f Differences in intracellular trafficking of CPV in association with variant TfRs

Alexa488-labeled CPV-2 uptake into cells expressing a subset of the receptor chimeras was examined by fixed and live-cell microscopy, and the receptors showed distinct patterns of uptake in some cases. The wild-type FelTfR allowed apparent rapid uptake from the cell surface and localization to a perinuclear region within the first 30 to

45 minutes of incubation, comparable to results previously obtained in feline cells

(Figure 3.7A) (22). In contrast, the chimeric TfRs with cytoplasmic and TM sequences

from viral proteins (PI4aHN-TfR and FluNA-TfR) bound virus at the cell surface, but

similar showed little apparent endocytosis within 10 minutes with the majority of virus

localized at the cellular periphery (Figure 3.7B and C).
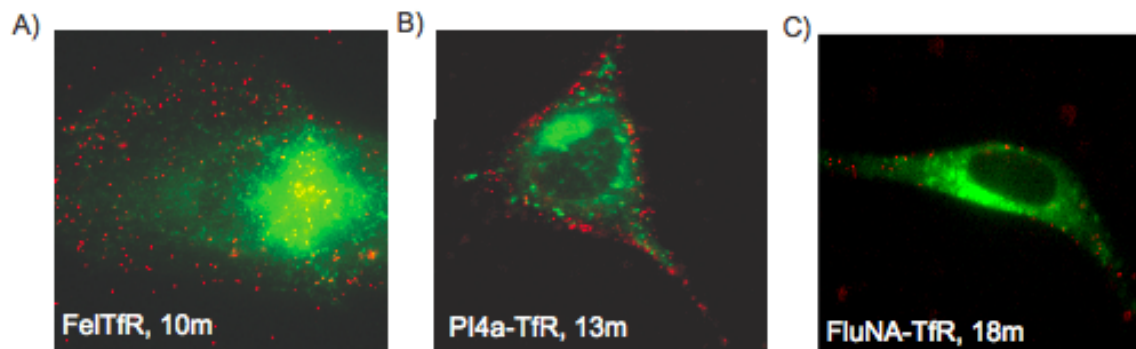
Figure 3.7. Altered endocytosis associated with mutant TfRs. Uptake of Alexa-594-fluorescently labeled virus into cells expressing mutant TfRs and Rab7-GFP, a marker of the late endosome, was examined by live-cell microscopy. Virus was incubated with cells for five minutes, then washed and imaged at 10-15 minutes total time. Shown are representative images of the different uptake patterns observed, including (A) wild type FelTfR demonstrating rapid uptake, and (B) PI4AHN-TfR or (C) FluNA-TfR showing the delay in uptake by the viral chimeras. In each image, viral particles are red, and the late endosomal compartment is depicted in green.

After a 45 minute incubation, the majority of capsids had concentrated in the

perinuclear region in cells expressing the wild-type FelTfR and could be readily

observed to co-localize with Rab7, a marker of the late endosome (Figure 3.8A). In cells

expressing FluNA-TfR, virions were still located in the cell periphery at later time points

(examined up to 2 hours) (Figure 3.8B), though by this later time point capsids had

begun to localize to the perinuclear area in the PI4aHN-TFR expressing cells (data not

shown).
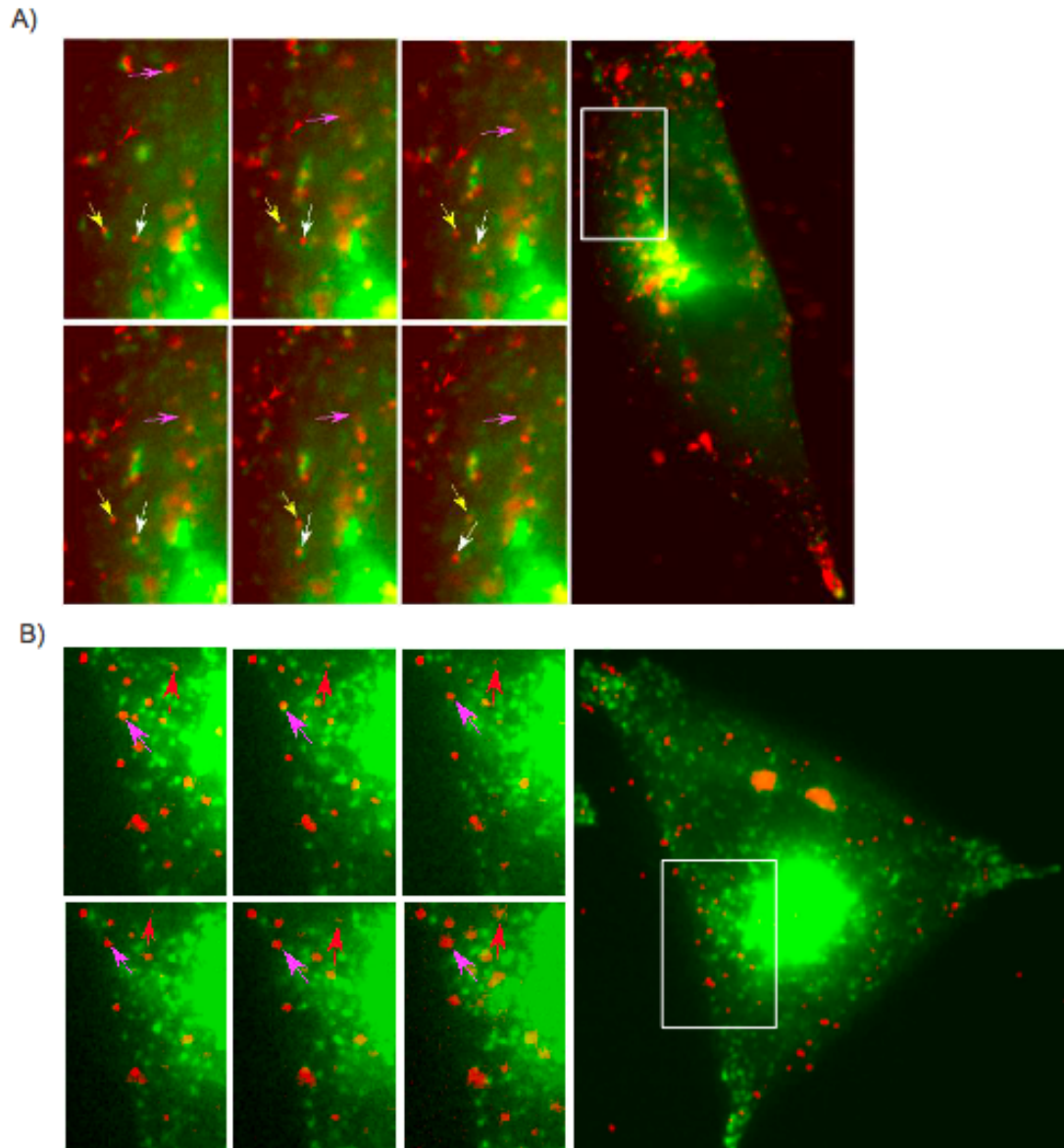
Figure 3.8. Intracellular trafficking patterns of virus associated with variant TfRs.
Endocytosis of Alexa 594-fluorescently labeled virus into cells co-expressing mutant
TfRs and Rab7-GFP was examined by live-cell microscopy for up to two hours after
binding. A) After 20 to 45 minutes, virus bound to the wild-type FeITfR reached the
perinuclear area and could be seen to co-localize and co-traffic (arrows) with the Rab7
marker of the late endosome. B) In cells expressing FluNA-TfR the virus remained
localized at the cell periphery with little movement for extended periods of time. A series
of six time-lapse images from a portion of each cell is shown at left, with frames set five
seconds apart. The complete image of the representative cell is shown at right,
highlighting the area shown in the time-lapse images (white box).

3.5 Discussion

The specific receptor binding interaction and the endocytic pathways followed by incoming virus capsids are important for the success of infection. While some of the requirements for cellular entry have been defined for parvoviruses, little is known about the requirements or flexibility for using specific uptake and intracellular trafficking pathways. Here we used a variety of approaches to assess the uptake and trafficking of the virus-receptor complex early in infection. The receptors were expressed in cells that do not otherwise bind the virus as they lack the endogenous TfR. This allows analysis of mutant TfR properties without the background of other receptors. The hamster-origin TRVb cells expressing wild-type FelTfR became susceptible to infection at levels similar to those of feline cells, suggesting that although the receptor was significantly overexpressed in many cells in this context, other aspects of the infection process are comparable between cells from the different species (cats and hamsters). In this study, the receptor uptake and trafficking properties were altered using mutant and chimeric TfRs with alternative cytoplasmic and transmembrane domains. The extracellular domain is identical between the mutants except for the first few residues of the stalk domain, which is not involved in ligand binding, so that the structural interaction between the virus and receptor is expected to be preserved. Thus the differences in virus uptake and infection are most likely explained by one or more alterations in cell surface receptor density and distribution, mechanism and efficiency of endocytosis, and intracellular trafficking.

3.5a Expression of variant receptors

Although expressed from the same promoter, the receptors varied in their levels of cellular expression as measured by antibody staining. The invariant chain chimera (Ii-TfR) showed only very low levels of cellular expression, likely due to the presence of a lysosomal targeting sequence in its cytoplasmic domain. The SV5 chimeric receptor (SV5HN-TfR) also expressed poorly, possibly due to misfolding or some other defect in expression or trafficking. The other receptors, except for FluNA-TfR, were expressed at levels approximately three times higher than in native feline cells, and bound antibody to levels within two-fold of wild-type FelTfR expressed in TRVb cells. This level of expression should be considered when analyzing the uptake patterns of these receptors, as the degree of cross-linking, mechanism of uptake, and/or other factors may be affected by receptor expression level and surface density.

3.5b Endocytosis of the variant TfRs

The sequences used to construct the receptor chimeras were derived from type II cellular or viral glycoproteins that traffic to the cell surface, a property clearly essential for a protein to act as a primary receptor for mediating infection by extracellular viruses. Binding of Tf for very short periods (15 to 30 seconds) can be taken as a rough measure of the amount of receptor present on the cell surface at any one time. The results show that all receptors were functionally expressed on the cell surface, although as with overall cellular expression, the surface levels were variable between the mutants. The mutant receptors also varied in their ability to bind and take up Tf over longer periods of time, and the timeframe used in Figure 3.4 (60 minutes at 37°C) was chosen to mimic the conditions used in infection. When this long incubation was used,

the patterns of binding for Tf and CPV-2 generally paralleled the whole-cell expression level as measured by antibody staining, although Tf was a more sensitive ligand for detecting deficiencies in uptake between the cellular mutants. Why most of the mutants bind comparatively less Tf than wild-type FeITfR after a one-hour incubation but do not show significant differences in CPV binding over this time frame is unclear. The large size of virus capsids and the ability to cross-link at least some receptors may result in reduced efficiency of endocytosis and receptor recycling that would limit the rate at which cumulative increase in viral association (and thus differences) could be detected.

Differences in the kinetics of Tf uptake over periods of seconds to minutes were also found between the mutant receptors. During cellular infection, CPV capsids attach to the cell surface and are endocytosed into clathrin-coated pits within approximately two minutes (D. Cureton, personal communication). In studies using Tf as a ligand, TfR uptake occurs rapidly with ~10% of the surface population endocytosed per minute (32). Thus the measured time points are appropriate given the expected uptake kinetics of the wild-type receptor. TfR uptake kinetics have been previously studied in vitro by binding Tf for varying amounts of time and then removing the residual surface proportion of Tf by an acid wash followed by a neutral pH wash. This treatment mimics the conditions seen in a normal round of endocytosis, and allows examination of how quickly bound Tf is endocytosed under different conditions. Acid washing did not remove the Alexa-488-labeled Tf from the surface of the cell (data not shown), so the results in Figure 3.5 show the kinetics of cumulative Tf association with the cell. While less transferrin is bound overall in those mutants where expression is less than wild-type FeITfR as measured by antibody staining, these data also indicate that the rate of

uptake varies between the receptors. While this experiment cannot specifically distinguish the contribution of endocytosis versus receptor recycling rates, it does begin to address the overall dynamics of the different mutant receptors. Further studies would be required to separate out the specific differences between the receptors during individual steps of the receptor trafficking cycle.

3.5c Association of the TfRs with membrane subdomains

The final aspect of receptor surface expression examined in this study involved determining association of the variant TfRs with lipid raft domains. The association of viral receptors with plasma membrane micro-domains rich in cholesterol and sphingolipids (lipid rafts) or non-raft-associated membrane domains can affect pathways available for uptake as well as intracellular destination. Often defined by their relative resistance to extraction with cold Triton X-100, raft association can give a crude indication of receptor properties related to membrane sub-localization (52). Although the composition and properties of these micro-domains are still unresolved, they appear to represent regions of different lipid composition that are small (five to 10 nm) and dynamic in size and composition (65). Clustering of protein and lipid components can increase the size and stability of these domains and can trigger endocytosis through raft-associated pathways. Raft association is also involved in the budding process of some viruses during viral egress, and specific transmembrane sequences can target individual viral proteins, such as the influenza virus neuraminidase, to these structures (7). Protein targeting to lipid rafts can also be achieved through association with additional proteins, as is the case with the HN protein of some paramyxoviruses (53). The NDV HN protein, for example, segregates to detergent resistant membranes only

through association with the viral fusion (F) protein and not based of any intrinsic feature of the HN protein itself (28). In the context of the chimeric receptors, the FluNA-TfR chimera has been previously shown to segregate to lipids rafts (24).

A subset of receptors were tested for lipid raft association in this study, but the sensitivity of Western blotting for the transfected receptors precluded visualization of the NDVHN-FelTfR and CD23-TfR chimeras. Without the presence of the viral F protein for targeting, the NDVHN-TfR would likely behave similarly to the PI4aHN-TfR construct and would not segregate to rafts; however, this remains to be confirmed experimentally. CD23-TfR was also unable to be visualized, but given its expected interaction with the clathrin machinery it is likely to behave like Asialo-GPR and wild-type FelTfR and segregate to non-lipid raft domains of the plasma membrane.

3.5d Pathways to parvoviral infection

Although CPV and FPV bind the wild-type feline TfR and are rapidly endocytosed, the subsequent fate of the virus and the requirements for specific pathways to infection are not well understood. Under normal cellular conditions, the Tf-TfR complex follows a well defined pathway of rapid clathrin-mediated uptake into the early endosome, with >99% of the complexes rapidly recycling to the plasma membrane through the pericentriolar recycling endosome (54). Cross-linking of the TfR alone is enough to retain the receptor in the endosomal system for longer periods of time, and may divert a higher percentage into the degradative compartment, regardless of the specific transmembrane and cytoplasmic sequences (32). This may be the case for the multivalent viral ligand, despite structural studies that have suggested that only one or a few receptors become associated with each viral capsid because, as with bivalent

antibodies, binding of only two receptors would be enough to facilitate cross-linking (21). The importance of the degradative compartment for infection was previously suggested by experiments where infection was inhibited in cells expressing a dominant negative form of the Rab7 protein normally associated with the late endosome, but not in cells expressing a dominant negative form of the Rab11 protein associated with the recycling endosome (22). The invariant chain chimera (Ii-TfR) was constructed as an attempt to determine the effects of diverting a higher percentage of receptor into the degradative compartment, but this receptor was not measurably expressed on the cell surface and was unable to be tested.

Previous results also showed that the virus rapidly disseminates to multiple intracellular compartments during a timeframe in which it is expected to remain associated with the receptor (22, 63). This result was also seen with the mutant TfRs in this study, though quantifying the proportion of virus-receptor complexes entering individual compartments during perinuclear accumulation was difficult due to poor resolution and high background GFP signal. However, the particle to infectivity ratio of CPV and FPV is very high, and simply characterizing the location where the majority of viral particles go may not reflect what compartments are actually important for infection. Additional studies will be required to clarify these requirements, specifically in the context of the signals that the virus requires in order to initiate infection, for example low pH and exposure to intracellular factors such as proteases.

In this study, mutant and chimeric transferrin receptors were examined to determine the importance of the transmembrane and cytoplasmic domains for cellular uptake and infection by parvoviruses. Chimeric and mutant receptors mutants were

identified that allowed entry and infection within two fold of the wild-type receptor,

indicating that there are no specific sequence requirements contained in the wild-type

version of these domains. The infection-permissive receptors had tails with sequences

from proteins expected to use clathrin-mediated endocytosis (asialoglycoprotein

receptor I, Fc epsilon receptor II), as well as receptor mutants that lacked the YTRF

internalization sequence (FeITfR-ATAA, FeITfR-Δ3-32) and thus had no known clathrin

interacting motifs. These results show that there is no absolute requirement for

sequences that interact with components of the clathrin-mediated mechanism of

endocytosis. Finally, while the receptors prepared from viral type II glycoproteins allow

some level of receptor expression and can bind capsids and mediate endocytosis, those

led to only very low levels of infection. Cellular infection by viruses requires a certain

threshold level of viral uptake, but beyond that these results indicate that the

transmembrane and cytoplasmic receptor domains do play a role in the infection

process by determining how the receptor is trafficked to and from the cell surface.

Further studies should seek to clarify the role for specific endocytic pathways and

intracellular trafficking destinations that are required by parvoviruses to trigger

uncoating in an environment that leads to productive infection.

3.6 Acknowledgements

3.7 References

1.   **Agbandje, M., R. McKenna, M. G. Rossmann, M. L. Strassheim, and C. R. Parrish.** 1993. Structure determination of feline panleukopenia virus empty particles. Proteins **16:** 155-171.

2.   **Anderson, H. A., Y. Chen, and L. C. Norkin.** 1996. Bound simian virus 40 translocates to caveolin-enriched membrane domains, and its entry is inhibited by drugs that selectively disrupt caveolae. Mol Biol Cell **7:**1825-34.

3.   **Bando, H., K. Kondo, M. Kawano, H. Komada, M. Tsurudome, M. Nishio, and Y. Ito.** 1990. Molecular cloning and sequence analysis of human parainfluenza type 4A virus HN gene: its irregularities on structure and activities. Virology **175:**307-12.

4.   **Bates, G. W., and M. R. Schlabach.** 1973. The reaction of ferric salts with transferrin. J Biol Chem **248:**3228-32.

5.   **Bates, G. W., and J. Wernicke.** 1971. The kinetics and mechanism of iron(3) exchange between chelates and transferrin. IV. The reaction of transferrin with iron(3) nitrilotriacetate. J Biol Chem **246:**3679-85.

6.   **Bennett, M. J., J. A. Lebron, and P. J. Bjorkman.** 2000. Crystal structure of the hereditary haemochromatosis protein HFE complexed with transferrin receptor. Nature **403:**46-53.

7.   **Campbell, S. M., S. M. Crowe, and J. Mak.** 2001. Lipid rafts and HIV-1: from viral entry to assembly of progeny virions. J Clin Virol **22:**217-27.

8.   **Chen, C., and X. Zhuang.** 2008. Epsin 1 is a cargo-specific adaptor for the clathrin-mediated endocytosis of the influenza virus. Proc Natl Acad Sci U S A **105:**11790-5.

9.   **Collawn, J. F., A. Lai, D. Domingo, M. Fitch, S. Hatton, and I. S. Trowbridge.** 1993. YTRF is the conserved internalization signal of the transferrin receptor, and a second YTRF signal at position 31-34 enhances endocytosis. J Biol Chem **268:**21686-92.

10.   **Coyne, C. B., and J. M. Bergelson.** 2006. Virus-induced Abl and Fyn kinase signals permit coxsackievirus entry through epithelial tight junctions. Cell **124:**119-31.

11.   **DeTulleo, L., and T. Kirchhausen.** 1998. The clathrin endocytic pathway in viral infection. Embo J **17:**4585-93.

12. **Ding, W., L. N. Zhang, C. Yeaman, and J. F. Engelhardt.** 2006. rAAV2 traffics through both the late and the recycling endosomes in a dose-dependent fashion. Mol Ther.

13. **Dudleenamjil, E., C. Y. Lin, D. Dredge, B. K. Murray, R. A. Robison, and F. B. Johnson.** 2010. Bovine parvovirus uses clathrin-mediated endocytosis for cell entry. J Gen Virol **91:**3032-41.

14. **Fuchs, H., U. Lucken, R. Tauber, A. Engel, and R. Gessner.** 1998. Structural model of phospholipid-reconstituted human transferrin receptor derived by electron microscopy. Structure **6:**1235-43.

15. **Geffen, I., C. Fuhrer, B. Leitinger, M. Weiss, K. Huggel, G. Griffiths, and M. Spiess.** 1993. Related signals for endocytosis and basolateral sorting of the asialoglycoprotein receptor. J Biol Chem **268:**20772-7.

16. **Gerondopoulos, A., T. Jackson, P. Monaghan, N. Doyle, and L. O. Roberts.** 2010. Murine norovirus-1 cell entry is mediated through a non-clathrin-, non-caveolae-, dynamin- and cholesterol-dependent pathway. J Gen Virol **91:**1428-38.

17. **Giannetti, A. M., P. M. Snow, O. Zak, and P. J. Bjorkman.** 2003. Mechanism for multiple ligand recognition by the human transferrin receptor. PLoS Biol **1:**E51.

18. **Gianni, T., G. Campadelli-Fiume, and L. Menotti.** 2004. Entry of herpes simplex virus mediated by chimeric forms of nectin1 retargeted to endosomes or to lipid rafts occurs through acidic endosomes. J Virol **78:**12268-76.

19. **Girod, A., C. E. Wobus, Z. Zadori, M. Ried, K. Leike, P. Tijssen, J. A. Kleinschmidt, and M. Hallek.** 2002. The VP1 capsid protein of adeno-associated virus type 2 is carrying a phospholipase A2 domain required for virus infectivity. J Gen Virol **83:**973-8.

20. **Govindasamy, L., K. Hueffer, C. R. Parrish, and M. Agbandje-McKenna.** 2003. Structures of host range-controlling regions of the capsids of canine and feline parvoviruses and mutants. J Virol **77:**12211-21.

21. **Hafenstein, S., L. M. Palermo, V. A. Kostyuchenko, C. Xiao, M. C. Morais, C. D. Nelson, V. D. Bowman, A. J. Battisti, P. R. Chipman, C. R. Parrish, and M. G. Rossmann.** 2007. Asymmetric binding of transferrin receptor to parvovirus capsids. Proc Natl Acad Sci U S A **104:**6585-9.

22. **Harbison, C. E., S. M. Lyi, W. S. Weichert, and C. R. Parrish.** 2009. Early steps in cell infection by parvoviruses: host-specific differences in cell receptor binding but similar endosomal trafficking. J Virol **83:**10504-14.

23. **Hueffer, K., L. Govindasamy, M. Agbandje-McKenna, and C. R. Parrish.** 2003. Combinations of two capsid regions controlling canine host range determine canine transferrin receptor binding by canine and feline parvoviruses. J Virol **77:**10099-10105.

24. **Hueffer, K., L. M. Palermo, and C. R. Parrish.** 2004. Parvovirus infection of cells by using variants of the feline transferrin receptor altering clathrin-mediated endocytosis, membrane domain localization, and capsid-binding domains. J Virol **78:**5601-11.

25. **Hueffer, K., J. S. Parker, W. S. Weichert, R. E. Geisel, J. Y. Sgro, and C. R. Parrish.** 2003. The natural host range shift and subsequent evolution of canine parvovirus resulted from virus-specific binding to the canine transferrin receptor. J. Virol. **77:**1718-1726.

26. **Jovic, M., M. Sharma, J. Rahajeng, and S. Caplan.** 2010. The early endosome: a busy sorting station for proteins at the crossroads. Histol Histopathol **25:**99-112.

27. **Kerr, J. R., S. F. Cotmore, M. E. Bloom, R. M. Linden, and C. R. Parrish.** 2006. Parvoviruses. Hodder Arnold, London.

28. **Kim, S. H., Y. Yan, and S. K. Samal.** 2009. Role of the cytoplasmic tail amino acid sequences of Newcastle disease virus hemagglutinin-neuraminidase protein in virion incorporation, cell fusion, and pathogenicity. J Virol **83:**10250-5.

29. **Lamb, R. A., R. G. Paterson, and T. S. Jardetzky.** 2006. Paramyxovirus membrane fusion: lessons from the F and HN atomic structures. Virology **344:**30-7.

30. **Lawrence, C. M., S. Ray, M. Babyonyshev, R. Galluser, D. W. Borhani, and S. C. Harrison.** 1999. Crystal structure of the ectodomain of human transferrin receptor. Science **286:**779-782.

31. **Leser, G. P., K. J. Ector, and R. A. Lamb.** 1996. The paramyxovirus simian virus 5 hemagglutinin-neuraminidaseglycoprotein, but not the fusion glycoprotein, is internalized via coated pits and enters endocytic pathway. Mol. Biol. Cell **7:**155-172.

32. **Marsh, E. W., P. L. Leopold, N. L. Jones, and F. R. Maxfield.** 1995. Oligomerized transferrin receptors are selectively retained by a lumenal sorting signal in a long-lived endocytic recycling compartment. J Cell Biol **129:**1509-1522.

33. **Mattera, R., M. Boehm, R. Chaudhuri, Y. Prabhu, and J. S. Bonifacino.** 2011. Conservation and diversification of dileucine signal recognition by adaptor protein (AP) complex variants. J Biol Chem **286:**2022-30.

34. **McCaffrey, M. W., A. Bielli, G. Cantalupo, S. Mora, V. Roberti, M. Santillo, F. Drummond, and C. Bucci.** 2001. Rab4 affects both recycling and degradative endosomal trafficking. FEBS Lett **495:**21-30.

35. **McGraw, T. E., L. Greenfield, and F. R. Maxfield.** 1987. Functional expression of the human transferrin receptor cDNA in Chinese hamster ovary cells deficient in endogenous transferrin receptor. J Cell Biol **105:**207-14.

36. **Meier, O., and U. F. Greber.** 2004. Adenovirus endocytosis. The journal of gene medicine **6 Suppl 1:**S152-63.

37. **Mercer, J., and A. Helenius.** 2008. Vaccinia virus uses macropinocytosis and apoptotic mimicry to enter host cells. Science **320:**531-5.

38. **Mercer, J., M. Schelhaas, and A. Helenius.** 2010. Virus entry by endocytosis. Annu Rev Biochem **79:**803-33.

39. **Mohrmann, K., and P. van der Sluijs.** 1999. Regulation of membrane transport through the endocytic pathway by rabGTPases. Mol Membr Biol **16:**81-7.

40. **Montagnac, G., A. Molla-Herman, J. Bouchet, L. C. Yu, D. H. Conrad, M. H. Perdue, and A. Benmerah.** 2005. Intracellular trafficking of CD23: differential regulation in humans and mice by both extracellular and intracellular exons. J Immunol **174:**5562-72.

41. **Munter, S., M. Way, and F. Frischknecht.** 2006. Signaling during pathogen infection. Sci STKE **2006:**re5.

42. **Norkin, L. C., and D. Kuksin.** 2005. The caveolae-mediated sv40 entry pathway bypasses the golgi complex en route to the endoplasmic reticulum. Virol J **2:**38.

43. **Novick, P., and M. Zerial.** 1997. The diversity of Rab proteins in vesicle transport. Curr Opin Cell Biol **9:**496-504.

44. **Palermo, L. M., K. Hueffer, and C. R. Parrish.** 2003. Residues in the apical domain of the feline and canine transferrin receptors control host-specific binding and cell infection of canine and feline parvoviruses. J Virol **77:**8915-8923.

45. **Pandey, K. N.** 2010. Small peptide recognition sequence for intracellular sorting. Curr Opin Biotechnol **21:**611-20.

46. **Parker, J. S., W. J. Murphy, D. Wang, S. J. O'Brien, and C. R. Parrish.** 2001. Canine and feline parvoviruses can use human or feline transferrin receptors to bind, enter, and infect cells. J Virol **75:**3896-902.

47. **Parker, J. S., and C. R. Parrish.** 1997. Canine parvovirus host range is determined by the specific conformation of an additional region of the capsid. J Virol **71:**9214-22.

48. **Parrish, C. R.** 1991. Mapping specific functions in the capsid structure of canine parvovirus and feline panleukopenia virus using infectious plasmid clones. Virology **183:**195-205.

49. **Parrish, C. R., P. Have, W. J. Foreyt, J. F. Evermann, M. Senda, and L. E. Carmichael.** 1988. The global spread and replacement of canine parvovirus strains. J Gen Virol **69 (Pt 5):**1111-6.

50. **Pelkmans, L., and A. Helenius.** 2003. Insider information: what viruses tell us about endocytosis. Curr Opin Cell Biol **15:**414-22.

51. **Querbes, W., B. A. O'Hara, G. Williams, and W. J. Atwood.** 2006. Invasion of host cells by JC virus identifies a novel role for caveolae in endosomal sorting of noncaveolar ligands. J Virol **80:**9402-13.

52. **Rajendran, L., and K. Simons.** 2005. Lipid rafts and membrane dynamics. J Cell Sci **118:**1099-102.

53. **Ravid, D., G. P. Leser, and R. A. Lamb.** 2010. A role for caveolin 1 in assembly and budding of the paramyxovirus parainfluenza virus 5. J Virol **84:**9749-59.

54. **Ren, M., G. Xu, J. Zeng, C. De Lemos-Chiarandini, M. Adesnik, and D. D. Sabatini.** 1998. Hydrolysis of GTP on rab11 is required for the direct delivery of transferrin from the pericentriolar recycling compartment to the cell surface but not from sorting endosomes. Proc Natl Acad Sci U S A **95:**6187-92.

55. **Sainte-Marie, J., V. Lafont, E. I. Pecheur, J. Favero, J. R. Philippot, and A. Bienvenue.** 1997. Transferrin receptor functions as a signal-transduction molecule for its own recycling via increases in the internal Ca2+ concentration. Eur J Biochem **250:**689-97.

56. **Scheiffele, P., A. Rietveld, T. Wilk, and K. Simons.** 1999. Influenza viruses select ordered lipid domains during budding from the plasma membrane. J Biol Chem **274:**2038-44.

57. **Sharma-Walia, N., H. H. Krishnan, P. P. Naranatt, L. Zeng, M. S. Smith, and B. Chandran.** 2005. ERK1/2 and MEK1/2 induced by Kaposi's sarcoma-associated herpesvirus (human herpesvirus 8) early during infection of target

cells are essential for expression of viral genes and for establishment of infection. J Virol **79:**10308-29.

58. **Sheff, D. R., E. A. Daro, M. Hull, and I. Mellman.** 1999. The receptor recycling pathway contains two distinct populations of early endosomes with different sorting functions. J Cell Biol **145:**123-139.

59. **Suikkanen, S., K. Saajarvi, J. Hirsimaki, O. Valilehto, H. Reunanen, M. Vihinen-Ranta, and M. Vuento.** 2002. Role of recycling endosomes and lysosomes in dynein-dependent entry of canine parvovirus. J Virol **76:**4401-11.

60. **Tsai, B.** 2007. Penetration of nonenveloped viruses into the cytoplasm. Annu Rev Cell Dev Biol **23:**23-43.

61. **Van Dam, E. M., T. Ten Broeke, K. Jansen, P. Spijkers, and W. Stoorvogel.** 2002. Endocytosed transferrin receptors recycle via distinct dynamin and phosphatidylinositol 3-kinase-dependent pathways. J Biol Chem **277:**48876-83.

62. **Vihinen-Ranta, M., L. Kakkola, A. Kalela, P. Vilja, and M. Vuento.** 1997. Characterization of a nuclear localization signal of canine parvovirus capsid proteins. Eur J Biochem **250:**389-394.

63. **Vihinen-Ranta, M., D. Wang, W. S. Weichert, and C. R. Parrish.** 2002. The VP1 N-terminal sequence of canine parvovirus affects nuclear transport of capsids and efficient cell infection. J Virol **76:**1884-91.

64. **Wang, X., R. Kumar, J. Navarre, J. E. Casanova, and J. R. Goldenring.** 2000. Regulation of vesicle trafficking in madin-darby canine kidney cells by Rab11a and Rab25. J Biol Chem **275:**29138-46.

65. **Wilson, B. S., S. L. Steinberg, K. Liederman, J. R. Pfeiffer, Z. Surviladze, J. Zhang, L. E. Samelson, L. H. Yang, P. G. Kotula, and J. M. Oliver.** 2004. Markers for detergent-resistant lipid rafts occupy distinct and dynamic domains in native membranes. Mol Biol Cell **15:**2580-92.

66. **Yeung, D. E., G. W. Brown, P. Tam, R. H. Russnak, G. Wilson, I. Clark-Lewis, and C. R. Astell.** 1991. Monoclonal antibodies to major nonstructural nuclear protein of minute virus of mice. Virology **181:**35-45.

CHAPTER FOUR: THE ROLE OF INTERMEDIATE HOSTS IN CROSS-SPECIES VIRUS TRANSMISSION DURING ADAPTATION OF CANINE PARVOVIRUS TO DOGS

4.1 Abstract

Understanding the factors that lead to the successful cross-species transmission of viruses is critical to anticipating and potentially controlling disease emergence. Here we show that the emergence of parvoviruses in raccoons resulted from multiple cross-species transmissions of feline panleukopenia virus (FPV) and canine parvovirus (CPV). CPV is a host range variant of FPV that caused a global pandemic in dogs when it emerged in 1978. By 1980, the original CPV type-2 (CPV-2) had been replaced in the wild by an antigenic variant designated CPV type-2a (CPV-2a), and additional CPV-2b and CPV-2c variants have arisen more recently as single point mutations of CPV-2a. Most raccoon isolates examined here fell between CPV-2 and CPV-2a in phylogenetic trees, identifying this species as an intermediate host that facilitated the evolution of later CPV strains. These strains had a spatial distribution covering much of the eastern United States and molecular clock estimates place their origin in the 1980s, suggesting that they have been circulating unrecognized for over 20 years. All CPV-like raccoon viruses had an aspartic acid at VP2 residue 300 that evolved in parallel multiple times across the parvovirus phylogeny. In the raccoon viruses derived from CPV, this 300Asp mutation, in combination with additional changes at other capsid surface residues, resulted in the inability to infect canine cells. These mutations were also associated with unique transferrin receptor (TfR) binding patterns and reactivity with monoclonal antibodies. The sequence of the raccoon TfR was intermediate between the feline and canine TfR, further supporting a role for raccoons in CPV evolution and adaptation.

4.2 Introduction

The transfer of viruses into new hosts is a cause of novel disease epidemics that pose a significant threat to human and animal health. However, the genetic and evolutionary mechanisms underlying cross-species virus transmission are still only partially understood. Well-documented historical examples of host-jumping events are rare, but provide opportunities to define the processes that underpin viral emergence. Here we examined a series of parvoviruses that have transferred from different hosts into raccoons (*Procyon lotor*) in North America, providing multiple examples of cross-species virus transmission and host adaptation.

Feline panleukopenia virus (FPV) and FPV-like viruses infect and cause disease in many animals within the order Carnivora, including large and small cats, mink, raccoons, and foxes. Previous studies have shown that these viruses are not readily distinguishable genetically or antigenically (36, 41). Canine parvovirus type-2 (CPV-2) emerged as a new virus of dogs in the late 1970s, and its capsid protein differs by only a few amino acids from FPV (14, 26, 33). The original 1978 CPV-2 strain was replaced worldwide between 1979 and 1980 by a genetic and antigenic variant, designated CPV type-2a (CPV-2a). All extant canine viruses are descendents of CPV-2a, including the mutants termed CPV-2b and CPV-2c that are defined by substitutions of residue 426 in the capsid protein VP2 (31).

The host ranges associated with FPV and CPV-2 are largely determined by mutations in the viral capsid proteins that control the ability to bind the transferrin receptor type 1 (TfR) on their host cells (13, 24). FPV does not infect dogs or canine cells *in vitro* due to the presence of a glycosylation specific for the canine TfR that

prevents FPV attachment (23). CPV-2 acquired the ability to bind the canine TfR and thus gained the canine host range by substitutions at VP2 residues 93 (Lys to Asn) and 323 (Asp to Asn) (5), but had lost the feline host range due to concurrent changes at residues 80, 564, and 568. The CPV-2a variant contained additional VP2 changes at residues 87 (Met to Tyr), 101 (Ile to Thr), 300 (Ala to Gly), and 305 (Asp to Tyr). These changes expanded the viral host range by allowing the virus to once again infect cats while simultaneously decreasing its binding affinity for the feline TfR (23, 42).

In addition to controlling viral host range, the genetic differences between parvovirus strains affect antigenicity. The capsid's two major antigenic sites are found near the top of the three-fold spike ("A site") and near the center of the asymmetric unit of the capsid, partially overlapping with the TfR binding site ("B site") (10, 37). Different reactivity with monoclonal antibodies (MAbs) can readily distinguish FPV, CPV-2, and the newer CPV variants (34, 37).

Raccoons are found throughout their native North American range, as well as in parts of Europe and Asia following introductions to those continents in the twentieth century (22, 44). They have long been recognized as a host for a virus antigenically indistinguishable from FPV that has been named raccoon parvovirus (RPV) (18, 43). Historically, raccoons were reported to be resistant to CPV-2 infection (2, 4). However, since 2007, parvovirus isolates have been recovered from raccoons in North America that appeared to be derived from CPV-2 (16). Here we show that multiple independent introductions of FPV- and CPV-like viruses into raccoons have occurred, and that these viruses harbor key changes in capsid residues associated with host adaptation, TfR binding, and viral antigenicity.

4.3 Materials and methods

4.3a Cells and cell culture

CHO-derived TRVb cells that lack an endogenous TfR (19) were grown in Ham's F12 media containing 10% fetal bovine serum. Crandell Reese feline kidney (CRFK) cells, Norden Laboratory feline kidney (NFLK) cells, and canine CF2Th and A72 cells were grown in 1:1 mixture of McCoy's 5A and Liebovitz L15 media with 5% fetal bovine serum.

4.3b Viruses and their preparation

The viruses examined here are listed in Table 4.1. For virus isolation, homogenized tissue or fecal samples were filtered and used to infect CRFK or NLFK cells. Viral DNA was amplified using polymerase chain reaction (PCR) directly from tissue extracts or after passage in cell culture. For formalin-fixed paraffin-embedded (FFPE) blocks, viral DNA was extracted using a commercial QuickExtract FFPE DNA Extraction Kit (Epicentre Biotechnologies, Madison, WI). Amplification was performed using Phusion Hot Start High Fidelity DNA polymerase (Finnzymes, Espoo, Finland). Amplicons covering the complete VP2 protein sequence, or the entire nonstructural and structural coding regions in some cases, were sequenced directly or after cloning using a PCR Cloning Kit (Qiagen, Valencia, CA). Products amplified from FFPE tissues were truncated (186 bp) and focused on the critical region that included VP2 residues 297, 300, 305, and 323. Control viruses were derived from infectious plasmid clones of FPV (FPV-b), CPV-2 (CPV-d), and CPV-2b (CPV-39) (13, 27) and purified as previously described (1). Viral inocula were prepared by passage in NLFK cells, homogenizing the

142

supernatant and cell fractions using freeze-thaw cycles, and clarifying the inoculum

through a Steriflip filter (Millipore, Billerica, MA).

Table 1. **Parvovirus isolates.** The prototype strains of FPV, CPV-2, and CPV-2b examined here and new isolates obtained in this study, grouped where appropriate when obtained from the same outbreak. Clinical features of the outbreak are included where available from the sample submission forms received with the diagnostic sample.

Isolate	Origin county, state, date	Number affected in outbreak, age, mortality
CPV/Rac/VA/118-A/07	Virginia Sept, 2007	8, 4-5 months old, 4 died.
CPV/Rac/GA/287/08 CPV/Rac/GA/289/08 CPV/Rac/GA/349/08	Georgia Oct-Nov, 2008	Several infections, 2-7 months, 3 died.
CPV/Rac/TN/351/09	Tennessee May, 2009	2 litters affected, <1.5 months old, multiple deaths
CPV/Rac/FL/381/09	Florida July, 2009	Several infected, ~1 month old, 1 death.
CPV/Rac/VA/278/09	Virginia Aug, 2009	Unknown number affected, <6months old, 4 deaths
CPV/Rac/KY/358/09 CPV/Rac/KY/9552/09 CPV/Rac/KY/3817/09	Kentucky Nov, 09	23 affected, unknown age, unknown mortality.
CPV/Rac/NY/92742/10	New York Aug, 2010	Several affected, <6 months old, 6 deaths.
CPV/Rac/NJ/76836/10	New Jersey Aug, 2010	8 affected, 14-16 weeks old, 7 deaths.
CPV/Rac/WI/37/10	Wisconsin 2010	Unknown
CPV/Bobcat/KS/44/10	Kansas 2010	Unknown
FPV/Rac/CA/208/10	California 2010	Unknown

4.3c Evolutionary analysis

The VP2 sequences of different carnivore parvovirus were compiled from GenBank (n = 498), one of which (GenBank accession M24005) was sampled from a raccoon in 1979. These sequences were combined with the 18 raccoon sequences determined here, resulting in a final data set of 516 sequences of length 1755 bp. All sequences included in this analysis covered at least 2/3 of the VP2 gene. Similar analyses were also conducted using full-length sequences of NS1 and VP2 where available (61 and 125 sequences, respectively). Sequence alignments were obtained using MUSCLE 3.7 (8). The phylogenetic relationships among these sequences were inferred using the maximum likelihood (ML) method implemented in PAUP* 4.0 (39), incorporating the general time-reversible substitution model with invariant sites and a gamma distribution of among-site rate variation (GTR+I+Γ_4), and were partitioned by codon positions as this was the best-fit nucleotide substitution model determined by Modeltest 3.7 (35). Tree-bisection-reconnection (TBR) branch swapping was also employed. To assess the robustness of the phylogenetic groupings observed, a bootstrap resampling analysis was performed using 1000 replicate neighbor-joining trees estimated under the ML substitution model described above, again utilizing PAUP* 4.0.

The time to the most recent common ancestor (TMRCA) of the raccoon sequences was estimated using the Bayesian Markov Chain Monte Carlo (MCMC) method available in the BEAST package (7). This analysis incorporated the nucleotide substitution model described above, as well as a relaxed (uncorrelated lognormal) molecular clock and the conservative Bayesian skyline model as a coalescent prior.

Statistical support was depicted as 95% Highest Probability Density (HPD) values, and the MCMC analysis was run until convergence was achieved in all parameters. The BEAST analysis also allowed us to infer the Maximum Clade Credibility (MCC) tree for these data, such that TMRCA values could be estimated for specific nodes. The MCC tree was topologically very similar to that produced in the ML analysis.

4.3d The raccoon transferrin receptor (rTfR)

Messenger RNA (mRNA) from raccoon PI 1Ut (NBL-9) cells (ATCC, Manassas, VA) or from raccoon tissues was extracted using the Oligotex Direct mRNA Mini kit (Qiagen), amplified using reverse transcriptase PCR (RT-PCR), and was cloned into the pcDNA3.1(+) plasmid and sequenced as previously described (24).

4.3e Antigenic analysis

28 mouse or rat monoclonal antibodies (MAbs) against CPV-2, FPV, or CPV-2b have been previously described (28, 30, 34). For hemagglutination inhibition (HI) assays, antibodies were tested using standard methods, and titers were compared to the virus against which the MAb was raised (37). Briefly, MAb hybridoma supernatant was serially diluted and incubated with 8 hemagglutinating (HA) units of virus for one hour at 20°C. Feline erythrocytes (0.5% v/v) in 20 mM Bis±Tris (pH 6.2) and 150 mM NaCl were added and the plates incubated at 4°C for 2 hours (3, 40). HI titer was scored as the first MAb dilution containing greater than 50% agglutinated cells, and was compared relative to the prototype virus against which the MAb was raised.

4.3f Cell infection and binding assays

Infection in NLFK, A72, or Cf2Th cells was assessed using standard methods for $TCID_{50}$ assays (42). Cell binding was analyzed using purified virus capsids as indicated

diluted to 10 μg/mL in DMEM 0.1% BSA and incubated in solution for 60 minutes at 37°C with NLFK or Cf2Th cells, or TRVb cells transfected with plasmids expressing the feline, canine, or raccoon TfR (9). Cells were fixed with 4% paraformaldehyde (PFA), and cell-associated virus capsids were detected with MAb 2 and goat anti-mouse-Alexa 488 (Sigma). Binding level was quantified using a Guava EasyCyte Plus flow cytometer (Guava Technologies).

4.4 Results

4.4a Parvoviruses in raccoons

We analyzed parvoviruses isolated between 2007 and 2010 from juvenile raccoons in several states in the USA, as well as raccoon viruses in our collections that were originally sampled between 1978 and 1990 (Table 4.1). All examined animals from 2007-2010 exhibited diarrhea associated with severe enteritis and had parvovirus antigen expression in the intestines, mesenteric lymph nodes, and/or less frequently in the cerebellum (data not shown).

The 19 VP2 sequences of viruses from raccoons were aligned with 497 FPV- and CPV partial VP2 sequences and subjected to phylogenetic analysis. Sequences of CPV-like viruses isolated from leopard cats (*Prionailurus bengalensis*) in Vietnam and Taiwan also fell within the major CPV-2a group, but were clearly distinct from the raccoon viruses. Notably, the lineages of raccoon isolates fell into several unrelated clusters across the carnivore virus phylogeny. These results indicate multiple cross-species transmission events into raccoons from both cats and dogs (Figure 4.1). While one raccoon isolate was most closely related to CPV-2b-like viruses and several

146

grouped among the FPV, most (n = 13) sequences of viruses from raccoons fell

between the CPV-2 and CPV-2a sequences (Figure 4.1). These latter raccoon isolates

were collected between 1982 and 2010 and were obtained from states along the

eastern seaboard of the US from Florida to New York State, as well as from Wisconsin,

Texas, and California (Table 4.1). This position on the phylogeny identifies these strains

as evolutionarily intermediates between CPV-2 and CPV-2a. Equivalent analyses of

NS1 gene sequences (61 samples) and the complete VP2 gene (125 samples)

confirmed these evolutionary relationships (data not shown).

Figure 4.1. Maximum likelihood (ML) phylogeny of carnivore parvoviruses based on 516 sequences of the VP2 gene. The sequences used represent feline panleukopenia viruses (green), viruses isolated from raccoons (blue), and the different strains of CPV (CPV-2, black; CPV-2a, red; CPV-2b, yellow; and CPV-2c, pink) are organized by their evolutionary relationship. As the mink enteritis viruses (MEV) clustered closely with those from cats they were also colored green. Sequences of viruses from leopard cats are indicated with stars. The tree is rooted using the oldest sequence included in the analysis (FPV/Cat/UK/62). Bootstrap values >0.90 are marked by asterisks. Branch lengths are drawn to scale of nucleotide substitutions per site. Insert: expansion of the phylogenetic tree section containing the main group of raccoon sequences, highlighting the amino acid substitutions that occurred on each branch.

148

Parvovirus variants:
FPV
Raccoon isolates
CPV-2
CPV-2a
CPV-2b
CPV-2c

CPV-2

CPV/Rac/WI/37/10
CPV/Bobcat/KS/44/10
CPV/Rac/VA/278/07
CPV/Rac/TN/351/09
CPV/Rac/KY/358-B/09
CPV/Rac/KY/39552/09
CPV/Rac/KY/33817/09
CPV/Rac/FL/381/09
CPV/Rac/NY/94742/10
CPV/Rac/VA/278/09
CPV/Rac/GA/289/08
CPV/Rac/GA/349/08
CPV/Rac/GA/287/08

RPV

I232T
G232R

M87L
I101T
A300D

S297A

D305H

CPV-2a

D300G
H305Y

0.005

149
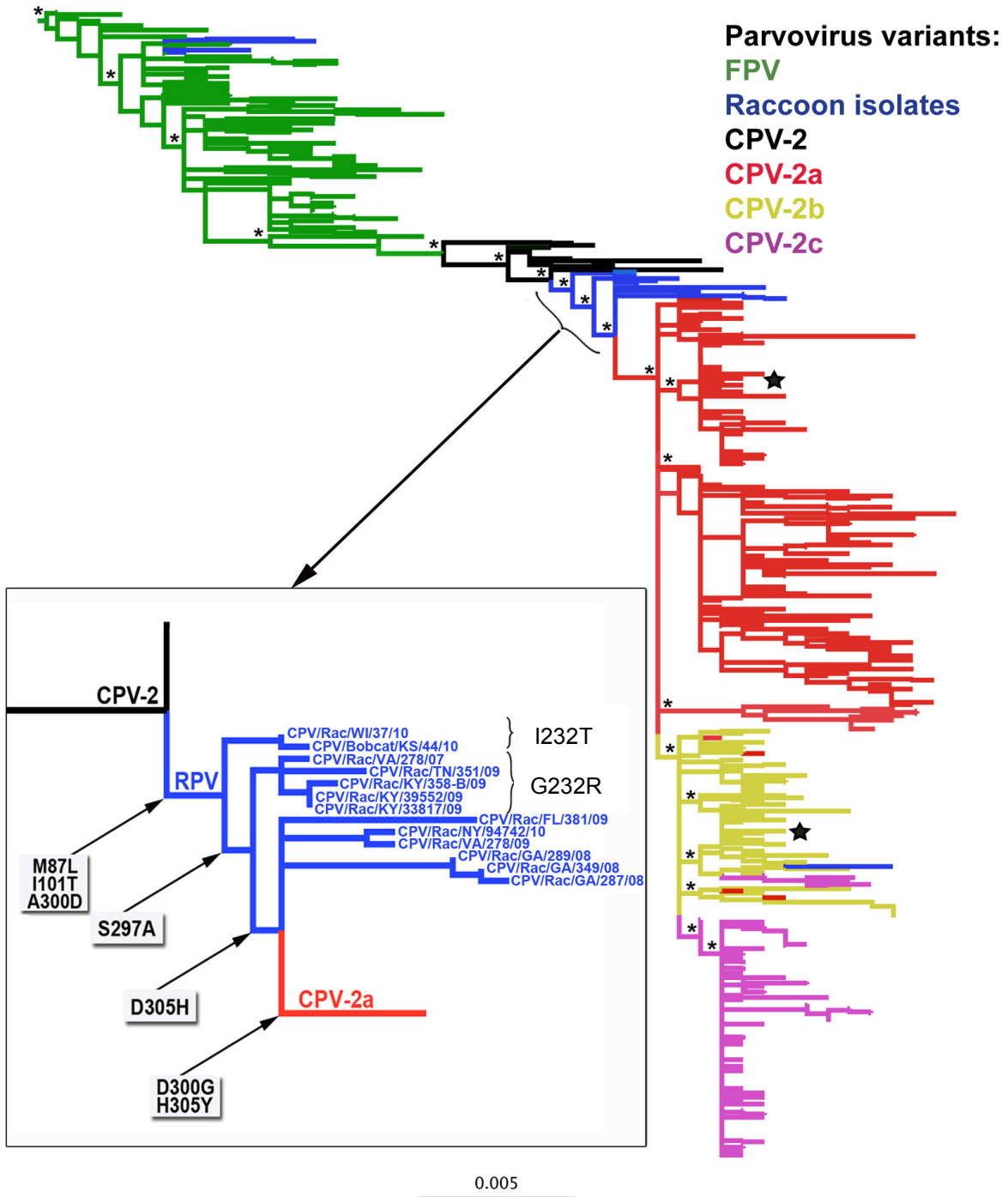
The emergence date of the raccoon viruses was inferred using a relaxed molecular clock analysis of the VP2 data set. Accordingly, the main group of raccoon isolates was estimated to have diverged from CPV between 20 to 30 years ago (95% HPD values), such that it has been undetected for at least 20 years. Raccoon isolates that fell outside of the main cluster, either within FPV or CPV-2b, had more recent origins (95% HPD values = 4-19 years ago). Comparable values were obtained using the full-length NS1 and VP2 data sets.

Many variant residues in the raccoon viruses were located within capsid protein structures that influence host range, TfR binding, and antibody binding (Figure 4.2). A key change occurred at VP2 residue 300, which is polymorphic among the carnivore parvoviruses (Figure 4.2). This residue was an Ala in the original RPV, FPV and CPV-2, and a Gly in CPV-2a-derived viruses in dogs. Most notably, residue 300 was Asp in all CPV-derived isolates from raccoons irrespective of their position on the phylogeny and hence whether they were derived from FPV or CPV (Figure 4.2). The CPV-derived raccoon viruses also contained polymorphisms at the following VP2 residues: 224 (Gly or Arg), 232 (Ile or Thr), 297 (Ser or Ala), and 305 (Asp or His) (Figures 4.1 and 4.2).

	VP2 Residue														
Name	80	87	93	101	103	190	224	232	297	300	305	323	426	564	568
FPV/Cat/UK/Philips_Roxane/62	K	M	K	T	V	M	G	I	S	A	D	D	N	N	A
FPV/Cat/NY/FPV-b/68	K	M	K	T	V	M	G	I	S	A	D	D	N	N	A
MEV/Mink/WI/Wolf/73	K	M	K	T	V	M	G	I	S	V	D	D	N	N	A
FPV/Raccoon/TX/AAA47118/79	K	M	K	T	V	M	G	V	S	A	D	D	N	N	A
FPV/Raccoon/NJ/6-727/90	K	M	K	T	V	M	G	V	S	A	D	D	N	N	A
FPV/Raccoon/CA/208-A/10	K	M	K	T	V	M	G	V	A	A	D	D	N	N	A
FPV/Raccoon/TX/79-4176/78	K	M	K	T	V	M	G	I	S	A	D	N	N	N	A
FPV/Raccoon/TX/8II82/82	K	M	K	T	V	M	G	I	S	A	D	N	N	N	A
CPV-2/Dog/IL/CPV-d/79	R	M	N	I	A	M	G	I	S	A	D	N	N	S	G
CPV/Raccoon/WI/37/10	R	L	N	T	A	M	G	T	S	D	D	N	N	S	G
CPV/Bobcat/KS/44/10	R	L	N	T	A	M	G	T	S	D	D	N	N	S	G
CPV/Raccoon/VA/118-A/07	R	L	N	T	A	M	R	I	A	D	D	N	N	S	G
CPV/Raccoon/TN/351/09	R	L	N	T	A	M	R	I	A	D	D	N	N	S	G
CPV/Raccoon/KY/358-B/09	R	L	N	T	A	M	R	I	A	D	D	N	N	S	G
CPV/Raccoon/KY/33817/09	R	L	N	T	A	M	R	I	A	D	D	N	N	S	G
CPV/Raccoon/KY/39552/09	R	L	N	T	A	M	R	I	A	D	D	N	N	S	G
CPV/Raccoon/GA/287/08	R	L	N	T	A	M	G	I	A	D	H	N	N	S	G
CPV/Raccoon/GA/289/08	R	L	N	T	A	M	G	I	A	D	H	N	N	S	G
CPV/Raccoon/GA/349/08	R	L	N	T	A	M	G	I	A	D	H	N	N	S	G
CPV/Raccoon/VA/278/09	R	L	N	T	A	M	G	I	A	D	H	N	N	S	G
CPV/Raccoon/FL/381/09	R	L	N	T	A	I	G	I	A	D	H	N	N	S	G
CPV/Raccoon/NY/94742/10	R	L	N	T	A	I	G	I	A	D	H	N	N	S	G
CPV/Raccoon/NJ/76836/10	R	L	N	T	A	M	G	I	A	D	H	N	N	S	G
CPV/Leopard cat/Viet Nam/V139	R	L	N	T	A	M	G	I	A	D	Y	N	N	S	G
CPV/Leopard cat/Viet Nam/V203	R	L	N	T	A	M	G	I	A	D	Y	N	D	S	G
CPV-2a/Dog/IL/CPV-15/84	R	L	N	T	A	M	G	I	A	G	Y	N	N	S	G
CPV-2b/Dog/TX/CPV-39/84	R	L	N	T	A	M	G	I	A	G	Y	N	D	S	G
CPV-2c/Dog/Italy/287/04	R	L	N	T	A	M	G	I	A	G	Y	N	E	S	G

Figure 4.2. Parvovirus VP2 capsid protein sequences. Shown are phylogenetically important positions associated with the viruses recovered from raccoons in different parts of the USA between 1979 and 2010, as well as viruses recovered from leopard cats in Vietnam in 1997, and a bobcat in Kansas USA in 2010. We also include the sequences at each position for the prototype FPV, CPV-2 and CPV-2a-related viruses.

4.4b Antigenic analysis

Many of the mutations in the raccoon virus capsids occurred within known antigenic sites, most notably at VP2 residue 224 ("A site") and VP2 residues 300 and 305 ("B site") (10, 37). Representative strains containing the most common combination of mutations (300Asp with 305His (e.g. CPV/Raccoon/GA/287/08) or 300Asp with 224Arg (e.g. CPV/Raccoon/VA/118-A/07)) were tested for reactivity with MAbs prepared against FPV, CPV-2, or CPV-2b and showed significant differences in their antigenic binding patterns (Figure 4.3). All CPV-derived raccoon strains tested showed decreased reactivity with "B site" antibodies, primarily due to the 300Asp mutation, and the

CPV/Raccoon/VA/118-A/07 virus (containing the additional mutation at "A site" residue 224Arg) showed decreased reactivity with 26 out of 28 MAbs tested, presumably due to loss of reactivity with antibodies at both sites.

4.4c In vitro host range and transferrin receptor binding

We tested the infectivity of representative raccoon virus isolates and the prototype FPV, CPV-2 and CPV-2b strains in feline and canine cells. All virus inocula infected feline cells to similarly high titers (10^5 to 10^7 TCID$_{50}$/mL). FPV, and the FPV- and CPV-derived viruses from raccoons showed 500- to >10,000-fold lower titers in canine cells (Figure 4.4). The CPV-2 isolate with the 300D mutant alone showed a one to two log reduction of infectivity for canine cells compared to feline cells, as was previously shown (17, 25).

To examine the specific binding of the raccoon viruses to different host receptors, we cloned the raccoon TfR complementary DNA (cDNA) from mRNA extracted from a raccoon cell line. This was found to be 88-89% identical at the amino acid level to dog and cat TfRs. The TfR apical domain, which controls virus binding, was more similar to the cat TfR as it did not contain the canine-specific glycosylation site at amino acid residue 384 (Asn in dog TfR, Lys in cat and raccoon TfR). The CPV-2 and CPV-2b capsids bound to cells expressing feline or raccoon TfR and, to a lower level, the canine TfR (Figure 4.5A, C, and E). FPV, an FPV-like raccoon isolate (RPV-79-4176/TX), and two representative CPV-derived raccoon isolates showed binding to the raccoon and feline TfRs, but did not bind the canine TfR above background levels (Figure 4.5B, D, and E).
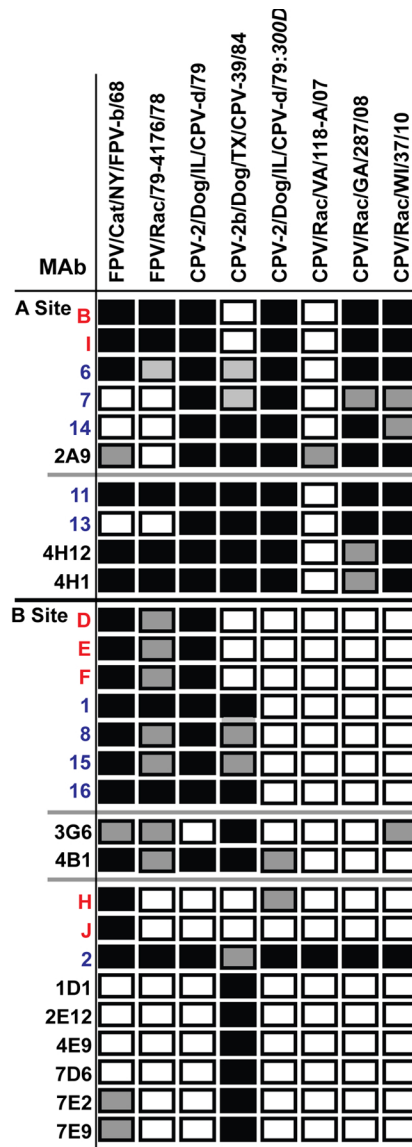
Figure 4.3. Antigenic analysis of viral variants. The hemagglutination inhibition assay and MAbs prepared against capsids of FPV (names in red), CPV-2 (names in blue), or CPV-2b (names in black) capsids were used to antigenically distinguish different raccoon isolates. Titers are compared to those of the capsid type used for immunization. Four different viruses from raccoons were tested, along with prototype FPV (FPV/Cat/NY/FPV-b/68), CPV-2 (CPV-2/Dog/IL/CPV-d/79), and CPV-2b (CPV-2b/Dog/TX/CPV-39/84), and the experimentally derived 300Asp mutant of CPV-2. Black squares indicate binding +/- 2-fold of the original titer, shaded squares indicate a 4- to 16-fold reduction in titer, and open squares indicate a >16-fold reduction in titer.
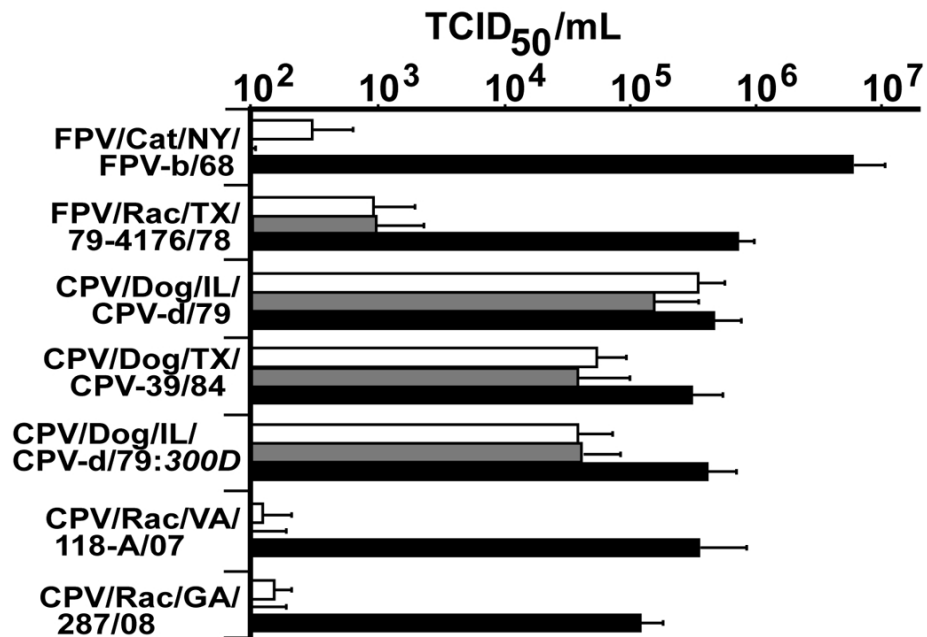
Figure 4.4. Relative infectivity of the raccoon isolates in canine and feline cells.
Infection assays were performed in NLFK feline cells (black bars), or A72 (gray bars) or Cf2Th (white bars) canine cells. Three different raccoon isolates (designations containing Rac, see also Table 4.1) were tested, along with prototype strains of FPV (FPV/Cat/NY/FPV-b/68), CPV-2 (CPV-2/Dog/IL/CPV-d/79), and CPV-2b (CPV-2b/Dog/TX/CPV-39/84), as well as the 300Asp mutant of CPV-2. Virus titers were determined by $TCID_{50}$ assay in each cell line. Error bars indicate $\pm$SD based on three independent experiments.
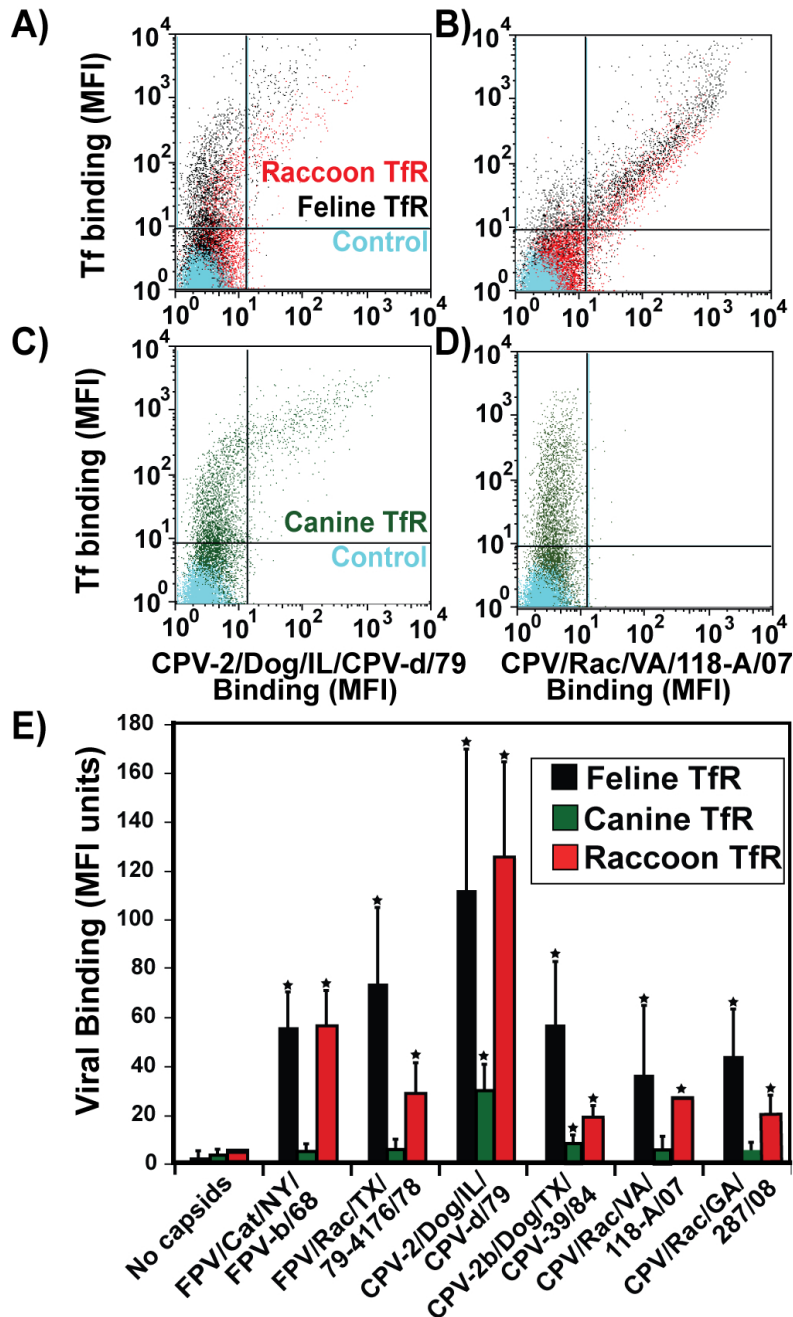
Figure 4.5. Binding of capsids and canine transferrin to the feline, raccoon, and canine TfRs. Receptors were expressed on TRVb cells that lack endogenous TfR, and binding levels were assayed by flow cytometry. Cells were incubated with Cy-5 conjugated-transferrin to detect TfR-expressing cells, and with virus capsids detected with MAb 2. (A) Tf and CPV-2 and (B) CPV/Rac/VA/118-A/07 bind to feline and raccoon TfRs. (C) Tf and CPV-2 (CPV-2/Dog/IL/CPV-d/79) bind to canine TfR. (D) The raccoon isolates (CPV/Rac/VA/118-A/07 shown) do not bind the canine TfR. E) Graphs of cell-associated Tf and virus are plotted as mean fluorescence intensity units (MFI); error bars $\pm$SD from the mean for 3 independent experiments ($\star$ = significant binding over background, $p<0.05$).

4.5 Discussion

Our studies of raccoon parvoviruses illustrate several key aspects of cross-species transmission and emergence of novel viruses. The most striking and surprising observation was that the major group of raccoon parvoviruses examined in this study fell between CPV-2 and CPV-2a on phylogenetic trees, such that they represent evolutionary intermediates between these antigenic variants and have been apparently circulating undetected for at least 20 years. In addition, these raccoon viruses contain key amino acid substitutions in the four VP2 codons that became fixed in CPV-2a after its global spread in dogs. Of these substitutions, those at residues 87 (Leu) and 101 (Thr) were the same in both CPV-derived raccoon viruses and CPV-2a compared with the more ancestral CPV-2 (Met and Ile, respectively). The two remaining strain-specific codons (300 and 305) exhibited different amino acid residues in CPV-2, CPV-derived raccoon viruses, and CPV-2a. Residue 300 was Asp in the raccoon isolates, rather than Ala (CPV-2) or Gly (CPV-2a), while residue 305 was either His (unique to raccoon isolates) or Tyr (also in CPV-2a), but not Asp (CPV-2). The Asp at residue 300 has been previously detected in some CPV-derived viruses from leopard cats in Vietnam and cats in Taiwan, and was also selected experimentally in a CPV-2 virus passaged in feline cells (15, 17, 20, 29). For the ancestral raccoon virus to give rise to CPV-2a, only a single change in codon 300 was required (Asp to Gly), which represents a single transitional mutation that could have occurred either before or after the transfer back to dogs. A previously studied experimental change of the neighboring VP2 residue 299 from Gly to Glu similarly blocked binding to the canine TfR and also prevents canine cell

infection, providing further support for the importance of this region in determining host range (13, 25).

4.5a A signature amino acid mutation was selected multiple times

Residue 300 in the viral capsid clearly plays a key role in the control of host range of carnivore parvoviruses. In particular, the 300Asp mutation appeared multiple times in the VP2 phylogeny and always associated with changes in host range, strongly suggesting that it is selectively favored and facilitates adaptation to raccoons and cats. The 300Asp mutation creates a novel hydrogen bond between surface loops of the capsid that likely stabilize the surface architecture. This interaction may play a role in inhibiting infection of canine cells by reducing the ability of the capsid to bind the canine TfR (17). The raccoon viruses also contained additional substitutions that further inhibited infection in canine cells; for example, VP2 224Arg or 305His were associated with the presence of residue 300Asp and had >100 fold reduced infection in canine cells compared to CPV-2 with the 300Asp mutation alone.

We observed other changes common to the raccoon viruses derived from different hosts, indicative of parallel changes in these viruses. The presence of residue 323Asn among the FPV-like viruses from raccoons was particularly interesting as this mutation was also associated with the species jump from cats (FPV) to dogs (CPV) (5). VP2 residue 297 was another notable example, as the change from Ser to Ala in CPV-2a in dogs was only seen after about 1990 (6, 12, 21), and this mutation was also largely fixed in the raccoon viruses derived from CPV.

4.5b Functional effects of changes on receptor and antibody binding

Many of the amino acid changes studied here fell within known binding sites for the TfR and antibodies and had effects on capsid functionality related to binding various carnivore TfRs and MAb reactivity (10, 11). Positive selection of virus variants that have specific structural interactions with the TfRs from cats, raccoons, and dogs would be expected, given the importance of this interaction for cell infection (13, 23). A role for antigenic selection is less easy to define, as the specific effects would depend on the immune status of the different hosts. In many cases immunity against parvoviruses, and immune selection in unvaccinated juveniles, depends on the nature of viruses infecting the mothers who contribute maternal antibodies that protect against infection. Some raccoon viruses reacted with only a small number of the 28 antibodies tested here, suggesting that immune escape is likely to be a source of selection pressure on some of these virus variants.

4.5c Virus evolution and emergence

Our study provides two more general insights into the process of cross-species virus transmission and emergence. First, natural selection of one or two necessary changes in the capsid amino acid sequence – such as the 300Asp in raccoons and 300Gly in dogs – is apparently readily accomplished as it has occurred on multiple occasions. Similar observations have been seen in the adaptation of influenza viruses among mammalian species (32, 33), indicating that, in many cases, successful emergence is not limited by mutational availability. This is particularly likely when the donor and recipient species are relatively closely related, such that the adaptive valley separating them is shallow (38). Second, as the major cluster of raccoon parvovirus

sequences fell between CPV and CPV-2a, we suggest that the potential role of intermediate hosts such as raccoons should be investigated in cases where major changes in viral phenotype occur even within in the same host species. Similarly, intermediate hosts may provide a bridge between two widely separated hosts, as has previously been reported or inferred for a number of other viruses (32). Furthermore, future studies of virus biodiversity will likely demonstrate the existence of intermediate hosts in other cases of cross-species transmission. However, the mutational pathways involved may be complex, some of the specific mutations found in viruses from the intermediate host will likely not be found, or will have been altered, in the final host. In the case studied here, the signature change of VP2 residue 300 from Ala to Asp in raccoons was followed by a change to Gly in CPV-2a. As such, these studies underscore the need for considering a variety of related hosts in order to fully understand the mechanisms of viral evolution allowing cross-species transmission.

4.7 References

1. **Agbandje, M., R. McKenna, M. G. Rossmann, M. L. Strassheim, and C. R. Parrish.** 1993. Structure determination of feline panleukopenia virus empty particles. Proteins **16:** 155-171.

2. **Appel, M. J. G., Parrish, C.R..** 1982. Raccoons are not susceptible to canine parvovirus. J.Am.Vet.Med.Assoc. **181:**489.

3. **Barbis, D. P., S.-F. Chang, and C. R. Parrish.** 1992. Mutations adjacent to the dimple of canine parvovirus capsid structure affect sialic acid binding. Virology **191:**301-308.

4. **Barker, I. K., R. C. Povey, and D. R. Voigt.** 1983. Response of mink, skunk, red fox and raccoon to inoculation with mink virus enteritis, feline panleukopenia and canine parvovirus and prevalence of antibody in wild carnivores in Ontario. Can.J.Comp.Med. **47: 188-197**.

5. **Chang, S. F., J. Y. Sgro, and C. R. Parrish.** 1992. Multiple amino acids in the capsid structure of canine parvovirus coordinately determine the canine host range and specific antigenic and hemagglutination properties. J Virol **66:**6858-6567.

6. **de Freitas, R. B., E. L. Durigon, D. D. Oliveira, C. M. Romano, M. R. de Freitas, A. D. Linhares, F. L. Melo, L. Walshkeller, M. L. Barbosa, E. M. Huatuco, E. C. Holmes, and P. M. Zanotto.** 2007. The "pressure pan" evolution of human erythrovirus B19 in the Amazon, Brazil. Virology.

7. **Drummond, A. J., and A. Rambaut.** 2007. BEAST: Bayesian evolutionary analysis by sampling trees. BMC Evol Biol **7:**214.

8. **Edgar, R. C.** 2004. MUSCLE: a multiple sequence alignment method with reduced time and space complexity. BMC Bioinformatics **5:**113.

9. **Goodman, L. B., S. M. Lyi, N. C. Johnson, J. O. Cifuente, S. L. Hafenstein, and C. R. Parrish.** 2010. Binding site on the transferrin receptor for the parvovirus capsid and effects of altered affinity on cell uptake and infection. J Virol **84:**4969-78.

10. **Hafenstein, S., V. D. Bowman, T. Sun, C. D. Nelson, L. M. Palermo, P. R. Chipman, A. J. Battisti, C. R. Parrish, and M. G. Rossmann.** 2009. Structural comparison of different antibodies interacting with parvovirus capsids. J Virol **83:**5556-66.

11. **Hafenstein, S., L. M. Palermo, V. A. Kostyuchenko, C. Xiao, M. C. Morais, C. D. Nelson, V. D. Bowman, A. J. Battisti, P. R. Chipman, C. R. Parrish, and M. G. Rossmann.** 2007. Asymmetric binding of transferrin receptor to parvovirus capsids. Proc Natl Acad Sci U S A **104:**6585-9.

12. **Hoelzer, K., L. A. Shackelton, C. R. Parrish, and E. C. Holmes.** 2008. Phylogenetic analysis reveals the emergence, evolution and dispersal of carnivore parvoviruses. J Gen Virol **89:**2280-9.

13. **Hueffer, K., J. S. Parker, W. S. Weichert, R. E. Geisel, J. Y. Sgro, and C. R. Parrish.** 2003. The natural host range shift and subsequent evolution of canine parvovirus resulted from virus-specific binding to the canine transferrin receptor. J. Virol. **77:**1718-1726.

14. **Hueffer, K., and C. R. Parrish.** 2003. Parvovirus host range, cell tropism and evolution. Curr Opin Microbiol **6:**392-398.

15. **Ikeda, Y., M. Mochizuki, R. Naito, K. Nakamura, T. Miyazawa, T. Mikami, and E. Takahashi.** 2000. Predominance of canine parvovirus (CPV) in unvaccinated cat populations and emergence of new antigenic types of CPVs in cats. Virology **278:**13-9.

16. **Kapil, S., G. Rezabek, B. Germany, and L. Johnston.** 2010. Isolation of a virus related to canine parvovirus type 2 from a raccoon (Procyon lotor). Vet Rec **166:**24-5.

17. **Llamas-Saiz, A. L., M. Agbandje-McKenna, J. S. L. Parker, A. T. M. Wahid, C. R. Parrish, and M. G. Rossmann.** 1996. Structural analysis of a mutation in canine parvovirus which controls antigenicity and host range. Virology **225:**65-71.

18. **Martin, H. D., and N. S. Zeidner.** 1992. Concomitant cryptosporidia, coronavirus and parvovirus infection in a raccoon (Procyon lotor). J Wildl Dis **28:**113-5.

19. **McGraw, T. E., L. Greenfield, and F. R. Maxfield.** 1987. Functional expression of the human transferrin receptor cDNA in Chinese hamster ovary cells deficient in endogenous transferrin receptor. J Cell Biol **105:**207-14.

20. **Miyazawa, T., Y. Ikeda, K. Nakamura, R. Naito, M. Mochizuki, Y. Tohya, D. Vu, T. Mikami, and E. Takahashi.** 1999. Isolation of feline parvovirus from peripheral blood mononuclear cells of cats in northern Vietnam. Microbiol Immunol **43:**609-12.

21. **Mohan Raj, J., H. K. Mukhopadhyay, J. Thanislass, P. X. Antony, and R. M. Pillai.** 2010. Isolation, molecular characterization and phylogenetic analysis of canine parvovirus. Infect Genet Evol **10:**1237-41.

22. **Nowak, R.** 1999. Carnivora: Family Procyonidae. Walker's Mammals of the World 6 Ed:694-704.

23. **Palermo, L. M., S. L. Hafenstein, and C. R. Parrish.** 2006. Purified feline and canine transferrin receptors reveal complex interactions with the capsids of canine and feline parvoviruses that correspond to their host ranges. J Virol **80:**8482-92.

24. **Parker, J. S., W. J. Murphy, D. Wang, S. J. O'Brien, and C. R. Parrish.** 2001. Canine and feline parvoviruses can use human or feline transferrin receptors to bind, enter, and infect cells. J Virol **75:**3896-902.

25. **Parker, J. S., and C. R. Parrish.** 1997. Canine parvovirus host range is determined by the specific conformation of an additional region of the capsid. J Virol **71:**9214-22.

26. **Parrish, C. R.** 1990. Emergence, natural history, and variation of canine, mink, and feline parvoviruses. Adv Virus Res **38:**403-450.

27. **Parrish, C. R.** 1991. Mapping specific functions in the capsid structure of canine parvovirus and feline panleukopenia virus using infectious plasmid clones. Virology **183:**195-205.

28. **Parrish, C. R., and L. E. Carmichael.** 1983. Antigenic structure and variation of canine parvovirus type-2, feline panleukopenia virus, and mink enteritis virus. Virology **129:**401-414.

29. **Parrish, C. R., and L. E. Carmichael.** 1986. Characterization and recombination mapping of an antigenic and hostrange mutation of canine parvovirus. Virology **148:**121-132.

30. **Parrish, C. R., Carmichael, L.E., Antczak, D.F.** 1982. Antigenic relationships between canine parvovirus type-2, feline panleukopenia virus and mink enteritis virus using conventional antisera and monoclonal antibodies. Arch.Virol. **72: 267-278**.

31. **Parrish, C. R., P. Have, W. J. Foreyt, J. F. Evermann, M. Senda, and L. E. Carmichael.** 1988. The global spread and replacement of canine parvovirus strains. J Gen Virol **69 (Pt 5):**1111-6.

32. **Parrish, C. R., E. C. Holmes, D. M. Morens, E. C. Park, D. S. Burke, C. H. Calisher, C. A. Laughlin, L. J. Saif, and P. Daszak.** 2008. Cross-species virus transmission and the emergence of new epidemic diseases. Microbiol Mol Biol Rev **72:**457-70.

33. **Parrish, C. R., and Y. Kawaoka.** 2005. The origins of new pandemic viruses: the acquisition of new host ranges by canine parvovirus and influenza A viruses. Annu Rev Microbiol **59:**553-86.

34. **Parrish, C. R., P. H. O'Connell, J. F. Evermann, and L. E. Carmichael.** 1985. Natural variation of canine parvovirus. Science **230:**1046-1048.

35. **Posada, D., and K. A. Crandall.** 1998. MODELTEST: testing the model of DNA substitution. Bioinformatics **14:**817-8.

36. **Steinel, A., C. R. Parrish, M. E. Bloom, and U. Truyen.** 2001. Parvovirus infections in wild carnivores. J Wildl Dis **37:**594-607.

37. **Strassheim, L. S., A. Gruenberg, P. Veijalainen, J.-Y. Sgro, and C. R. Parrish.** 1994. Two dominant neutralizing antigenic determinants of canine parvovirus are found on the threefold spike of the virus capsid. Virology **198:**175-184.

38. **Streicker, D. G., A. S. Turmelle, M. J. Vonhof, I. V. Kuzmin, G. F. McCracken, and C. E. Rupprecht.** Host phylogeny constrains cross-species emergence and establishment of rabies virus in bats. Science **329:**676-9.

39. **Swofford , D. L.** 2003. PAUP*. Phylogenetic Analysis Using Parsimony (*and other methods). . Version 4. Sinauer Associates. Sunderland, Mass.

40. **Tresnan, D. B., L. Southard, W. Weichert, J. Y. Sgro, and C. R. Parrish.** 1995. Analysis of the cell and erythrocyte binding activities of the dimple and canyon regions of the canine parvovirus capsid. Virology **211:**123-132.

41. **Truyen, U., A. Gruenberg, S. F. Chang, B. Obermaier, P. Veijalainen, and C. R. Parrish.** 1995. Evolution of the feline-subgroup parvoviruses and the control of canine host range in vivo. J. Virol. **69:**4702-4710.

42. **Truyen, U., and C. R. Parrish.** 1992. Canine and feline host ranges of canine parvovirus and feline panleukopenia virus: distinct host cell tropisms of each virus in vitro and in vivo. J Virol **66:**5399-5408.

43. **Waller, E. F.** 1940. Infectious gastroenteritis in raccoons (Procyon lotor). J.Am.Vet.Med.Assoc. **96: 266-268**.

44. **Zeveloff, S.** 2002. Raccoons: a natural history. Smithsonian Books, Washington, DC.

CHAPTER 5: NEUTRALIZING PROPERTIES OF

ANTIBODIES AGAINST AAV1 AND AAV5 CAPSIDS

5.1 Abstract

Monoclonal antibodies (MAbs) were prepared against AAV type 1 (AAV1) and 5 (AAV5) capsids and were purified as intact antibodies and, in some cases, Fab fragments. Four IgG and 3 IgM antibodies were prepared against AAV1. One IgG and 6 IgM antibodies were prepared against AAV5 from mice pre-immunized with AAV1 capsids and boostered with AAV5 four days before hybridoma preparation. The anti-AAV1 MAbs showed cross-reactivity only with AAV6, while the AAV5 antibodies were slightly cross-reactive with AAV1 but not other serotypes. All antibodies were specific for assembled capsids and were able to neutralize the homologous virus, though with different efficiencies. Fab fragments of the MAbs were generally poorly neutralizing. Different antibodies appeared to have various mechanisms of neutralization that primarily included inhibition of receptor binding but also post-attachment neutralization in one case.

5.2 Introduction

Adeno-associated viruses (AAVs) are non-pathogenic, non-enveloped viruses with a single stranded DNA genome packaged into an ~25 nm diameter icosahedral capsid. They are classified within the Parvoviridae family, genus Dependovirus. The 4.7 kb genome lacks a viral DNA polymerase gene, and these viruses are dependent on cellular polymerases as well as on their helper viruses, usually adenovirus, to provide functions essential for replication. Many AAV strains are currently under investigation as vectors for therapeutic gene delivery due to a variety of features that make them

attractive vector candidates (1, 7, 32). These include the a) stability of the capsid that facilitates handling of the vectors during production and transport, b) inability of the virus to replicate without helper gene products, c) lack of disease associated with infection, d) ability to induce long term expression of packaged genes in some cases lasting up to months or years, and e) ability to transduce a variety of dividing and non-dividing cells (47). Since their initial discovery in the 1960s as contaminants of Adenovirus preparations, more than 12 AAV serotypes have been identified in a variety of host species that possess varying natural tissue tropisms and receptor binding properties (14, 52). Genetic modification of viral capsids has further expanded this repertoire for targeting to cell types of specific gene therapy interest (5, 34).

The capsid is assembled from a total of 60 copies of three overlapping capsid proteins, VP1, VP2, and VP3, in an approximately 1:1:10 ratio. The core of the capsid is formed by an eight-stranded β-barrel, with the intervening loops between the β strands responsible for the specific features of the capsid surface. The different serotypes of AAV have capsid proteins that are ~60-80% identical in amino acid sequence (10, 11), and the differences in antigenicity and tissue tropism between the serotypes stem primarily from mutations within the surface loops.

AAV2 was initially isolated from a human genital lesion. It was the first serotype to be studied in detail and is the capsid type with the largest number of ongoing clinical gene therapy trials for delivery of genes to treat disease states such as cystic fibrosis and hemophilia (13, 41). The primary cellular receptor for AAV2 is heparin sulfate proteoglycan (HSPG), though the virus can use a variety of co-receptors including $\alpha V\beta 5$

integrins and human fibroblast growth factor receptor 1 (FGF1) (16, 35, 42).

Despite a relatively low immunogenicity compared to other viral vector systems, humoral immunity leading to virus neutralization has been a major barrier to clinical trials involving AAV2 in humans (46). Anti-AAV2 neutralizing antibodies can be detected in up to 30%-80% of human subjects in different studies, and these antibodies may be capable of neutralizing the virus and preventing transgene expression even during the first administration (2, 3, 27, 56). Furthermore, in immunologically naive individuals, even one therapeutic application of AAV2 vectors can elicit the generation of memory B cell responses that can preclude the effectiveness of repeat dosing where that is necessary for sustained gene expression (39). These responses are affected by the route, dose, and serotype of the administered virus, as well as the identity, expression level, and promoter of the transgene product (21, 44).

More recently, additional serotypes have been evaluated as alternate gene therapy vectors. AAV1 originates from non-human primates, and is of interest because of its superior ability to transduce muscle and hematopoitic stem cells compared to other AAV serotypes. Another serotype, AAV5, has higher levels of muscle, airway epithelia, and brain tissue transduction compared to AAV2 (18, 55, 57). Both of these serotypes utilize sialic acids as the primary cellular receptor, and AAV5 also binds to the platelet derived growth factor receptor (PDGF) as a co-receptor (23, 48). Serotypes 5, 7, and 8, and other genetically modified variants are of specific interest because they are the most divergent from AAV2 and in some studies appear to have lower levels of pre-existing immunity in humans (4, 12, 15).

Repeated administration of transgenes packaged by sequentially different AAV capsid serotypes has been attempted to circumvent the problems encountered with the development of anti-vector antibodies. The capsids of different serotypes can vary up to 20% in amino acid sequence, so that antibodies tend not to significantly cross-react, and thus this strategy has met with some success in reducing vector neutralization (19, 54). Another approach is to concurrently administer immunosuppressants (such as cyclosporin) with the AAV vector to temporarily reduce immune responses to the virus capsid and/or transgene, and that has also been successful in some clinical trials (30).

Despite the importance of antibodies in the anti-viral response to AAV, little is known about the major antigenic epitopes on the capsid surface or the mechanism(s) of antibody neutralization. Antibodies can neutralize viruses by a variety of mechanisms (36). The "single hit model" describes neutralization by as few as one antibody binding to one key site on the viral capsid. Inactivation is achieved by rendering the capsid non-infectious, for example, by the antibody mimicking the structural interaction of the virus with the cellular receptor to induce conformational changes associated with genome release or another aspect of entry (8). This model of neutralization has been suggested to act in the anti-viral response against picornaviruses, but appears not to be involved in viral neutralization in most cases (24). The "multi-hit model" explains neutralization as the result of antibodies coating the surface of the capsid by occupying a certain threshold percentage of available epitopes to directly or sterically prevent interactions with target cells. A variety of factors affect the number of antibodies per viral capsid needed to prevent cellular infection *in vivo*, including epitope accessibility and

organization as well as overall capsid size (25). For icosahedral viruses, capsid surface area is generally proportional to the number of antibodies needed for neutralization. However, in some cases not all of the accessible epitopes need to be coated in order to neutralize the virus, and the threshold stoichiometry varies by antibody and virus (40). Furthermore, these antibodies may neutralize by varying mechanisms, including aggregating viral particles, directly or indirectly preventing receptor binding, inhibiting viral uncoating and genome release, and by Fc region interaction with other components of the immune system (26, 31, 49).

Some information has been gathered for antibody neutralization mechanisms of parvoviruses, primarily for AAV2 and for the autonomous parvoviruses canine parvovirus (CPV) and minute virus of mice (MVM). Studies of CPV and MVM antigenic epitopes examined naturally antigenically variant CPV strains with changes at residues that also affect viral host range as well as experimentally derived escape mutants from neutralizing MAbs (29, 37, 43). The structures of eight different anti-CPV Fab antibody fragments bound to the virus capsid were determined using cryo-electron microscopy, and those showed that ~62% of the capsid surface was involved in antibody binding. The only regions not covered by those antibodies in that study were two depressed regions, and the cylinder surrounding the fivefold axis of symmetry. (17). Interestingly, the major epitopes that varied between antigenically distinct naturally occurring CPV strains fell into two small regions of the capsid surface. This suggests that although most antibodies bind on or near the protrusions at or surrounding the icosahedral threefold axis, a complex interaction exists between the capsid surface and the host

antibody response. Thus the sites involved in antibody binding may be constrained by other required functions of the capsid surface.

Studies of AAV2 examining a small number of MAbs or polyclonal anti-capsid antibodies show that antibody binding is affected by changes in only a small number of sites on the capsid, and that reactivity can be reduced by mutations of residues within those sites (22, 33). Some of the mutations also change the receptor binding properties of the capsid, particularly those that affect binding to HSPG. Nonetheless, many of those mutants retained similar infectivity to wild-type capsids (28). For AAV2, binding of antibodies to different epitopes as described by mutational analysis show neutralization of infectivity by either inhibition of receptor binding or at post-attachment steps (50). A panel of mutant AAV2 capsids with surface residue mutations to Ala or other amino acids was examined for binding to HSPG and reactivity with an anti-AAV2 MAb (A20), polyclonal antibodies in three human sera, or to a pool of human IgGs (28). Some mutations prevented A20 antibody binding and neutralization, and others reduced virus sensitivity to neutralization by the individual sera by up to 42-fold, or by a pool of sera up to four-fold. There was not always a direct relationship between the change in IgG binding and neutralization, indicating that not all IgGs were equally efficient.

Here we describe a number of MAbs (both IgGs and IgMs) produced against the capsids of AAV1 and AAV5. The structural analysis of the specific antibody-capsid interaction for a subset of these antibodies has been described elsewhere (Figure 5.1, B. Gurda, manuscript in preparation). The results of these studies showed that most antibodies recognize a small region on the virus capsid, close to known receptor-binding

sites on the three-fold axis. The stoichiometry of binding by these antibodies varied, with most antibodies binding only once per three-fold spike (e.g. anti AAV1 antibodies 5H7 and 4E4, Figure 5.1A and B). The consequence of this low occupancy is that even at saturation, 40 out of 60 VP monomers remain potentially open for receptor interaction depending on the area of steric inhibition provided by the antibody. In contrast, the Anti-AAV5 antibody 3C5 (Figure 5.1C) bound to all three monomers around the three-fold axis, such that the capsid was nearly completely covered by Fabs at saturation. The orientation of Fab binding also differed between the AAV1 antibodies, with 5H7 binding nearly perpendicular to the capsid surface (Figure 5.1A, top panel) and 4E4 binding at an angle (Figure 5.1B, top panel). Of the anti-AAV1 antibodies, 4E4 had a larger surface area of interaction extending down the shoulder of the three-fold axis, and possessed the only binding footprint that crossed the two-fold axis for potential interaction with neighbouring VP subunits (Figure 5.1A and B, bottom panels). By comparing the reactivities of these various mouse antibodies with their homologous capsids we seek to define the efficiency of antibody attachment to these viruses and the processes of neutralization that may negatively impact the delivery of AAV-mediated gene therapy products.
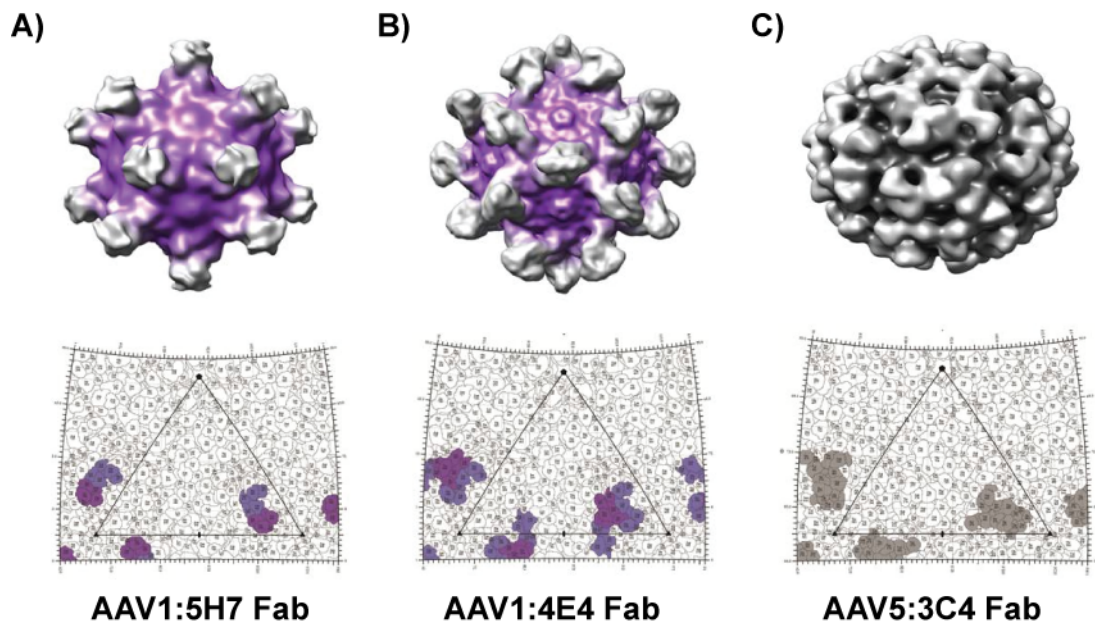
Figure 5.1. Structures of selected Fabs in complex with AAV capsids. Shown are the structures of AAV1 bound by the A) 5H7 or B) 4E4 Fab fragment (top panels) and the footprint of binding on the viral asymmetric unit (bottom panels). The viral capsid is depicted in purple, and the Fab density in light gray. The structure of the AAV1:9A8 complex was not determined in this study and is not shown. C) Structure and footprint of AAV5 bound by the 3C5 Fab fragment, similar to A and B above except that the capsid is depicted in dark gray. (From B. Gurda, manuscript in preparation, with permission.)

5.3 Materials and methods

5.3a Capsid production and immunizations

Empty AAV1, AAV2 and AAV5 capsids comprised of VP1, 2 and 3 proteins were expressed from baculoviruses under the control of the late promoter, grown in HI5 insect cells and purified using cesium chloride and sucrose gradients as previously described (20, 45). Mice were immunized with 0.1 μg AAV1 capsids initially by the

subcutaneous route, with Freund's complete adjuvant in the first immunization and Freund's incomplete adjuvant for the later immunizations. For the final booster, purified AAV1 or AAV5 capsids were administered intravenously in PBS. Three days later the spleen cells were recovered and the lymphocytes were fused to mouse myeloma Sp2/0 cells according to standard methods using polyethylene glycol to create antibody-secreting hybridomas (38). Hybrid cells were selected in the presence of hypoxanthine-aminopterin-thymidine (HAT) and screened for anti-AAV antibody production by ELISA or immunohistochemistry. Positive cells were cloned three times.

5.3b Viruses and cells

GFP-pseudopackaged AAV1 and AAV5 capsids were prepared as previously described (6). Briefly, 293T cells were transfected with pAAV1RC or pAAV5cap and pAAV2 rep78, a plasmid containing the adenovirus helper genes, and a plasmid containing the GFP gene controlled by a mammalian promoter and flanked by the AAV2 genome inverted terminal repeats. Virus capsids were harvested 48 hours after transfection and purified using a cesium chloride step gradient. The highest titer fractions were identified by qPCR and $TCID_{50}$ analysis in Cos-1 or HeLa cells.

Empty AAV1 and AAV5 virus like particles were fluorescently labeled with Alexa-488 dyes (Invitrogen, Carlsbad, CA), following the manufacturer's instructions, with purification as previously described. The degree of labeling was determined to be 10-15 days per capsid, and the capsids were identified to be primarily single particles using the method outlined in (20).

5.3c Production and purification of MAb and Fab fragments

MAb-producing hybridomas were grown in 500 mL culture bags, and the IgGs were isolated from the supernatant using HiTrap Protein G columns (GE LIfesciences, Piscataway, NJ). To produce Fabs, the IgGs were digested using a Fab preparation kit (Thermo Scientific, Rockford, IL), and the monomeric Fab were further purified by chromatography using a Sephadex G100 column (Sigma, St. Louis, MO). IgG and ELISA and/or immunofluorescence confirmed Fab specificity and reactivity.

5.3d ELISA and dot blot analysis of viral binding

To examine the reactivity of the MAbs against different strains of AAV, both ELISA and dot blots of purified capsids were performed. Purified capsids (4 µg/ml in bicarbonate buffer (pH 9.6)) were adsorbed to Probind polystyrene ELISA plates (Corning, Lowell, MA). Antibodies were added and incubated for one hour at 22°C, followed by addition of a secondary horseradish peroxidase (HRP)-conjugated goat anti-mouse antibody and AEC substrate. For membrane dot-blots, capsids of each AAV were spotted on nylon membranes, incubated with the antibody supernatant for one hour followed by a secondary anti-mouse HRP antibody (Sigma). The bound antibody-conjugated HRP was detected with Supersignal luminescent substrate (Thermo Scientific) and exposed to X-ray film.

5.3e Neutralization assays

AAV1 and AAV5 capsids packaging GFP under the control of the CMV promoter were incubated with ten-fold dilutions of purified intact IgGs or Fab fragments as

indicated for 60 minutes at room temperature (22°C). This mixture was incubated with

Cos-1 or HeLa cells at a fixed genome per cell ratio and incubated for one hour at 37°C.

The cells were washed, and fresh growth media was added to the cells. The percentage

of infected cells was measured by quantifying the number of cells expressing GFP at 48

hours post infection using flow cytometry, and was compared to a control well with no

antibody added. Post attachment neutralization was performed by mixing the same

concentration of virus as above with cells for 30 minutes at 4°C prior to the addition of

antibody at the same dilutions as above. After an additional hour at 4°C the cells were

washed extensively, and warm growth media was added. Cells were assayed for GFP

expression at 48 hours post infection as above.

5.3f Assay for antibody-mediated inhibition of cellular binding

Alexa-488-labeled empty AAV1 and AAV5 capsids were incubated in solution with

serial 10-fold dilutions of purified intact IgGs or Fab fragments as indicated for 60

minutes at room temperature. This mixture was incubated with Cos-1 or HeLa cells at a

concentration of 25,000 genomes per cell and incubated for one hour at 4°C. The cells

were washed extensively in cold growth media and assayed for viral binding compared

to a control well with no antibody added, as measured by Alexa-488 mean fluorescence

intensity (MFI) using flow cytometry.

5.4 Results

5.4a Antibody production

We prepared panels of MAbs against AAV1 and AAV5 capsids using two

different immunization strategies. The first involved repeated immunization of AAV1

capsids two to three months prior to the fusion of spleen cells. This protocol resulted in

the production of four IgG- and four IgM-secreting hybridomas against AAV1. Seeking

to prepare cross-reactive antibodies by the sequential administration of alternate

serotypes, we immunized mice twice with AAV1 capsids, then gave a final intravenous

immunization of AAV5 capsids four days prior to the fusion. That protocol resulted in the

isolation of nine IgM- and one IgG-secreting hybridomas against AAV5. A subset of the

antibodies selected for further analysis is shown in Table 5.1.

Table 5.1. Mouse anti-AAV MAbs selected for further studies. The immunizing
antigen and isotype are indicated. *=IgM antibodies were tested for cross-reactivity in
dot blot analysis but were not further tested for neutralizing ability.

Monoclonal antibody (MAb)	Designation in text	Parental AAV antigen	Isotype
AA4E4.G7	4E4	AAV1	IgG2a
AA5H7.D11	5H7	AAV1	IgG2a
AA9A8.B12	9A8	AAV1	IgG1
BB3C5.F4	3C5	AAV5	IgG3
BB9F7.F12	9F7	AAV5	IgM*
BB8F1.E8	8F1	AAV5	IgM*

5.4b Cross-reactivity among different AAV serotypes

Cross-reactivity between the AAV1 and AAV5 MAb hybridoma supernatant and

several AAV serotypes was tested by ELISA and Western dot blot analysis (ELISA data

not shown) (Figure 5.2 and 5.3). The B1 antibody was used to confirm the presence of

virus capsids in the dot blot assay; this antibody was raised against AAV2 and is

directed at a linear peptide at the C-terminus of the VP3 common region present in all

AAVs tested except AAV4 (50). A commercial antibody generated against AAV4

capsids, ADK4, was used as a positive control to verify the presence of this virus during the dot blot assays.
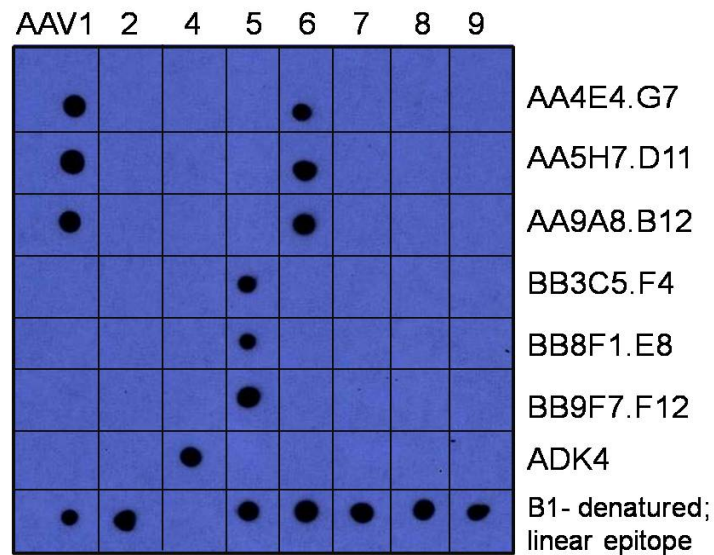
Figure 5.2. Native dot blot analysis of the anti-AAV1 and anti-AAV5 MAbs against AAV1, 2, and 4-9. No cross-reactivity of AAV1 or AAV5 MAbs for other serotypes is seen, except for anti-AAV1 antibody recognition of AAV6 capsids. The B1 antibody recognizes a linear epitope in denatured capsids near the two-fold axis and is used as a positive control to demonstrate the presence of non-parental AAV serotypes. The ADK4 monoclonal antibody (AAV4 specific) is used as a positive control for AAV4 capsids since the B1 epitope is not present in this serotype.

The MAbs were found to recognize conformational epitopes on assembled capsids as they did not react with any linear epitopes in denatured capsids (data not shown, J. Chiorini, personal communication). Dot blots of a subset of the antibody panel binding to intact capsids are shown in Figure 5.2. The eight anti AAV-1 antibodies were specific for the capsids used to immunize the mice, and showed cross-reactivity with serotype 6 but not with any other strain tested (AAV1, 2, 4, 5, 7-9). The anti-AAV5 MAbs displayed no

cross-reactivity in this initial analysis, but when tested at high concentrations had a

weak reaction with AAV1 (Figure 5.3A). However, this reaction was abrogated at even

slightly higher dilutions of hybridoma supernatant (Figure 5.3B).
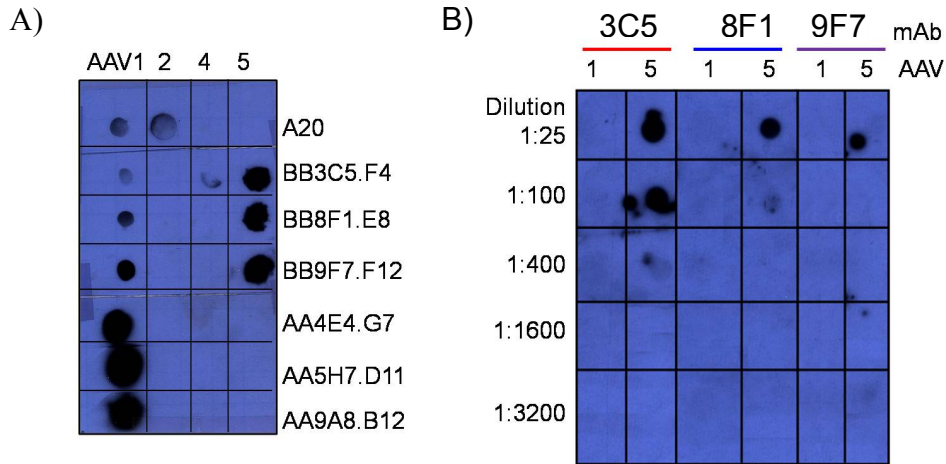
Figure 5.3 MAb characterization and cross-reactivity at high concentrations. A)
Native blot using a MAb hybridoma supernatant dilution of 1:4. Recognition of native
AAV1 by the anti-AAV5 monoclonals is evident at this dilution. B) Serial dilutions of the
anti-AAV5 MAb hybridoma supernatant tested against native AAV1 and 5 capsids. A
lack of recognition is already seen at a 1:25 dilution.

5.4c Neutralization ability of the MAbs

The selected anti-AAV1 and anti-AAV5 IgGs (Table 5.1) were tested for the ability

to neutralize virus infection; the anti-AAV5 IgMs were not tested. Neutralization was

defined as the dilution that gave a 50% or greater reduction of cellular transduction by

AAV1 and AAV5 vectors packaging the GFP-gene, scored as the percentage of GFP-

expressing cells 48 hours after infection and compared to a control well with no antibody

added. All of the antibodies neutralized as intact IgGs although with different efficiencies

(Figure 5.4A). The 4E4 IgG was the most efficient and neutralized at 50- and 500- fold

lower concentrations than the 5H7 and 9A8 antibodies, respectively. The Fabs were each less neutralizing than their IgG counterparts, with the 5H7 antibody retaining the highest level of neutralizing ability as a Fab fragment. The 4E4 and 9A8 Fab fragments reached 50% neutralization only at the highest concentration tested (Figure 5.4B). A similar pattern was seen with the anti AAV5 antibody, 3C5 (Figure 5.4C). This antibody was neutralizing as an intact IgG at a level similar to the 9A8 anti-AAV1 antibody, but was non-neutralizing as a Fab fragment. Figure 5.4D shows the specificity of the antibody-virus interaction as neither IgGs nor Fabs raised against CPV (MAbs 15 and 16) nor an anti-bovine serum albumin IgG were neutralizing even at the highest concentration.
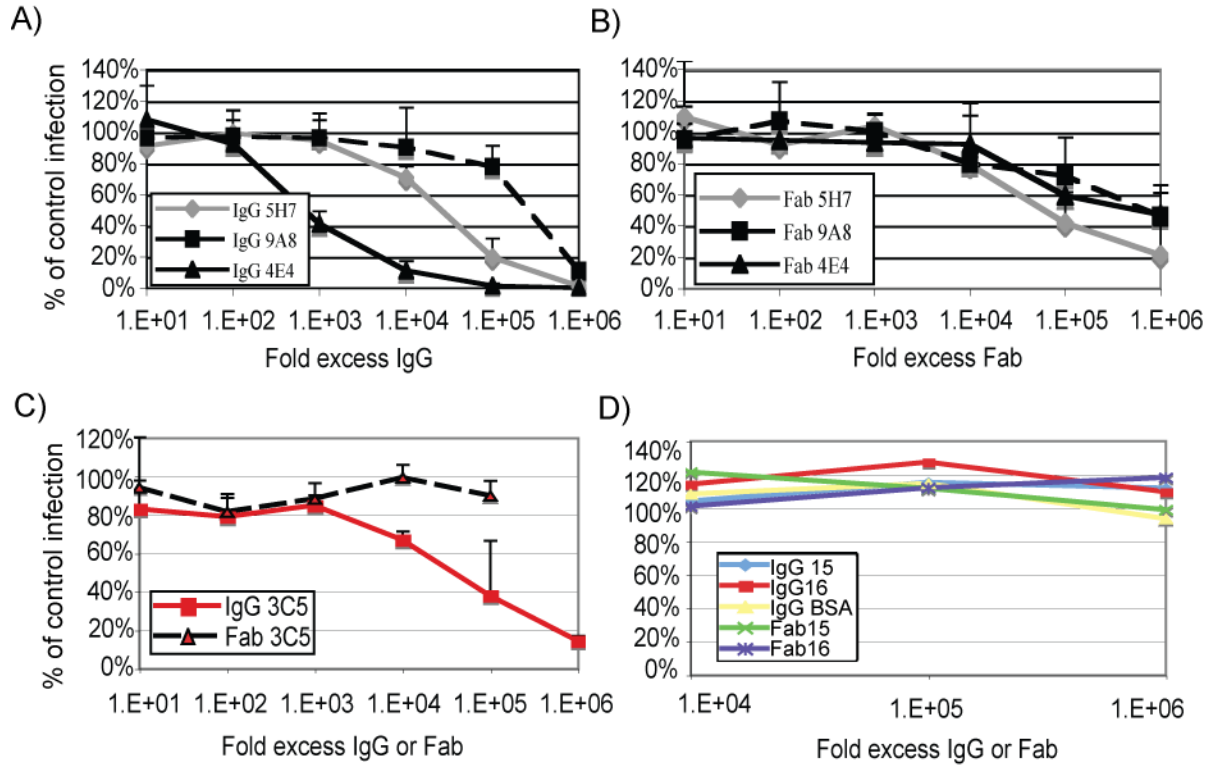
Figure 5.4. Neutralization of AAV1 and AAV5 by MAb IgGs and Fabs. A and B) Serial dilutions of selected anti-AAV1 (A) IgGs or (B) Fabs were pre-incubated with AAV1 capsids packaging the GFP gene under the control of the CMV promoter, then inoculated on Cos-1 cells and scored for infection after 48 hours by flow cytometry. Data are normalized to a control where no antibody was added C) Serial dilutions of the single anti-AAV5 IgG and Fab were tested for the ability to neutralize AAV5 transduction of HeLa cells as in (A) and (B). D) Control IgGs and Fabs directed against canine parvovirus or bovine serum albumin are unable to neutralize when added under the same conditions as above (AAV1 data shown).

5.4d Mechanism of antibody neutralization

The antibodies were tested for their ability to inhibit receptor binding (Figure 5.5). Each anti-AAV1 IgG was able to inhibit receptor binding to <20% of control levels, but they varied in efficiency (Figure 5.5A). Similar to the findings in the infection neutralization assay, the 4E4 antibody reduced viral association with cells at the lowest concentrations out of the three antibodies tested. The Fab fragments were less

inhibitory of receptor binding than their IgG counterparts, and only the 5H7 antibody

reduced the level of cell-associated virus to <50% of control levels as a Fab (Figure

5.5B). Neither the anti-AAV5 3C5 IgG nor Fab fragment reduced the level of cell-

associated virus to <80% of control levels (Figure 5.5C). Control antibodies did not

inhibit the viruses' ability to attach to cells (Figure 5.5D).
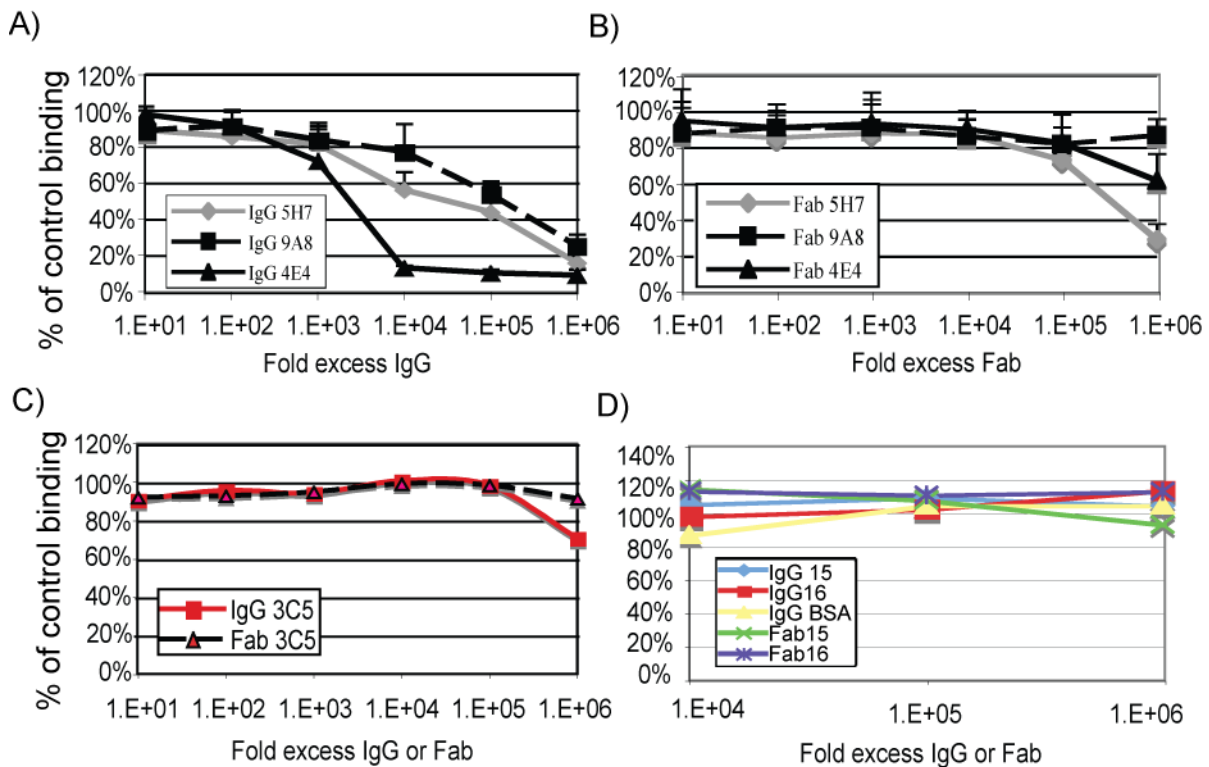
Figure 5.5. Ability of the anti AAV1 and anti-AAV5 MAbs to inhibit receptor binding. A and B) Serial dilutions of selected anti-AAV1 (A) IgGs or (B) Fabs were pre-incubated with Alexa-488 fluorescently labeled empty AAV1 capsids, and then were added to Cos-1 cells. Flow cytometry was used to determine the level of cell-associated fluorescent virus and was compared to a control where no antibody was added. C) Serial dilutions of the anti-AAV5 3C5 IgG and Fab were tested for the ability to inhibit Alexa-488 labeled AAV5 receptor binding to HeLa cells as in (A) and (B). D) Control IgGs and Fabs directed against canine parvovirus or bovine serum albumin are unable to inhibit receptor binding when added under the same conditions as above (AAV1 data shown).

To identify potential neutralization mechanisms other than inhibition of receptor binding, the antibodies were tested for their ability to neutralize AAV infection after the virus had already attached to cells (Figure 5.6). Of the anti-AAV1 antibodies, only the 4E4 IgG gave 50% neutralization at the highest two concentrations tested when added after virus attachment (Figure 5.6A), and none of the Fabs significantly neutralized the virus (Figure 5.6B). Neither the anti-AAV5 3C5 IgG nor Fab inhibited infection after the virus had bound to cells (Figure 5.6C).
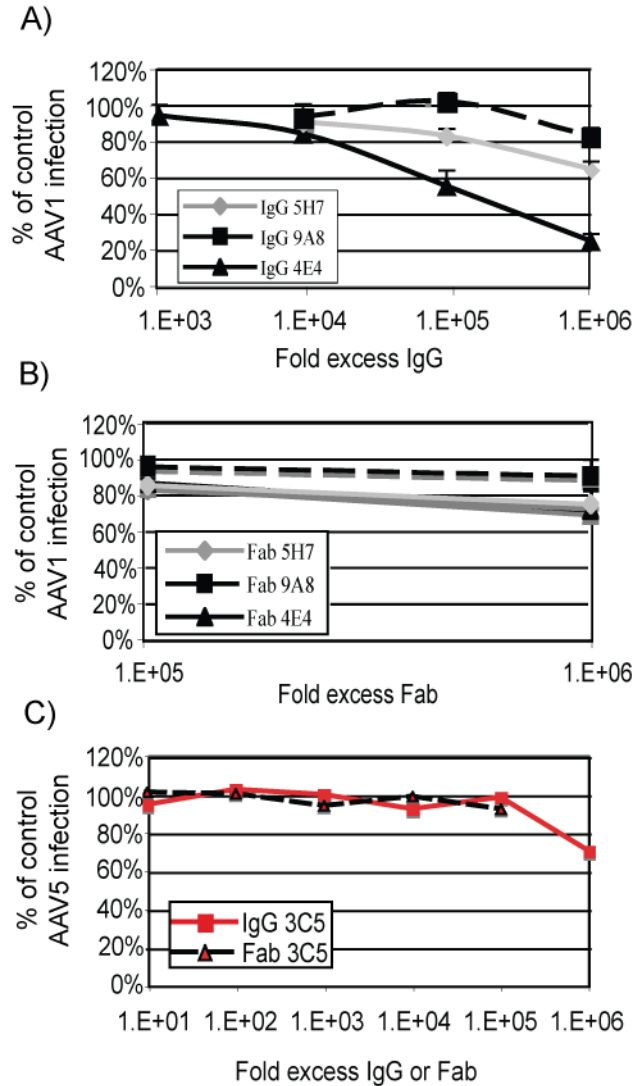
Figure 5.6. Ability of the anti AAV1 and anti-AAV5 MAbs to neutralize at a post-attachment step. A and B) AAV1 capsids packaging the GFP gene were inoculated onto Cos-1 cells at 4°C to allow virus attachment but not endocytosis. Serial dilutions of selected anti-AAV1 (A) IgGs or (B) Fabs were added after 30 minutes for one hour, then unbound antibodies and virus were removed by extensive washing. Cells were warmed to 37°C and scored for infection after 48 hours by flow cytometry. Data are normalized to a control where no antibody was added C) Serial dilutions of the anti-AAV5 3C5 IgG and Fab were tested for the ability to neutralize AAV5 capsids packaging the GFP gene after attachment to HeLa cells as in (A) and (B).

5.5 Discussion

5.5a Anti-AAV monoclonal antibody production

Antibodies are an essential component of the immune response to AAV. The antibody response develops shortly after infection and can protect against subsequent exposures to both the initial immunizing virus and antigenically related viruses in some cases. Here we developed IgG and IgM antibodies reactive against AAV1 and AAV5 capsids to examine the antigenic structures of the capsids, as well as the cross-reactivity and neutralization properties of the antibodies. The AAV capsid was a potent antigen for stimulating antibody production, and only four days after immunization with AAV5 (in mice previously immunized with AAV1) we were able to prepare a panel of several anti-capsid antibodies. Multivalent viral capsids are effective B cell antigens that may elicit some immediate T-cell independent responses, and this is likely the reason for the vigorous anti-AAV5 response seen here (9). T-helper cell epitopes may also be shared between the AAV1 used for pre-immunization and the AAV5 capsids given in the final boost, and may that affect the response against the second virus. Although the mice had been previously immunized with AAV1, most of the antibodies produced were IgMs directed against AAV5, with only one IgG. In similar studies of canine parvovirus capsids we prepared anti-capsid IgM hybridomas four days after primary immunization of naïve mice, suggesting that the pre-immunization with AAV1 was not necessary for the early response seen here (C Parrish, unpublished data).

The structures of the antibody-capsid complexes were solved by cryo-electron microscopy for some of the antibodies examined here, and all were found to bind within

a relatively limited footprint on the capsid surface. The antibodies all bound to the prominent spike near the three-fold axis of the capsid, adjacent to the receptor-binding domain. Only the binding site of the anti-AAV1 4E4 antibody extended across the two-fold axis with the potential to cross-link VP subunits. Although the area around the five-fold axis protrudes from the capsid surface and might be expected to be an attractive feature for antibodies, structural analysis has previously identified flexibility in the surface loops at this location in CPV capsids (17). This property, if also present in the AAV capsid, could be expected to interfere with the tightly controlled structural interactions required for antibody binding and may account for the lack of antibodies found directed against this area.

5.5b Cross-reactivity of the anti-AAV monoclonal antibodies

The MAbs produced in this study react with AAV1 and AAV5 capsids and provide a variety of useful reagents for the study of AAV immunogenicity and cellular entry. The antibodies were generally not cross-reactive between serotypes, except for the anti-AAV1 antibodies that also reacted with AAV6 capsids. These two serotypes share 99.2% sequence identity, and the capsid proteins differ by only six amino acids. While these viruses do show some differences in receptor binding and transduction efficiency, they are the most closely related of any of the serotypes and thus it is not necessarily surprising to see some antibody cross-reactivity (51, 53). The anti-AAV5 antibodies showed only weak cross-reactivity with AAV1, despite that the mice were immunized twice with AAV1 and only once with AAV5 shortly before lymphocyte harvesting. The hybridomas obtained from these mice were screened and cloned based only on their

185

reactivity with AAV5, and strongly-reactive anti-AAV1 B cells produced during the initial

two immunizations were not selected for by this screening method. The particular

features of each capsid type that attract the antibody response therefore must differ

between serotypes, supporting their separation as distinct serotypes and the practice of

using sequential administration of different AAVs for repeat transgene delivery in clinical

trials to reduce vector neutralization.

5.5c Neutralizing ability of the anti-AAV antibodies

All the anti-AAV specific antibodies neutralized the viruses as intact IgGs, but

they had different neutralization abilities across the six-log concentration profile tested.

Of the three anti-AAV1 IgGs tested, 4E4 was able to neutralize at the lowest

concentration and had the largest coverage of any antibody where the structure was

solved. As it binds at an angle to the capsid surface, it likely provides more steric

hindrance to prevent interaction of the virus with the target cell. The structural

interaction of 9A8 with AAV1 has not been solved and its epitope is unknown, but it was

poorly neutralizing. Thus, it may have a different structural interaction, poor affinity, or

may be less able to cross-link particles than the other two antibodies examined in this

study.

The anti-AAV5 3C5 IgG possessed a neutralization profile similar to that of the

least efficient anti-AAV1 antibody, 9A8. This MAb binds to all 60 VP capsid protein

monomers so that the entire capsid appears to be coated by antibodies at saturation

(Figure 5.1C). However, this antibody was produced only after four days of

immunization with AAV5 and may represent an immature antibody with a relatively low

affinity that is easily displaced to allow the virus to infect cells. Further studies would be needed to compare the reactivity of this antibody to those produced by a three-step immunization as was done for AAV1 in this study.

Given that the location of the antibody footprints appeared at or near the receptor-binding sites, inhibition of receptor binding was hypothesized to be a logical mechanism of neutralization. The shapes of the infection neutralization curves were similar to the binding inhibition curves for the anti-AAV1 antibodies, suggesting that this was in fact a major mechanism used. The most highly neutralizing IgG (4E4) and Fab (5H7) were the most effective in interference with receptor binding. As a whole, the Fabs were poorly inhibitory of receptor binding compared to the intact IgGs, and were also poorly neutralizing. The could be a result of the smaller area of steric inhibition provided by the Fab fragments that lack the bulky Fc domain and second Fab arm, rendering them less able to prevent the access of sialic acids to the capsid surface. Alternatively, the inability of Fab fragments to cross link viral particles may also be a factor contributing to their low efficacy of neutralization.

When tested for the ability to neutralize the virus after it had already attached to receptors, only the 4E4 IgG, and none of the Fabs, was able to significantly inhibit infection. The mechanism by which this post-attachment neutralization occurred was not determined, but the structure of the 4E4 antibody-virus complex provides some clues. The 4E4 antibody is the only MAb with a binding site that extends across the two-fold axis of symmetry and has the potential to cross link subunits, stabilize the capsid structure, and interfere with required conformational changes during entry. As the Fab

fragment did not neutralize the virus after attachment, the implication is either that the antibody is binding bivalently to stabilize the capsid structure or that another mechanism is at work. For example, the post-attachment neutralization may be due to an isotype specific constant region (Fc) mediated function within the cell, as the 4E4 antibody is of a different subclass than the other two anti-AV1 antibodies. A recent study has identified a TRIM-21 dependent, Fc mediated, intracellular neutralization mechanism, and this or a related functionality may be of some relevance here (31).

The antigenic structures of viral capsids recognized by antibodies are key to the development of protective immune responses. The AAVs provide an important model system to examine the antigenic structure of simple capsids, as there are several genetically and antigenically distinct viruses that have been classified by DNA sequence analysis. The results of these studies provide insights into the particular features of the AAV capsids that draw the antibody response, and highlight that, while other mechanisms may be used in some cases, inhibition of receptor binding is a major mechanism by which antibodies neutralize AAVs. Future studies are ongoing to develop antibody escape mutants that retain the receptor-binding properties of the wild-type virus. These efforts seek to circumvent the interference of humoral immunity on the delivery of AAV-derived gene therapy vectors, and if successful would be relevant for the many ongoing clinical trials using AAV to deliver genes of interest for a variety of disease states.

5.6 Acknowledgements

Infectious Diseases. The authors would like to thank Sandra Wainer and Beverly

Handleman for excellent technical support. Wendy Weichert performed the mouse

immunizations and hybridoma production. J. Chiorini performed the dot blot assays for

cross-reactivity. B. Gurda performed the cryo-electron microscopy and structural

interpretations.

5.7 References

1. **Allocca, M., A. Tessitore, G. Cotugno, and A. Auricchio.** 2006. AAV-mediated gene transfer for retinal diseases. Expert Opin Biol Ther **6:**1279-94.

2. **Boutin, S., V. Monteilhet, P. Veron, C. Leborgne, O. Benveniste, M. F. Montus, and C. Masurier.** 2010. Prevalence of serum IgG and neutralizing factors against adeno-associated virus (AAV) types 1, 2, 5, 6, 8, and 9 in the healthy population: implications for gene therapy using AAV vectors. Hum Gene Ther **21:**704-12.

3. **Calcedo, R., L. H. Vandenberghe, G. Gao, J. Lin, and J. M. Wilson.** 2009. Worldwide epidemiology of neutralizing antibodies to adeno-associated viruses. J Infect Dis **199:**381-90.

4. **Chiorini, J. A., F. Kim, L. Yang, and R. M. Kotin.** 1999. Cloning and characterization of adeno-associated virus type 5. J Virol **73:**1309-19.

5. **Choi, V. W., D. M. McCarty, and R. J. Samulski.** 2005. AAV hybrid serotypes: improved vectors for gene delivery. Curr Gene Ther **5:**299-310.

6. **Conway, J. E., C. M. Rhys, I. Zolotukhin, S. Zolotukhin, N. Muzyczka, G. S. Hayward, and B. J. Byrne.** 1999. High-titer recombinant adeno-associated virus production utilizing a recombinant herpes simplex virus type I vector expressing AAV-2 Rep and Cap. Gene Ther **6:**986-93.

7. **Dai, J., and A. B. Rabie.** 2007. The use of recombinant adeno-associated virus for skeletal gene therapy. Orthod Craniofac Res **10:**1-14.

8. **Dimmock, N. J.** 1993. Neutralization of animal viruses. Curr Top Microbiol Immunol **183:**1-149.

9. **Fehr, T., D. Skrastina, P. Pumpens, and R. M. Zinkernagel.** 1998. T cell-independent type I antibody response against B cell epitopes expressed

repetitively on recombinant virus particles. Proc Natl Acad Sci U S A **95:**9477-81.

10. **Gao, G., M. R. Alvira, S. Somanathan, Y. Lu, L. H. Vandenberghe, J. J. Rux, R. Calcedo, J. Sanmiguel, Z. Abbas, and J. M. Wilson.** 2003. Adeno-associated viruses undergo substantial evolution in primates during natural infections. Proc Natl Acad Sci U S A **100:**6081-6.

11. **Gao, G., L. H. Vandenberghe, M. R. Alvira, Y. Lu, R. Calcedo, X. Zhou, and J. M. Wilson.** 2004. Clades of Adeno-associated viruses are widely disseminated in human tissues. J Virol **78:**6381-8.

12. **Gao, G. P., M. R. Alvira, L. Wang, R. Calcedo, J. Johnston, and J. M. Wilson.** 2002. Novel adeno-associated viruses from rhesus monkeys as vectors for human gene therapy. Proc Natl Acad Sci U S A **99:**11854-9.

13. **Grieger, J. C., and R. J. Samulski.** 2005. Adeno-associated virus as a gene therapy vector: vector development, production and clinical applications. Adv Biochem Eng Biotechnol **99:**119-45.

14. **Grimm, D., and M. A. Kay.** 2003. From virus evolution to vector revolution: use of naturally occurring serotypes of adeno-associated virus (AAV) as novel vectors for human gene therapy. Curr Gene Ther **3:**281-304.

15. **Grimm, D., J. S. Lee, L. Wang, T. Desai, B. Akache, T. A. Storm, and M. A. Kay.** 2008. In vitro and in vivo gene therapy vector evolution via multispecies interbreeding and retargeting of adeno-associated viruses. J Virol **82:**5887-911.

16. **Hacker, U. T., F. M. Gerner, H. Buning, M. Hutter, H. Reichenspurner, M. Stangl, and M. Hallek.** 2001. Standard heparin, low molecular weight heparin, low molecular weight heparinoid, and recombinant hirudin differ in their ability to inhibit transduction by recombinant adeno-associated virus type 2 vectors. Gene Ther **8:**966-8.

17. **Hafenstein, S., V. D. Bowman, T. Sun, C. D. Nelson, L. M. Palermo, P. R. Chipman, A. J. Battisti, C. R. Parrish, and M. G. Rossmann.** 2009. Structural comparison of different antibodies interacting with parvovirus capsids. J Virol **83:**5556-66.

18. **Halbert, C. L., A. D. Miller, S. McNamara, J. Emerson, R. L. Gibson, B. Ramsey, and M. L. Aitken.** 2006. Prevalence of neutralizing antibodies against adeno-associated virus (AAV) types 2, 5, and 6 in cystic fibrosis and normal populations: Implications for gene therapy using AAV vectors. Hum Gene Ther **17:**440-7.

19. **Halbert, C. L., E. A. Rutledge, J. M. Allen, D. W. Russell, and A. D. Miller.**

2000. Repeat transduction in the mouse lung by using adeno-associated virus vectors with different serotypes. J Virol **74:**1524-32.

20. **Harbison, C. E., S. M. Lyi, W. S. Weichert, and C. R. Parrish.** 2009. Early steps in cell infection by parvoviruses: host-specific differences in cell receptor binding but similar endosomal trafficking. J Virol **83:**10504-14.

21. **Hernandez, Y. J., J. Wang, W. G. Kearns, S. Loiler, A. Poirier, and T. R. Flotte.** 1999. Latent adeno-associated virus infection elicits humoral but not cell-mediated immune responses in a nonhuman primate model. J Virol **73:**8549-58.

22. **Huttner, N. A., A. Girod, L. Perabo, D. Edbauer, J. A. Kleinschmidt, H. Buning, and M. Hallek.** 2003. Genetic modifications of the adeno-associated virus type 2 capsid reduce the affinity and the neutralizing effects of human serum antibodies. Gene Ther **10:**2139-47.

23. **Kaludov, N., K. E. Brown, R. W. Walters, J. Zabner, and J. A. Chiorini.** 2001. Adeno-associated virus serotype 4 (AAV4) and AAV5 both require sialic acid binding for hemagglutination and efficient transduction but differ in sialic acid linkage specificity. J Virol **75:**6884-93.

24. **Klasse, P. J., and Q. J. Sattentau.** 2001. Mechanisms of virus neutralization by antibody. Curr Top Microbiol Immunol **260:**87-108.

25. **Klasse, P. J., and Q. J. Sattentau.** 2002. Occupancy and mechanism in antibody-mediated neutralization of animal viruses. J Gen Virol **83:**2091-108.

26. **Law, M., and L. Hangartner.** 2008. Antibodies against viruses: passive and active immunization. Curr Opin Immunol **20:**486-92.

27. **Lin, J., R. Calcedo, L. H. Vandenberghe, J. M. Figueredo, and J. M. Wilson.** 2008. Impact of preexisting vector immunity on the efficacy of adeno-associated virus-based HIV-1 Gag vaccines. Hum Gene Ther **19:**663-9.

28. **Lochrie, M. A., G. P. Tatsuno, B. Christie, J. W. McDonnell, S. Zhou, R. Surosky, G. F. Pierce, and P. Colosi.** 2006. Mutations on the external surfaces of adeno-associated virus type 2 capsids that affect transduction and neutralization. J Virol **80:**821-34.

29. **Lopez-Bueno, A., M. G. Mateu, and J. M. Almendral.** 2003. High mutant frequency in populations of a DNA virus allows evasion from antibody therapy in an immunodeficient host. J. Virol. **77:**2701-2708.

30. **Lorain, S., D. A. Gross, A. Goyenvalle, O. Danos, J. Davoust, and L. Garcia.** 2008. Transient Immunomodulation Allows Repeated Injections of AAV1 and

Correction of Muscular Dystrophy in Multiple Muscles. Mol Ther **16:**541-7.

31. **Mallery, D. L., W. A. McEwan, S. R. Bidgood, G. J. Towers, C. M. Johnson, and L. C. James.** 2010. Antibodies mediate intracellular immunity through tripartite motif-containing 21 (TRIM21). Proc Natl Acad Sci U S A **107:**19985-90.

32. **Michelfelder, S., and M. Trepel.** 2009. Adeno-associated viral vectors and their redirection to cell-type specific receptors. Adv Genet **67:**29-60.

33. **Moskalenko, M., L. Chen, M. van Roey, B. A. Donahue, R. O. Snyder, J. G. McArthur, and S. D. Patel.** 2000. Epitope mapping of human anti-adeno-associated virus type 2 neutralizing antibodies: implications for gene therapy and virus structure. J Virol **74:**1761-6.

34. **Muller, O. J., F. Kaul, M. D. Weitzman, R. Pasqualini, W. Arap, J. A. Kleinschmidt, and M. Trepel.** 2003. Random peptide libraries displayed on adeno-associated virus to select for targeted gene therapy vectors. Nat Biotechnol **21:**1040-6.

35. **Negishi, A., J. Chen, D. M. McCarty, R. J. Samulski, J. Liu, and R. Superfine.** 2004. Analysis of the interaction between adeno-associated virus and heparan sulfate using atomic force microscopy. Glycobiology **14:**969-77.

36. **Parren, P. W., and D. R. Burton.** 2001. The antiviral activity of antibodies in vitro and in vivo. Adv Immunol **77:**195-262.

37. **Parrish, C. R., C. Aquadro, M. L. Strassheim, J. F. Evermann, J.-Y. Sgro, and H. Mohammed.** 1991. Rapid antigenic-type replacement and DNA sequence evolution of canine parvovirus. J Virol **65:**6544-6552.

38. **Parrish, C. R., and L. E. Carmichael.** 1983. Antigenic structure and variation of canine parvovirus type-2, feline panleukopenia virus, and mink enteritis virus. Virology **129:**401-414.

39. **Petry, H., A. Brooks, A. Orme, P. Wang, P. Liu, J. Xie, P. Kretschmer, H. S. Qian, T. W. Hermiston, and R. N. Harkins.** 2008. Effect of viral dose on neutralizing antibody response and transgene expression after AAV1 vector re-administration in mice. Gene Ther **15:**54-60.

40. **Pierson, T. C., D. H. Fremont, R. J. Kuhn, and M. S. Diamond.** 2008. Structural insights into the mechanisms of antibody-mediated neutralization of flavivirus infection: implications for vaccine development. Cell Host Microbe **4:**229-38.

41. **Scallan, C. D., D. Lillicrap, H. Jiang, X. Qian, S. L. Patarroyo-White, A. E.**

Parker, T. Liu, J. Vargas, D. Nagy, S. K. Powell, J. F. Wright, P. V. Turner, S. J. Tinlin, S. E. Webster, A. McClelland, and L. B. Couto. 2003. Sustained phenotypic correction of canine hemophilia A using an adeno-associated viral vector. Blood.

42. **Shi, W., G. S. Arnold, and J. S. Bartlett.** 2001. Insertional mutagenesis of the adeno-associated virus type 2 (aav2) capsid gene and generation of aav2 vectors targeted to alternative cell-surface receptors. Hum Gene Ther **12:**1697-711.

43. **Strassheim, L. S., A. Gruenberg, P. Veijalainen, J.-Y. Sgro, and C. R. Parrish.** 1994. Two dominant neutralizing antigenic determinants of canine parvovirus are found on the threefold spike of the virus capsid. Virology **198:**175-184.

44. **Sun, J. Y., V. Anand-Jawa, S. Chatterjee, and K. K. Wong.** 2003. Immune responses to adeno-associated virus and its recombinant vectors. Gene Ther **10:**964-76.

45. **Urabe, M., C. Ding, and R. M. Kotin.** 2002. Insect cells as a factory to produce adeno-associated virus type 2 vectors. Hum Gene Ther **13:**1935-43.

46. **van der Marel, S., E. M. Comijn, H. W. Verspaget, S. van Deventer, G. R. van den Brink, H. Petry, D. W. Hommes, and V. Ferreira.** 2011. Neutralizing antibodies against adeno-associated viruses in inflammatory bowel disease patients: Implications for gene therapy. Inflamm Bowel Dis.

47. **Van Vliet, K. M., V. Blouin, N. Brument, M. Agbandje-McKenna, and R. O. Snyder.** 2008. The role of the adeno-associated virus capsid in gene transfer. Methods Mol Biol **437:**51-91.

48. **Walters, R. W., S. Yi, S. Keshavjee, K. E. Brown, M. J. Welsh, J. A. Chiorini, and J. Zabner.** 2001. Binding of adeno-associated virus type 5 to 2,3-linked sialic acid is required for gene transfer. J Biol Chem **2766:**20610-2061.

49. **Willey, S., and M. M. Aasa-Chapman.** 2008. Humoral immunity to HIV-1: neutralisation and antibody effector functions. Trends Microbiol **16:**596-604.

50. **Wobus, C. E., B. Hugle-Dorr, A. Girod, G. Petersen, M. Hallek, and J. A. Kleinschmidt.** 2000. Monoclonal antibodies against the adeno-associated virus type 2 (AAV-2) capsid: epitope mapping and identification of capsid domains involved in AAV-2-cell interaction and neutralization of AAV-2 infection. J Virol **74:**9281-93.

51. **Wu, Z., A. Asokan, J. C. Grieger, L. Govindasamy, M. Agbandje-McKenna,**

and R. J. Samulski. 2006. Single amino acid changes can influence titer, heparin binding, and tissue tropism in different adeno-associated virus serotypes. J Virol **80:**11393-7.

52. **Wu, Z., A. Asokan, and R. J. Samulski.** 2006. Adeno-associated virus serotypes: vector toolkit for human gene therapy. Mol Ther **14:**316-27.

53. **Wu, Z., E. Miller, M. Agbandje-McKenna, and R. J. Samulski.** 2006. Alpha2,3 and alpha2,6 N-linked sialic acids facilitate efficient binding and transduction by adeno-associated virus types 1 and 6. Journal of virology **80:**9093-103.

54. **Xiao, W., N. Chirmule, S. C. Berta, B. McCullough, G. Gao, and J. M. Wilson.** 1999. Gene therapy vectors based on adeno-associated virus type 1. J Virol **73:**3994-4003.

55. **Zabner, J., M. Seiler, R. Walters, R. M. Kotin, W. Fulgeras, B. L. Davidson, and J. A. Chiorini.** 2000. Adeno-associated virus type 5 (AAV5) but not AAV2 binds to the apical surfaces of airway epithelia and facilitates gene transfer. J Virol **74:**3852-3858.

56. **Zaiss, A. K., and D. A. Muruve.** 2008. Immunity to adeno-associated virus vectors in animals and humans: a continued challenge. Gene Ther **15:**808-16.

57. **Zhong, L., W. Li, Y. Li, W. Zhao, J. Wu, B. Li, N. Maina, D. Bischof, K. Qing, K. A. Weigel-Kelley, I. Zolotukhin, K. H. Warrington, Jr., X. Li, W. B. Slayton, M. C. Yoder, and A. Srivastava.** 2006. Evaluation of primitive murine hematopoietic stem and progenitor cell transduction in vitro and in vivo by recombinant adeno-associated virus vector serotypes 1 through 5. Hum Gene Ther **17:**321-33.

CHAPTER 6: CONCLUSIONS AND FUTURE DIRECTIONS

6.1 Contextual framework

Parvoviruses must cross a number of hurdles to reach the nuclei of host cells and complete their replication cycle. In nature they must first survive in the environment long enough to reach the host and gain access to target tissues with cells permissive for replication. Inside the host, they must also evade a variety of innate and adaptive immune mechanisms, such as neutralizing antibodies, specifically tailored to combat incoming pathogens. Even once they gain access to a target cell, to reach the nucleus the virus must still traverse the dense cellular landscape that includes obstacles at the plasma membrane, the network of interconnected endosomal compartments, the cytoplasm with its tightly compacted cytoskeletal networks, and finally the nuclear envelope and lamina. The studies contained herein advance our understanding of how parvoviruses navigate a pathway to infection despite the numerous roadblocks imparted by the host.

Furthermore, the landscape of obstacles changes on both short and long time scales, as both the host and the virus continue to evolve in concert with each other in what has been termed the "host-pathogen arms race" (4). As a relatively recent virus that emerged about 35 years ago, CPV-2 and its relatives provide a model for viral emergence which is broadly applicable to a variety of contemporary emerging diseases. Given the ever-increasing contact between wildlife and domestic animal species and between animals and humans, the occurrence of these types of outbreaks is likely only to increase in the future. Though they are still relatively rare, we have witnessed several examples of rapid changes in viral host range or virulence in recent years, including Hendra virus, SARS corononavirus, avian and swine influenza that have emerged in

humans, the jump of A/H3N8 equine influenza virus into dogs, and the rapid emergence of a virulent systemic strain of feline calicivirus from a normally innocuous upper respiratory pathogen in cats (VS-FCV) (1, 5, 6). Understanding the effects that small differences among viral strains can have on host range, tissue tropism, antigenicity, and virulence is essential for being able to predict and manage outbreaks of new or newly recognized diseases, particularly those that arise from a host-jumping event.

6.2 Parvovirus receptor recognition and cellular uptake

The cellular receptor is the key to viral entry into host cells, and is important for determining host range and tissue tropism. The virus attaches to the receptor at the cell surface, and in the case of carnivore parvoviruses the TfR is used for receptor-mediated endocytosis and trafficking to specific intracellular locations. Chapter 2 further elucidated the details of this entry process in the context of the evolutionary variation of different viruses and hosts. The results showed that despite differing by only a few amino acids, the feline and canine viruses have somewhat different interactions with the receptor on the surface of canine and feline cells. Not only do they bind with an apparently different affinity (as evidenced by the level of cell-associated virus), but they also bind with a different surface distribution (on filopodia of canine cells), and are taken up with different kinetics in canine and feline cells. These features likely affect the efficiency of cellular infection, given the importance of the specific interaction of the virus with the TfR and the requirements for certain (as yet poorly defined) intracellular signals that alert the virus it is in an environment permissive for genome release.

The requirements for specific interactions between the TfR and cellular components were analyzed in Chapter 3 using variant feline TfRs with transmembrane

and cytoplasmic domains derived from alternate cellular and viral type II membrane proteins, or with mutations in the native cytoplasmic domain. A total of 10 different receptors, including wild-type, were analyzed for expression and functionality in allowing binding, endocytosis, and infection by CPV and FPV. Of these, eight out of the 10 were expressed at sufficient level to warrant further study. Although these receptors showed some variation in the ability to endocytose transferrin and virus capsids, these results confirm that some chimeric receptors can be expressed in a functionally intact way on the cell surface. However, of the eight receptors tested, only the two feline TfRs with mutated cytoplasmic domains allowed infection at wild type levels. The chimeric receptors fell into two groups based on sequence of origin; chimeras with cellular proteins allowed intermediate levels of infection while viral protein chimeras allowed only low levels. Future studies will further elucidate the mechanisms behind these differences in infection efficiency. The results presented in Chapter 3 begin to address these questions by showing that viruses bound to the least permissive receptors had slower uptake kinetics and different intracellular distributions following endocytosis, suggesting that alternate pathways of uptake may be directing most of these viruses to non-productive compartments.

6.3 Intracellular trafficking of parvoviruses

Despite variations in behavior between wild-type feline and canine parvoviruses at the cell surface, differences in the intracellular trafficking patterns between the viral strains analyzed were not easily distinguishable and only subtle differences of unknown importance were identified. The results presented here show that after uptake by wild-type receptors on healthy cells, virus capsids became rapidly dispersed throughout

several endosomal compartments and could be found in early, late, and recycling compartments within the first 10 minutes after uptake. However, the particle-to-infectivity ratio for parvoviruses is very high and simply observing where the majority of the particles go may not necessarily identify the infectious pathway. For this, confirmation by a variety of additional approaches is required.

The importance of the degradative pathway in infection was supported in Chapter 2 by the finding that disrupting membrane trafficking within the early and late endosomes using dominant negative forms of Rab5 or Rab7 inhibited infection, while disrupting the recycling endosome with a dominant negative Rab11 protein did not. Furthermore, in Chapter 3, capsids bound to chimeric receptors with cytoplasmic tails from viral proteins that did not efficiently traffic to the perinuclear area were also the most deficient in infection. However, the proportion of viruses entering specific different endosomal compartments at this location was not determined in these studies due to the limited resolution of our imaging technology. Furthermore, in neither of these studies was virus directly observed escaping the late endosomal or lysosomal compartments, and the mechanisms by which membrane penetration, cytoplasmic trafficking, and nuclear entry occur have remained elusive. Further experiments will seek to examine these issues, as the later steps of entry between endosomal trafficking and nuclear import appear to be major bottlenecks in the parvovirus infection process. Specific areas of interest include the potential role of intra-endosomal cellular factors in modifying the viral capsid or facilitating conformational changes involved with exposure of the VP1 N terminus or genome, and the specific roles for the phospholipase A_2 domain and nuclear localization signals contained within the VP1 N terminus.

Finally, these studies demonstrated the utility of fluorescently-labeled capsids in the study of the early steps of virus interactions with cells. They appear to behave very similarly to unlabeled capsids, allow for easy quantitative detection of the level of cell-associated virus, and allow us to follow virus entry into live cells in real time. As such, this technology was utilized in each study contained within this dissertation, and is also being applied to studies by others in the laboratory.

6.4 The role of antibodies in parvoviral infection and evolution

Antibodies play a central role in the control of parvoviral infections, and no doubt exert a selective pressure on the viral capsid as it passes from host to host. However, the ability of the host immune response to select for viral mutations that escape from this pressure is constrained by structural limitations imposed by the need to preserve vital functions such as receptor binding and the flexibility to package and release the genome in the proper environment. In the case of FPV and CPV, the appearance of antigenically variant strains has occurred simultaneously with alterations in host range, suggesting a multi-factorial driving force for viral evolution. Presumably, this is also the case in the evolution of CPV-2 as it passed through raccoons, which were identified in Chapter 4 as a newly-recognized intermediate host in the adaptation of CPV to dogs. The CPV-2-like strains isolated from raccoons were found to have alterations in both reactivity with antibodies and in the ability to bind the canine TfR and use it to infect canine cells.

The major antigenic sites on the CPV capsid have been defined, and those overlap with structures important for receptor binding. In general, these sites are thought to be easy targets for the immune response as they tend to be located on

prominent features of the viral capsid, maximizing presentation to the host cell and as a byproduct, to the immune response. For CPV and FPV, receptor binding is a key determinant in host range and is dependent on specific features of both the host TfR and the virus capsid. On the receptor side, the TfR contains species-specific mutations throughout different carnivore families and genera, and ongoing studies in the lab are teasing out the significance of these differences in the evolution and host-switching of carnivore parvoviruses (J. Kaelber, personal communication).

On the capsid side, of particular relevance to the mutations seen in the CPV-2 derived isolates from raccoons as detailed in Chapter 3, VP2 residue 300 is located in the "B" antigenic site and has mutated more than once since the virus first emerged in the 1970s. Other key changes in raccoon strains also fell within antigenic sites, including VP2 residue 224 in the "A site" and VP2 residue 305, also in the "B site" (3). Combinations of changes at those two sites led to loss of reactivity with all but a small number of mouse and rat monoclonal anti-FPV or anti-CPV antibodies. The raccoon strain with changes of residues 300 and 224 together evaded detection by nearly all of the 30 anti-FPV and -CPV antibodies tested, which may be taken as an approximation of the polyclonal antibody response. It remains to be seen whether the emergence of strains similar to these will cause a problem for our domestic animals; however, despite that changes at these sites are apparently relatively readily selected, these viruses have been circulating undetected in raccoons for 20 years and they have failed to cause a detectable disease epidemic among companion animals, possibly due to the varying fitness landscapes traversed during passage between different hosts.

Serological studies would be beneficial in determining the prevalence of seropositivity in raccoons from different geographic locations. Other carnivores such as foxes and mustelids should also be examined more closely for seropositivity and incidence of parvoviral disease, and the viral sequences determined in cases when active infections are found. This effort would be useful for tracking the ongoing incidence and evolution of virus strains in different hosts and may be helpful in detecting and managing novel and potentially dangerous viruses in the future. In addition, analysis of specific antibodies produced by raccoons and other natural hosts would be interesting to determine whether the epitopes recognized fall into these same antigenic sites as defined by the mouse and rat antibody response, or are unique.

Future studies addressing the antibody response of the dog should also be undertaken, as the epitopes recognized by the canine B cell repertoire have not been specifically defined. Though they likely share similarities with the sites identified by rodent antibodies, a specific study in dogs may be useful for designing future generation vaccines, especially in light of (so far mostly unfounded) concerns about escape of the virus from vaccine immunity. Beginning in 2000, the appearance of the CPV-2c antigenic variant containing a single point mutation at VP2 residue 426 sparked a controversy and near-panic about this issue. While current evidence is that contemporary vaccines protect effectively against this strain, the potential for emergence of a virus variant that is not protected against does exist. In each case of viral evolution of CPV, only a small number of changes (though always more than one) were necessary to achieve the major jumps in host range. In fact, within the last few years, there has been mounting anecdotal evidence for increased incidence of

parvoviral enteritis in dogs older than the normal six to16 weeks, including fully

vaccinated adult dogs. A limited amount of VP2 sequencing has been undertaken from

diagnostic samples submitted to the diagnostic lab at Cornell University, and while

some recurring mutations have been seen, no conclusive patterns of accumulated

mutations have been found (unpublished data, and E. Dubovi, personal

communication). Once again, only ongoing surveillance will be able to tease out the

significance of any individual or combined mutations.

6.5 Antibody limitations to parvoviruses as gene therapy vectors

The antibody response is also a key hurdle in the development of adeno-

associated viruses as gene therapy vectors. Humoral immunity can prevent the

application of these vectors in a significant proportion of the human population, as

studies have identified anti-capsid antibodies in up to 80% of the population in some

cases (2). The study in Chapter 5 sought to define the functionality of antibodies

produced in mice against AAV1 and AAV5. Previous structural studies showed that like

the autonomous parvoviruses, these antibodies were directed against a limited footprint

on the viral capsid that overlapped with the receptor-binding site (B. Gurda, personal

communication). The results presented here showed that despite binding to a similar

location, the antibodies were variably effective at neutralizing cellular transduction and

that this neutralization was likely favored by the larger area of steric hindrance, the

bivalency, or the Fc region of the intact IgG as most Fab fragments were poorly

neutralizing. The mechanism of neutralization was primarily associated with inhibition of

receptor binding in many cases, although for one antibody (3C5, anti-AAV5) the inferred

affinity was too low to show this directly. Only one antibody (4E4, anti-AAV1) was able

to neutralize after the virus had bound to cells, indicating that it may have an alternate mechanism of neutralization.

Future studies should seek to examine the neutralization properties of additional antibodies, preferably isolated from human lymphocytes, as only a small number of mouse antibodies were tested in the current study. Increasing the diversity of antibodies may allow for the identification of additional epitopes and mechanisms of neutralization, or may simply strengthen the hypothesis that inhibition of receptor binding is truly the most important target for the antibody response. In addition, AAV escape mutants that reduce or eliminate binding by the various antibodies should be experimentally selected or designed *in silico*. This work is currently ongoing (M. Agbanje-McKenna, personal communication). Despite the limited footprint of interaction with MAbs, a full AAV1 escape mutant would likely involve changes at more than one residue, based on the slightly different binding sites antibodies 5H7 and 4E4. In addition, given that escape mutations would be very near the site for receptor interaction, these mutants must be rigorously tested to ensure that they maintain the correct receptor binding properties and tissue tropism(s) before being developed as gene-delivery vectors. If successful, these strains could have tremendous clinical impact as they would circumvent the current major hurdle preventing therapeutic gene delivery by parvoviruses.

6.6 References

1.   **Aguilar, H. C., and B. Lee.** Emerging paramyxoviruses: molecular mechanisms and antiviral strategies. Expert Rev Mol Med **13:**e6.

2.   **Erles, K., P. Sebokova, and J. R. Schlehofer.** 1999. Update on the prevalence of serum antibodies (IgG and IgM) to adeno-associated virus (AAV). J Med Virol **59:**406-11.

3.   **Hafenstein, S., V. D. Bowman, T. Sun, C. D. Nelson, L. M. Palermo, P. R. Chipman, A. J. Battisti, C. R. Parrish, and M. G. Rossmann.** 2009. Structural comparison of different antibodies interacting with parvovirus capsids. J Virol **83:**5556-66.

4.   **Kuijl, C., and J. Neefjes.** 2009. New insight into the everlasting host-pathogen arms race. Nat Immunol **10:**808-9.

5.   **Ossiboff, R. J., A. Sheh, J. Shotton, P. A. Pesavento, and J. S. Parker.** 2007. Feline caliciviruses (FCVs) isolated from cats with virulent systemic disease possess in vitro phenotypes distinct from those of other FCV isolates. J Gen Virol **88:**506-17.

6.   **Taubenberger, J. K., and J. C. Kash.** Influenza virus evolution, host adaptation, and pandemic formation. Cell Host Microbe **7:**440-51.